University of Alberta

Macrophage and T cell interactions: The role of T-cell associated products in arginase-1 induction

by

Lisa Billesberger

A thesis submitted to the Faculty of Graduate Studies and Research in partial fulfillment of the requirements for the degree of

Master of Science

Department of Medical Microbiology and Immunology

Edmonton, Alberta
Fall 2008

Library and Archives Canada

Published Heritage Branch

395 Wellington Street
Ottawa ON K1A 0N4
Canada

Bibliothèque et Archives Canada

Direction du Patrimoine de l'édition

395, rue Wellington
Ottawa ON K1A 0N4
Canada

Your file Votre référence
ISBN: 978-0-494-47183-8
Our file Notre référence
ISBN: 978-0-494-47183-8

NOTICE:
The author has granted a non-exclusive license allowing Library and Archives Canada to reproduce, publish, archive, preserve, conserve, communicate to the public by telecommunication or on the Internet, loan, distribute and sell theses worldwide, for commercial or non-commercial purposes, in microform, paper, electronic and/or any other formats.

The author retains copyright ownership and moral rights in this thesis. Neither the thesis nor substantial extracts from it may be printed or otherwise reproduced without the author's permission.

AVIS:
L'auteur a accordé une licence non exclusive permettant à la Bibliothèque et Archives Canada de reproduire, publier, archiver, sauvegarder, conserver, transmettre au public par télécommunication ou par l'Internet, prêter, distribuer et vendre des thèses partout dans le monde, à des fins commerciales ou autres, sur support microforme, papier, électronique et/ou autres formats.

L'auteur conserve la propriété du droit d'auteur et des droits moraux qui protège cette thèse. Ni la thèse ni des extraits substantiels de celle-ci ne doivent être imprimés ou autrement reproduits sans son autorisation.

In compliance with the Canadian Privacy Act some supporting forms may have been removed from this thesis.

While these forms may be included in the document page count, their removal does not represent any loss of content from the thesis.

Conformément à la loi canadienne sur la protection de la vie privée, quelques formulaires secondaires ont été enlevés de cette thèse.

Bien que ces formulaires aient inclus dans la pagination, il n'y aura aucun contenu manquant.

Canada

Dedicated to:

Leroy Michael Billesberger

&

Janice Colleen Billesberger

ABSTRACT

Macrophages and T cells are the most common immune cells infiltrating rejecting allografts. Macrophages are activated towards either an alternative (AMA) or classical activation phenotype by a network of cytokines, largely produced by activated T cells (ATC). Transcript expression of AMA marker Arginase 1 (Arg1) was increased in advanced stages of mouse kidney allograft rejection despite concomitant expression of Ifng, which inhibits AMA. I found that IL-4 and IL-13 independent and dependent mechanisms could lead to Arg1 induction. Activin A likely plays a major role in IL-4 and IL-13 independent induction of Arg1 –both *in vitro* co-cultures, and *in vivo* allograft rejection. Contact between macrophages and ATC did not significantly change macrophage Arg1 induction unless ATC produced IFN-γ. Co-cultures that contained IFN-γ contained low levels of IL-4 and IL-13 and our data suggests that activin A plays an important role for Arg1 induction in the presence of IFN-γ. These studies redefine the current paradigm of AMA and enhance our understanding of the role of the alternatively-activated macrophage in the allograft.

ACKNOWLEDGEMENTS

The last three years have been a whirlwind of activity and I have many people to thank for supporting me through this time.

Firstly, I would like to acknowledge my family: My father Leroy Billesberger, my mother Janice Billesberger, and my sisters Amanda and Cathryn Billesberger. Mom and Dad, you are my heroes. Thank you for your encouragement during my post-secondary years and for constantly supporting me in whatever I choose to do. Kyle Fisher, in the short time that I've known you, you've already changed my life. Your humor and generous nature are unparalleled and I look forward to many more of our adventures.

I have been fortunate to work in a laboratory that, in addition to offering world-class research in a stimulating environment, is home to some of the most fantastic people I have ever met. Luis Hidalgo, I first knew you as a teaching mentor but I now know you as one of my very best friends. Kara Allanach, you are like a sister to me and I appreciate you so much. Gunilla Einecke, fellow grad-student and confidante, I know that our friendship will last for many years to come. While there are too many people in the Halloran laboratory to single out in detail, I'd like to briefly acknowledge Joan Urmson, Stacey Lacoste, Suja Guttikonda, Anna Hutton, Vido Ramassar, Michael Mengel, and Konrad Famulski for their help and support. I developed close friendships with our many phenomenal summer students and I thank Brett Danielson, Joe LaBosserie, Jeffrey Venner, and Rebeca Psutka. I would especially like to thank Eric Milne for his sense of humor and advice. To my supervisor, Phil Halloran, you have taught me so much and I

consider you both a mentor and friend. The caliber of your personnel reflects positively on you, and I am convinced that I couldn't have found a better supervisor anywhere.

Members of the ex-'IMIN posse' I'd like to thank you: Stephanie Campbell, Nikki Barsby, and Logan Banadyga. Stephanie, you have been there for me during both the worst and best days 'EVER', and Nikki you have always been a loyal and honest friend and I appreciate you immensely. Maryam Nakhei, you have been so supportive and I appreciate your friendship. Finally, my roommates have been patient and heartening and I thank Joelle St. Pierre, Deanna Hockley, and Melany Wagner.

TABLE OF CONTENTS

CHAPTER 1: BACKGROUND **PAGE**

1.1 Introduction....1

1.2 Transplantation Overview....3

1.3 General Macrophage Overview....5

1.4 Activation Phenotypes of Macrophages....7

1.5 Regulation and Effects of Arginase-1....10

1.6 Effector T cells Overview. 12

1.7 Cytokines of Alternative Macrophage Activation....16

1.8 Prototypical TH_2 Cytokines IL-4 and IL-13....17

1.9 TGF-β Superfamily Member Activin A....21

1.10 Justification of Project....27

1.11 Figures 29

CHAPTER 2: MATERIALS AND METHODS

2.1 Introduction....34

2.2 Reagents, Cell-Culture Maintenance, and Mice....35

2.3 Renal Transplantation and Sample Preparation....37

2.4 Generation of Primary Immune Cells and *in vitro* Co-cultures....38

2.5 Cell RNA Extractions, Reverse Transcriptase Polymerase Chain Reaction, and Quantitative Real-Time Polymerase Chain Reaction....41

2.6 Experimental Procedures on Co-cultures....43

2.7 Tables....46

CHAPTER 3: EFFECTS OF T CELL-CONTACT ON MACROPHAGE ARGINASE-1 INDUCTION

3.1 Alternative Activation Markers Found in The Allograft Despite Interferon-γ.....47

3.2 Establishment of Macrophage/ T Cell Co-Cultures..... 48

3.3 Macrophage Activation in Macrophage/ Activated T Cell Co-cultures.....49

3.4 The Cytokine Profile in Macrophage/ Activated T Cell Co-Culture Supernatant...51

3.5 The Effect of Interferon-γ on Co-culture Macrophage Arginase-1 Induction.....52

3.6 Effect of Interferon-γ On Cytokine Profile in Macrophage/ Activated T Cell Co-culture Supernatant.....53

3.7 Effect of H2-T23 on Co-culture Macrophage Arginase-1 Induction.....53

3.8 Effect of H2-T23 On Cytokine Profile In Macrophage/ Activated T Cell Co-Culture Supernatant.....54

3.9 Neutralizing α-CD94 And α-NKG2/A/C/E Antibodies Do Not Increase IL-4 Production By Activated BALB/c T Cells.....55

3.10 Tables..... 56

3.11 Figures.....60

CHAPTER 4: ACTIVIN A AND THE ALTERNATIVE MACROPHAGE ACTIVATION PARADIGM

4.1 Soluble T Cell-Associated Products Induce Macrophage Arginase-1 Expression..... 72

4.2 IL-4 And IL-13 are Sufficient in our Culture System to Induce Macrophage Arginase-1 Expression.....72

4.3 IL-4 and IL-13-Independent Induction of Macrophage Arginase-1 *in vitro*.....73

4.4 Activin A Expression is Found in Allografts at Time-Points that Correspond with High Arginase-1 and High Interferon-γ Expression. 75

4.5 Activin A is Present in Macrophage/ Activated T Cell Co-culture Supernatant....77

4.6 Activin A Directly Induces Macrophage Arginase-1 Expression *in vitro*..... 78

4.7 Neutralizing Activin A in Macrophage/ Activated T Cell Co-Cultures Attenuates Macrophage Arginase-1 Induction.....79

4.8 Macrophages in Co-Culture with Activated T Cells Express High Levels of Activin A..... 80

4.9 Tables..... 82

4.10 Figures..... 84

CHAPTER 5: GENERAL DISCUSSION

5.1 Summary of Data.....103

5.2 T Cell-Associated Products induce Macrophage Arginase-1 Expression..... 105

5.3 Macrophage/ T cell Contact and Macrophage Arginase-1 Expression.....111

5.4 Future Directions..... 116

5.5 Conclusions..... 118

5.6 Figures..... 121

REFERENCES.....124

LIST OF TABLES

CHAPTER 2: MATERIALS AND METHODS PAGE

2.1 Gene-specific primer and probe sequences used in quantitative RT-PCR studies using the ABI PRISM 7700 and 7900 Sequence Detector.....46

CHAPTER 3: EFFECTS OF T CELL-CONTACT ON MACROPHAGE ARGINASE-1 INDUCTION

3.1 Summary of Arg1 induction in co-culture experiments using RAW MΦ and whole ATC.....56

3.2 Summary of Arg1 induction in co-culture experiments using RAW or primary MΦ and/ or 'whole' or $CD3^+$ ATC.....57

3.3 Summary of IL-4, IL-13, and IFN-γ levels in co-culture supernatant in experiments using RAW or primary MΦ and/ or 'whole' or $CD3^+$ ATC.....58

3.4 Summary of Arg1 induction in co-culture experiments using RAW MΦ and whole BALB/c WT or BALB/c $Ifng^{-/-}$ (GKO) ATC.....59

CHAPTER 4: ACTIVIN A AND THE ALTERNATIVE MACROPHAGE ACTIVATION PARADIGM

4.1 Summary of activin A concentration levels in direct-contact and no-contact conditions in co-culture experiments using RAW or primary BALB/c WT or IL-4RKO MΦ/ BALB/c WT or GKO 'whole' or $CD3^+$ ATC Arg1 induction in co-culture experiments using RAW MΦ and whole ATC.....82

4.2 Summary of IL-4, IL-13, IFN-γ, and activin A levels in co-cultures supernatant in BALB/c WT or IL-4RKO MΦ/ BALB/c WT $CD3^+$ ATC no-contact co-cultures..... 83

LIST OF FIGURES

CHAPTER 1: BACKGROUND PAGE

1a. General overview of allograft rejection.....30

1b. Cartoon of the AMA/ CMA paradigm.....31

1c. Alloantigen recognition by T cells during the course of allograft rejection.....32

1d. General structure of the inhibins and activins.....33

CHAPTER 3: EFFECTS OF T CELL-CONTACT ON MACROPHAGE ARGINASE-1 INDUCTION

3a. Time-course of macrophage activation-associated cytokine transcripts in CBA kidney allografts transplanted into B6 hosts.....61

3b. Time course of macrophage activation-associated transcripts in CBA kidney allografts transplanted into B6 hosts.....62

3c. Flow cytometric analysis of F4/80$^+$ purity in mouse peritoneal preparations following two different methods of macrophage purification.....63

3d. Whole or CD3$^+$-enriched ATC used in the co-culture assay.....64

3e. Quantitative RT-PCR of AMA marker Arg1 in RAW MΦ/ whole ATC co-cultures.....65

3f. Quantitative RT-PCR of AMA marker Chi3L3 and CMA marker Nos2 in RAW MΦ/ whole ATC co-cultures.....66

3g. ELISA analysis of cytokine levels in RAW MΦ/ BALB/c WT ATC co-culture supernatant.....67

3h. Quantitative RT-PCR of AMA marker Arg1 in RAW MΦ/ whole BALB/c WT or GKO ATC co-cultures.....68

3i. ELISA analysis of cytokine levels in RAW MΦ/ BALB/c GKO 'whole' co-culture supernatant..... 69

3j. Quantitative RT-PCR of AMA marker Arg1 in RAW MΦ/ whole BALB/c or DBA/2 ATC co-cultures..... 70

3k. ELISA analysis of cytokine levels in RAW MΦ/ DBA/2 'whole' ATC co-culture supernatant..... 71

CHAPTER 4: ACTIVIN A AND THE ALTERNATIVE MACROPHAGE ACTIVATION PARADIGM

4a. Quantitative RT-PCR of AMA marker Arg1 in F4/80$^+$ peritoneal BALB/c WT macrophages treated with increasing concentrations of recombinant IL-4 or IL-13..... 85

4b. Quantitative RT-PCR of AMA marker Arg1 in F4/80$^+$ peritoneal BALB/c WT macrophages treated with 0.1 ng/mL IL-4 and/ or 5.0 ng/mL IL-13..... 86

4c. Quantitative RT-PCR of AMA marker Arg1 in BALB/c WT or IL-4RKO MΦ treated with recombinant IL-4 and IL-13..... 87

4d. Quantitative RT-PCR of AMA marker Arg1in BALB/c WT or IL-4RKO MΦ incubated in no-contact with BALB/c WT CD3$^+$ ATC..... 88

4e. ELISA analysis of cytokine levels in BALB/c WT or IL-4RKO MΦ/ BALB/c WT ATC co-culture supernatant..... 89

4f. Time-course of macrophage activation-associated cytokine transcripts in CBA kidney allografts transplanted into B6 hosts..... 90

4g. Microarray analysis of transcript levels in normal (N) CBA WT kidneys, And in CBA WT or GRKO kidneys transplanted into BALB/c WT or IL-4RKO hosts..... 91

4h. Microarray analysis of transcript levels in MLRs and primary F4/80$^+$

MΦ cultures....92

4i. ELISA analysis of cytokine levels in RAW MΦ/ BALB/c WT ATC co-culture supernatant....93

4j. Quantitative RT-PCR of AMA marker Arg1 in BALB/c WT MΦ treated with increasing doses of recombinant activin A....94

4k. Quantitative RT-PCR of AMA marker Arg1in BALB/c WT MΦ treated with 100 ng/mL of activin A and/ or 100 ng/mL of LPS....95

4l. Quantitative RT-PCR of AMA marker Arg1 in BALB/c WT MΦ treated with 100ng/mL of activin A and/ or 0.1 ng/mL of recombinant IL-4 and 5.0 ng/mL of recombinant IL-13....96

4m. Quantitative RT-PCR of AMA marker Arg1 in BALB/c WT or IL-4RKO MΦ/ $CD3^+$ BALB/c WT ATC no-contact co-cultures....97

4n. Quantitative RT-PCR of AMA marker Arg1in BALB/c WT or IL-4RKO MΦ/ $CD3^+$ BALB/c WT ATC co-cultures....98

4o. Flow chart of purification protocol to re-isolate $F4/80^+$ cells from MΦ/ ATC co-cultures....99

4p. Flow cytometry analysis of MΦ purity....100

4q. Quantitative RT-PCR analysis of T cell-associated and MΦ-associated transcripts in cells from MΦ/ ATC co-cultures....101

4r. Quantitative RT-PCR of Inhba in cells in BALB/c WT MΦ/ ATC co-cultures....102

CHAPTER 5: GENERAL DISCUSSION

5a. Activin A in the context of an immune response....122

5b. The big picture of allograft rejection....123

LIST OF ABBREVIATIONS

Arg1	–Arginase1
ATC	–Activated T cell
AMA	–Alternative macrophage activation
APC	–Antigen presenting cell
AP-1	–Activator protein
CMA	–Classical macrophage activation
CSF	–Colony stimulating factor
DC	–Dendritic cells
EGF	–Epidermal growth factor
IFN	–Interferon
Ig	–Immunoglobulin
IRF	–Interferon regulatory factor
IRS	–Insulin receptor substrate family
ITIM	–Immunoreceptor tyrosine-based inhibition motif
JAK	–Janus kinases
LPS	–Lipopolysaccharide
MΦ	–Macrophage
MARE	–Maf-recognition elements
MHC	–Major histocompatibility complex
MLR	–Mixed lymphocyte reaction
MMP	–Matrix metalloproteinases

NFAT –Nuclear-factor of activated T cells

NF-κB –Nuclear factor-kappa

NK cell –Natural killer cell

Nos –Nitric oxide synthetase

NO –Nitric oxide

PRR –Pattern recognition receptor

PI3K –Phosphoinositide 3-kinase

PTB –Protein binding tyrosine binding

SLO –Secondary lymphoid organ

STAT –Signal transducer and activator of transcription

T-bet –T box expressed in T cells

TGF-β –Transforming growth factor

T_{reg} –Regulatory T cell

TLR –Toll-like receptor

TNF –Tumor necrosis factor

T_H –T helper cell

WT –Wildtype

CHAPTER 1

BACKGROUND

1.1 INTRODUCTION

MΦs can be activated by a large number of pathways, including innate stimuli, humoral activation, or the action of T cell-secreted cytokines (1). MΦs activated through the action of cytokines are typically categorized into classical MΦ activation (CMA) or alternative MΦ activation (AMA) phenotypes. In rejecting allografts, MΦ phenotypes vary depending on the presence of interferon (IFN)-γ and components of the major histocompatibility complex (MHC) class I antigen presentation machinery. We have observed that kidney allografts with an impaired ability to respond to IFN-γ or compromised MHC class I presentation pathways exhibit accelerated graft necrosis and elevated transcript levels of the AMA marker arginase-1 (Arg1) (2). The increase in Arg1 in these cases occurs despite abundant IFN-γ expression in the allograft. This implies that the regulation of AMA is more complex than the current model of MΦ activation suggests. Recently activin A, a pluripotent member of the TGF-β superfamily, was shown to be secreted by α-CD3-activated effector T cells and induce Arg1 expression in peritoneal MΦs (3).

For many patients facing end-stage kidney failure the survival-advantage and enhanced quality-of-life conferred by kidney-transplantation is a distant hope, and dialysis is a grim reality: Despite the 60, 000 patients on the 2005 United States waiting list for kidney transplantation, in 2004 only 16, 879 kidney transplants were preformed (4). Faced with a shortage of donor-kidneys, it is important that steps are taken to promote and sustain long-term graft-survival in transplant recipients.

The vast majority of transplants performed are between non-genetically identical, or allogeneic, individuals. Allogeneic transplants often trigger a recipient-mediated immune-response against the foreign transplant that leads to rejection and, ultimately, transplant loss. To better understand the process of allograft rejection, our laboratory has characterized murine models of human kidney transplantation. Together with information gathered from human kidney transplant biopsies, these models indicate that alloreactive T cells and macrophages (MΦ) play important roles in allograft rejection. Indeed, MΦs and activated T cells are the most abundant immune cells infiltrating rejecting allografts (5).

Traditionally, transplantation rejection dogma contends that rejection is a process mediated largely by the cytolytic-effects of T cells on the allograft. Despite their association with rejection, we and others have shown that the cytolytic activity of CD8+ T cells is not essential to allograft destruction (6;7). Rather, we hypothesize that damage to rejecting transplants is a result of T cell-activated MΦs. This project focused on the effects of T cell contact and associated soluble mediators on MΦ Arg1 induction.

1.2 TRANSPLANTATION OVERVIEW

(a) Types of transplantation. Transplants are xenogeneic, syngeneic, or allogeneic. In xenotransplantation, a graft is transplanted from one species to another and, although it has been touted as the solution to the donor-organ shortage, xenotransplantation is currently impractical for a number of reasons including species-specific growth factor receptors and endogenous viruses (8;9). In contrast to xenotransplantation, syngeneic and allogeneic transplantation occur within the same species; more specifically, syngeneic transplantation is between genetically identical individuals such as monozygotic twins and allogeneic transplantation is between genetically non-identical individuals. Identical twins are rare, thus syngeneic transplantation is uncommon and the vast majority of human transplants are allogeneic. Up to 5 % of the T cells within a given individual's T cell repertoire may recognize and instigate a response against allogeneic major-histocompatibility complex (MHC). In the context of transplantation, recognition of alloantigen invokes a powerful immune response that can result in rejection and ultimate destruction of the allograft.

(b) On the recognition of alloantigen by T cells. T cells recognizing alloantigen are generated in much the same manner as pathogen-specific T cells and will be discussed in more detail in subsequent text.

(c) Non-specific instigators of allograft rejection. The surgery associated with the donation process and ischemic/ reperfusion time of the donor organ during

transplantation results in injuries to the allograft. For example, MHC, cytokine, and chemokine expression is increased in response to ischemic injury, and these changes can invoke an inflammatory response that is independent of a specific recipient-mediated alloimmune response (10;11). However, the adaptive immune response is often triggered following the activation of the innate immune response by factors such as tissue stress (12). Thus, the specific immune response against an allograft may be enhanced by the actual process of transplantation, likely by activation and maturation of antigen presenting cells (APC) in response to tissue stress and subsequent co-stimulation and activation of allospecific T cells.

(d) Disturbances in the force: Effects of rejection on the allograft. After activation, allospecific B and T cells enter the graft and enhance the inflammatory cascade, leading to increased extravasation of cellular filtrate into the graft (13). In addition, injury to the allograft during the transplantation process likely contributes to endothelial activation and facilitates entry of leukocytes. Many allograft cells present class I and II MHC to allospecific lymphocytes and during rejection increased IFN-γ expression enhances MHC expression by graft epithelial cells, parenchymal cells, and vascular endothelial cells. In the rejecting allograft, changes in expression of cytokines, such as IFN-γ and TNF, and cytotoxic-T lymphocyte molecules, such as perforin and granzyme A/B, are all observed (14).

Although the mechanisms of allograft rejection remain elusive, the initial stages are primarily dependent on T cells: Transplantation into immunoglobulin-deficient mice results in early rejection-phenotypes that are similar to transplantation into wild-type

mice. Despite the strong induction of cytotoxic-genes in rejection, transplants into perforin-deficient mice still reject suggesting that the cytotoxic effects of T cells are not sufficient for mediating injury to transplanted tissues (7). Nonetheless, direct contact between cytotoxic T cells and allograft tissue is observed in rejection and correlates with functional decline of the graft (15). MΦs and effector T cells are the two most common immune cells observed by histology in the rejecting allograft and our laboratory now believes that rejection is a process mediated by effector T cell-activated MΦs (Figure 1a) (5).

1.3 GENERAL MACROPHAGE OVERVIEW

(a) General overview of macrophages. MΦ precursors and neutrophils are thought to arise from a common myeloid progenitor. Initially, MΦs were grouped as part of the reticularendothelial system; however, this method of classification was later discarded as it failed to differentiate between endothelial cells and resident MΦs (16). Instead the mononuclear-phagocyte method of classification was introduced, which included only MΦs and their monocyte-precursors, as well as lineage-committed bone marrow precursors (16). Later in differentiation, most tissue-resident MΦs are derived from bone-marrow monocytes that also give rise to dendritic cells and osteoclasts (16). Between 5 and 10% of circulating blood mononuclear leukocytes are monocytes that display varying degrees of granularity (16). The original definition of mononuclear phagocyte included stipulations on morphology and ultra-structural features, expression of certain enzymes,

non-specific uptake of particles, and expression of certain endocytic receptors (17). However, cells of the monocytic phagocyte lineage are notorious for their plasticity and heterogeneity, and this heterogeneity is believed to reflect specialization of function within different microenvironments. For example, when cultured human monocyte subsets differentiate into dendritic cells in the presence of granulocyte/ MΦ colony-stimulating factor and IL-4 (16;17).

(b) Macrophages are potent presenters of antigen. MΦs are extensively characterized as efficient APCs, and a broad range of plasma membrane receptors mediate interaction with host-endogenous normal and altered proteins, as well as with microbial molecules (18). Unlike the specific receptors found in adaptive immunity, the pattern recognition receptors (PRRs) of innate immunity are germ-line encoded and recognize conserved molecular patterns on pathogens. The identification of a pan-MΦ marker has been fraught with difficulty due to MΦ heterogeneity. To date F4/80, the expressed protein of the gene Emr1, is the most reliable MΦ marker found in the mouse as it is expressed on most resident MΦs including red pulp-associated splenic MΦs, brain microglia, liver Kupffer's cells, and skin Langerhan's cells (17;19;20). Interestingly, expression of F4/80 appears to be tightly linked to the physiological states of MΦs. For instance, blood monocytes express less F4/80+ than tissue MΦs (21). In addition, activated MΦs from animals infected with bacille Calmette-Guerin have decreased F4/80+ expression compared to unstimulated MΦs (22). Activation through the PRRs on MΦs leads to surface marker changes, phagocytosis of antigen, signaling, and altered gene expression.

Ultimately, pathogen recognition results in the instigation of homeostatic mechanisms, innate effector mechanisms, and the induction of acquired immunity (18).

1.4 ACT IVATION PHENOTYPES OF MACROPHAGES

(a) General overview of macrophage activation. MΦs may be activated through their PRRs or altered-self stimuli, Fc or complement receptors, or a network of cytokines that is primarily produced by activated T cells (1). MΦs that are activated by microbial or altered-self stimuli display innate activation; in contrast, MΦs that are activated by binding of Fc receptors display humoral activation. Conventionally, MΦ activation states that are augmented by T-cell associated cytokines are classified into one of two activation phenotypes: Classical MΦ activation (CMA) or alternative MΦ activation (AMA). Although Procrustean in nature, dichotomizing activation phenotypes enables the categorization of MΦ activation into easily-understood patterns that will predict a generalized outcome (Figure 1b).

(b) Innate and humoral MΦ *activation.* MΦs possess a diverse collection of PRRs that recognize innate and humoral ligands through direct recognition of carbohydrate, lipid, proteins, or nucleic acids, or through the use of opsonins such as antibody (23), collectins (24;25), lipopolysaccharide (LPS)-binding protein, or complement (1). In addition, MΦs respond to a variety of endogenous host-ligands such as modified lipoproteins and heat-shock proteins (1). Recognition of ligand through PRR leads to the production of pro-

inflammatory cytokines such as type-one IFNs (α/β) and the expression of reactive oxygen species (26) and nitric oxide. Inflammation is followed by a tightly regulated anti-inflammatory response. In addition to the induction of pro-inflammatory cytokines, exogenous and endogenous MΦ stimuli promote phagocytosis and endocytosis through scavenger receptors and the mannose receptor, and enhance antigen presentation through increased expression of co-stimulatory surface molecules (1). MΦs may be further activated by a complex network of predominantly T cell secreted cytokines independently of, or in conjunction with, innate or humoral stimuli (26).

(c) Classical macrophage activation. Classical MΦ activation (CMA) can be thought of as the "Mr. Hyde" side of MΦ phenotypes: CMA is usually associated with destruction. More specifically, MΦs with a CMA phenotype are associated with the induction of apoptosis, responses against intracellular-microorganisms, tumor-clearance, matrix degradation and tissue damage, phagocytosis of opsonized complexes, and delayed-type hypersensitivity (1;27). In addition, CMA MΦs phagocytose apoptotic cells and cellular debris (26).

The prototypical Th1 cytokine IFN-γ drives CMA, alone or in concert with additional cytokines (e.g. tumour-necrosis factor; TNF) or microbial stimuli (e.g. LPS). IFN-γ rapidly primes MΦs for action through a JAK-STAT1α-mediated pathway, that induces the interferon regulatory factor (IRF1-9) family of transcription factors (28). Binding of the IRFs to IRF-binding elements results in the induction of antiviral and antibacterial states by upregulating IFN-α/β production and nitric oxide synthetase 2 (Nos2) expression, respectively (28). Nos2 expression shifts cellular L-arginine

metabolism towards production of citrulline and nitric oxide (NO). In addition to being bactericidal, NO has been shown to induce apoptosis in certain cell-types (26;28;29). In addition, CMA MΦs have an overall phenotype of proteolytic activity and contribute to tissue matrix destruction through the direct production of matrix metalloproteinases (MMPs) such as MMP-7 (30), and the induction of other cell types to produce MMPs. For instance, MΦs induce lung fibroblasts to produce MMP-13 (31) and myofibroblast mesangial cells to produce MMP-3 (32).

The typical CMA MΦ has an IL-12^{high}, IL-23^{high}, IL-10^{low} profile and secretes pro-inflammatory cytokines such as IL-1β, TNF, and IL-6 and effector molecules such as reactive oxygen and nitrogen intermediates (33). CMA is important in many experimental inflammatory models such as experimental autoimmune encephalomyelitis (34) and progressive nephritis (35). Interestingly, recent research has shown that CMA MΦs are not necessarily doomed to a hostile life as Mr. Hyde. Rather, it seems that MΦs can exhibit a plasticity of phenotype in that CMA MΦs satiated by phagocytosis of apoptotic cells acquire a phenotype that is similar, albeit not functionally identical, to the alternatively activated MΦ (26).

(d) Alternative macrophage activation. Alternative MΦ activation (AMA) can be thought of as the 'Dr. Jekyll' side of MΦ activation: In contrast to the destructive-tendencies of CMA MΦs, mild-mannered AMA MΦs are usually associated with remodeling and resolution of inflammation. In particular, AMA MΦs generate anti-inflammatory cytokines, promote angiogenesis, respond against extra-cellular pathogens, enhance antigen-presentation, induce cell survival and proliferation, and participate in matrix

synthesis and stabilization (26). Like CMA MΦs, AMA MΦs also phagocytose apoptotic cells and debris.

Cytokine mediators of AMA will be discussed in detail in subsequent text. Briefly, IL-4 and IL-13 have been extensively characterized as inducers of AMA and, more recently, the transforming growth factor-β (TGF-β) superfamily member activin A has also been associated with AMA.

Induction of AMA leads to an increase in mannose receptor (CD206) and scavenger receptors (CD163), MHC class II expression, fusion of cells, production of arginase-1 (Arg1) and a modest decrease in the expression of pro-inflammatory cytokines and the respiratory burst (1;36). FIZZ1 and Ym1/2 have also been associated with AMA (37). AMA is associated with wound healing (1) and with the fibrotic disease pathologies seen in chronic parasite infections, such as leshmaniasis (38), and perhaps atherosclerosis (1).

1.5 REGULATION AND EFFECTS OF ARGINASE-1

(a) General overview of arginase-1. Arginase is a homotrimeric 105 kD enzyme that hydrolyzes its substrate L-arginine into L-ornithine and urea. Two distinct isozymes have been identified in mammals that act in distinct sub-cellular compartments: cytosolic Arg1 is usually found in the liver and catalyzes the last step of the urea cycle, whereas mitochondrial arginase (Arg2) distribution is more ubiquitous (e.g. liver, brain, kidney, skeletal muscle) and does not appear to play a role in the urea cycle. Importantly, Arg1

found in MΦs is an indicator of AMA, and will be the focus of this discussion (39). Unlike liver Arg1, MΦ Arg1 is not constitutively expressed throughout life; it is tightly regulated and in resting murine MΦs Arg1 is not detectable at the mRNA, protein, or enzymatic levels (40). Interestingly, Arg1 is upregulated in mononuclear immune cells after trauma (41).

(b) Structure and biochemical properties of arginase-1. Arg1 requires manganese for action and recognizes its sole biological substrate, L-arginine, with high fidelity (39). Indeed, Arg1 is unable to act on arginine with altered structure or stereochemistry and will not recognize D-arginine or arginine with altered substituents. The fluoride ion is a simple uncompetitive inhibitor of Arg1 activity: The fluoride ion binds to the substrate-enzyme complex and prevents enzymatic activity by displacing a metal-bridging hydroxide ion. The most effective Arg1 inhibitors, however, are those that bridge the binuclear manganese cluster activity. For example, NO-hydroxy-L-arginine (NOHA) is a modest inhibitor of Arg1 activity. NOHA is an intermediate of NO biosynthesis and provides at least a partial explanation for the inhibition of CMA products on AMA. In addition to specific inhibition mechanisms, Arg1 and Nos2 both vie for the same substrate: L-arginine. As a result, both enzymes can effectively inhibit the action of the other through depletion of their common substrate and this principal has aroused much clinical interest. Interestingly, specific inhibitors of Arg1 are used to prevent arginase-dependent depletion of L-arginine which increases the bioavailability of L-arginine for the synthesis of NO – an important first messenger in male erectile function (39).

(c) Gene regulation of arginase-1. Transcription of Arg1 mRNA is inducible in response to various stimuli including IL-4, IL-13, cAMP, and TGF-β. Elements involved in transcriptional responses to these stimuli are found in the 5' flanking region of the murine arginase I gene (42). In the case of IL-4 and IL-13, transcription of Arg1 is dependent on an enhancer region that is located approximately 3 kb from the transcriptional start site. In response to signaling through the IL-4/13 receptor, STAT-6 directly binds the enhancer and instigates the transcription of other genes required for Arg1 expression. Other factors that bind to the enhancer region include C/EBP β, the co-activator CBP and PU.1, a transcription factor that is crucial to MΦ biology and development (40;43). Arg1 shifts L-arginine metabolism in AMA MΦs towards the production of L-ornithine and urea; L-ornithine is further metabolized to prolines and polyamines, which are associated with collagen production and cell proliferation respectively (1;44). Polyamines can be exploited by intracellular pathogens, such as Leishmania, to support their proliferation (45). Additionally, induction of Arg1 in MΦs likely plays a role in wound healing (46) and in the formation of granulomas during infection (44). Finally, induction of MΦ Arg1 likely contributes to airway remodeling and hyper-responsiveness in asthma (47).

1.6 EFFECTOR T CELLS OVERVIEW

(a) Generation of effector T cells. After genesis and stochastic gene rearrangement of the T cell receptor in the bone marrow, T cells mature in the thymus where they undergo specific positive and negative selection processes before being released into the

peripheral circulation. Naïve T cells, or T cells that have not met their cognate antigen, are restricted from entering peripheral tissues. Rather, naïve CD8 and CD4 T cells traffic from blood into secondary lymphoid organs (SLO), through lymphoid vessels to the lymph, and back to the blood where they enter other SLOs. Examples of SLOs include the spleen, lymph nodes, and Peyer's patches. Whilst in the SLO, T cells sample antigen presented on APCs, which have migrated from the periphery in response to infection or injury.

Dendritic cells (DC) are the predominant APC that T cells meet in the SLOs. DC reside in the periphery in an inactivated state where they continually endocytose material from their extracellular environment thereby surveying their surroundings for insults such as infection or injury. DCs, like MΦs, recognize danger signals through PRRs such as the Toll-like receptors. Recognition of a pathogenic disturbance leads to DC activation and exodus to SLOs. DCs can discriminate the threat that each endocytosed antigen presents to the host: Recognition does not necessarily lead to an active immune response and can even lead to tolerance of the antigen. Indeed, DC can traffic to SLOs and induce tolerance to certain antigens (48). For example, DC can induce tolerance to self-antigens or even suppress disease in experimental models of autoimmunity such as autoimmune thyroiditis (49).

Naïve T cells and DC in SLOs are coordinated to move in a manner that brings them into contact with each other; a process driven by changes in chemokine and chemokine receptor expression. After recognition of their cognate antigen on mature DC, naïve T cells are activated, undergo clonal expansion, acquire effector functions, and move to the periphery. CD4 T cells move to the periphery or to B cell regions of SLOs

where they provide essential co-stimulation to B cells and enable antibody isotype class-switching and promote B cell progression to plasma cells. Once in the periphery, CD8 and CD4 T cells can act as effector cells. For example, CD4 T cells secrete a plethora of cytokines that modulate the immune response. These include Th1-type cytokines, like IFN-γ, IL-2, and lymphotoxin, and Th2-type cytokines like IL-4, IL-5, IL-10, and IL-13. CD8 T cells also produce a number of cytokines and, in addition, are important mediators of cytotoxicity.

Subsequent to the eradication of antigenic threat, most activated T cells are deleted from the T cell repertoire. Deletion occurs by activation-induced cell death or by antigenic withdrawal. Only a limited number of activated T cells are spared this fate, and these will become memory cells that ensure a rapid and highly effective immune response upon secondary-exposure to the same specific antigen (50).

(b) Generation of allospecific-effector T cells. After clonal expansion and acquisition of effector functions, allospecific T cells exit SLOs and are recruited into the allograft in response to chemokines and other inflammatory mediators induced in the allograft. Pre-existing allospecific memory T cells may be present in the transplant recipient as a result of previous immunological-priming from blood transfusions or transplants. Pre-existing memory cells have been linked with increased early-rejection episodes (51). Interestingly, allospecific memory T cells have been detected in naïve individuals; that is, in individuals who have not been immunologically primed with a previous transplant or blood transfusion. Alloreactive memory T cells in 'naïve' individuals are speculated to arise from an unrelated pathogenic challenge that happen to cross-react with alloantigens

(52). Recipient T cells encounter their cognate alloantigen on APCs through direct or indirect presentation pathways or by a pathway combining both (Figure 1c) (53).

Indirect presentation is the stereotypical presentation of antigen during the course of an immune response: Antigen is taken up by the APC, processed intracellularly, and presented as short, linear fragments of peptide to recipient T cells in the context of recipient MHC class II. In transplantation, graft-derived cells or released antigens are taken up by recipient APC and donor-derived MHC peptides are presented to alloreactive T cells that subsequently initiate the alloimmune response.

Direct presentation of antigen involves the direct recognition of intact donor-derived MHC molecules by recipient T cells. Recipient T cells recognize allogeneic MHC directly on cells within the allograft; alternately, donor APCs may travel from the allograft to SLOs and activate allospecific T cells. Direct presentation responses are demonstrated by the strong *in vitro* response generated by T cells incubated with allogeneic APCs in mixed lymphocyte reactions.

A third mechanism of antigen presentation has recently been proposed: Allogeneic MHC is acquired by recipient APCs, and instead of being processed intracellularly, is presented intact to recipient T cells. Theoretically, this could occur by recipient APCs acquiring membrane fragments from donor cells that contain intact MHC which directly activates recipient allospecific T cells (53).

1.7 CYTOKINES OF ALTERNATIVE MACROPHAGE ACTIVATION

(a) General overview of cytokines associated with alternative macrophage activation.

The prototypical Th2 cytokines IL-4 and IL-13 are well characterized as inducers of AMA. The TGF family of cytokines, MΦ colony stimulating factor (CSF), IFN-α/β, and TGF-β all induce MΦ gene expression profiles that partially overlap with IL-4/13-induced MΦ responses (1). Activin A, a pluripotent member of the TGF-β superfamily, also induces Arg1 expression in MΦs (3). IL-10 is a part of the Th2 milieu and has been grouped with other AMA-inducing cytokines in the past. However, IL-10 acts through a separate plasma-membrane receptor than IL-4 and IL-13 and results in MΦ deactivation through inhibition of antigen presentation and effector functions (1). For example, IL-10 decreases MHC class II expression and potently inhibits nitric oxide and pro-inflammatory cytokine production (54;55). To this end, IL-10 is better classified as a MΦ-deactivator that is distinct of AMA. In summary, as each immunomodulatory cytokine has different effects on MΦ activation phenotype it has been suggested that the definition of AMA be limited only the effects of IL-4 and IL-13 so as to avoid confusion (1). In light of recent findings that activin A elicits a MΦ phenotype very similar to IL-4/13 induced AMA, this text will also discuss activin A (3).

1.8 PROTOTYPICAL TH_2 CYTOKINES IL-4 AND IL-13

(a) General overview of IL-4 and IL-13. IL-4 and IL-13 belong to the same protein family and share several structural similarities. The genes for both IL-4 and IL-13 are found on chromosome 5 of the human genome or chromosome 11 of the mouse genome; IL-4 and IL-13 proteins are approximately 18 kDa and 12 kDa in size, respectively. The structure of human IL-13 is predicted to be similar to IL-4, which consists of a four helix bundle lined with hydrophobic residues and of polar residues on the surface that display a high degree of solvent accessibility (56). IL-4, but not IL-13, induces T cell differentiation, although both have similar effects on B cells and monocytes (1). There are multiple cellular sources of IL-4 and IL-13. IL-4 and IL-13 are produced by Th2 T cells in response to T-cell receptor engagement, or by mast cells, basophils, and eosinophils in response to cross-linking of high affinity immunoglobulin-E (IgE) receptors (57).

(b) Regulation of IL-4 and IL-13 expression. Like many other genes, transcription of IL-4 and IL-13 is dependent on the ubiquitous transcription factor nuclear-factor of activated T cells (NF-AT) and activator protein-1 (AP-1). However, restricted expression of IL-13 and IL-4 relies on GATA proteins and *c-maf* (58). AP-1 is a dimeric complex of a Jun family protein and a Fos family protein that interacts with GATA proteins (59). AP-1 activity is higher in TH_2 cells than in TH_1 cells, and binds sites near the IL-4 promoter elements. Structural analysis of NFAT revealed an interface that can mediate interactions with AP-1 when it is bound adjacently on DNA, providing an explanation for the cooperation observed in transactivation via proximal IL-4 promoter elements. Furthermore, a similar interaction between *c-maf* and AP-1 has been reported, providing

a basis for TH_2 selective synergistic interactions on the IL-4 promoter (58). GATA proteins are tissue-restricted transcription factors that use a zinc-finger DNA-binding domain to bind a specific DNA motif. Two families of GATA proteins have been proposed: GATA-1—3, which are predominantly expressed in hematopoietic stem cells, and GATA-4—6, which are predominantly expressed in mesoderm- and endoderm-derived tissues (59). IL-4 and IL-13 expression relies on different members of the GATA-1—3 family in a cell-specific manner. In mast cells, GATA-1 and 2 play important roles in IL-4 gene transcription, and GATA-1 plays an important role in IL-13 transcription (59). In T cells GATA-3 is involved in chromatin remodeling of IL-4 and IL-13 genes and renders promoter regions more accessible to transcription factors (60). GATA-3 is expressed by CD4+ T cells until differentiation into TH_1 cells and also directly regulates transcription of IL-5, thus serving as a global TH_2 cytokine marker. *c-maf*, a proto-oncogene, cannot initiate transcription but is important for high levels of IL-4 production by enhancing promoter activity (61).

(c) Signaling of IL-4 and IL-13. IL-4 signals through heterodimeric type I or type II receptor complexes. The type I receptor complex assembles in hematopoietic cells when IL-4 binds the IL-4Rα chain, which then dimerizes with the common gamma chain (γC). The type II receptor complex forms in hematopoietic cells of the myeloid lineage as well as other cell types including epithelial cells, endothelial cells, and fibroblasts (57). IL-4 binds to the IL-4Rα chain, and IL-4Rα forms a dimer with IL-13Rα1 to form the type II receptor. Dimerization of the IL-4 receptor activates Janus kinases (Jaks) associated with the cytoplasmic tail of the receptor. Jak1 and Jak3 are activated in type I receptors, while

Jak 1, Jak 2, and Tyk2 are activated in type II receptors. Subsequent to kinase activation, tyrosine residues in the cytoplasmic tail of IL-4Rα are phosphorylated and become docking sites for signaling molecules. The first tyrosine residue interacts with protein binding tyrosine binding domains (PTB) found in members of the insulin receptor substrate family (IRS) and Sic, while the 2nd through 4th tyrosine residues interact with the SH2 domain of signal transducer and activator of transcription 6 (STAT6), and the fifth tyrosine residue is found within an immunoreceptor tyrosine-based inhibition motif (ITIM) and interacts with the SHP-1 phosphatase (57). At the receptor complex, these signaling molecules are tyrosine-phosphorylated. Phosphorylated STAT6 dimerizes and translocates to the nucleus where it binds to the promoters of many genes including CD23 and class II major histocompatibility complex (MHC). STAT6 can be dephosphorylated by SHP-1. Depending on the cell type, cellular environment, and activation state of the cell STAT6 can act as a transcriptional activator or repressor. Phosphorlyated IRS binds to the p85 subunit of phosphoinositide 3-kinase (PI3K) and to the adaptor Grb2. In cell lines, the IRS family has been linked to cell proliferation pathways; in contrast, in primary cell lines STAT6 has been linked to cell proliferation and apoptosis protection pathways (62).

IL-13 also requires the IL-4Rα subunit for active signaling, thus intertwining the IL-4 and IL-13 signaling pathways. Indeed, the type II IL-4 receptor is homologous to the IL-13Rα1/ IL-4Rα heterodimeric IL-13 receptor. The IL-13/ type II receptor is ubiquitously expressed including in epithelial tissues, MΦs, fibroblasts, and eosinophils (63). The fact that IL-4 and IL-13 share a receptor explains how they both elicit many of the same cellular responses. IL-13 signals through heterodimeric transmembrane

receptors. IL-13 binds to IL-13Rα1 with moderate affinity, which leads to the recruitment of the IL-4Rα chain to the receptor complex. IL-13 also binds with high affinity to IL-13Rα2. However, this subunit does not lead to active signaling; rather it acts as a decoy receptor and decreases IL-13 signaling through IL-13Rα1/ IL-4Rα. Dimerization of IL-13Rα1 with IL-4Rα leads to activation of Jaks associated with the cytoplasmic tail of the receptor complex: IL-13Rα1 is associated with Jak2 and Tyk2 while IL-4Rα is associated with Jak1. Jak activation leads to the phosphorylation of docking sites on specific cytosolic tyrosine residues, and signaling molecules are recruited that lead to downstream effects of IL-13. For instance, signaling through the PI3K pathway leads to cell survival and growth, while signaling through the STAT6 pathway alters gene transcription that leads to eosinophilic inflammation and airway hyperreactivity (63).

(d) Effects of IL-4 and IL-13. IL-4 and IL-13 induce similar physiological effects and are associated predominantly with allergy, asthma, and autoimmunity (57). Both IL-4 and IL-13 promote expression of markers of AMA in MΦs including: IL-1 decoy receptor, Arg1, mannose receptor, CD23 (IgE F_c receptor), FIZZ1, MMP-1 and MMP-9 (1).

IL-4 regulates expression of leukotriene C4 synthase by mast cells, chemokine production and mucous secretion by epithelial cells, collagen production by fibroblasts, and AMA (64). In the developing immune response, IL-12 is produced by DC and MΦs and is essential for TH_1 development. IL-4 inhibits this pathway of development by down-regulating expression of the IL-12 receptor thus promoting TH_2 development and suppressing the development of TH_1 cells (61). Therefore, IL-4 plays an anti-

inflammatory role in disease processes characterized by high production of inflammatory mediators such as IL-1, IL-6, IL-8, and TNF. In addition, IL-4 is a growth factor for mast cells, B cells, and T cells, increases class II MHC expression on B cells, and promotes IgE and IgG_1 isotype class-switching (65). IL-4 may play a role in fibrotic diseases such as systemic sclerosis –IL-4 stimulates production of extracellular-matrix protein collagen by fibroblasts (66).

IL-13 also regulates AMA and may also play a significant role in asthma and allergy by regulating airway hypersensitivity, mucus hypersecretion, and TH_2 type inflammation of the bowel (67). In human peripheral blood monocytes treated with LPS, IL-13 inhibits the production of anti-inflammatory cytokines IL-1β, TNF, IL-6, and IL-8 (68). IL-13 enhances B cell and monocyte differentiation and proliferation, induces IgG_4 and IgE isotype class-switching, and, like IL-4, increases CD23 expression (69).

1.9 TGF-β SUPERFAMILY MEMBER ACTIVIN A

(a) General overview of activin A. The activins and inhibins are pluripotent members of the TGF-β superfamily and exist as disulfide-linked dimers. The inhibins are built from Inhb and Inha subunits; in contrast, the activins are built from only Inhb subunits (Figure 1d). For example, activin A is a homo-dimer of inhba, whereas activin AB is a hetero-dimer of Inhba and Inhbb, and activin B is a homo-dimer of Inhbb (70). Inhibins and activins are multifunctional cytokines found in many cell-types and tissues, including

neuronal and endocrine tissues, bone marrow cells, myeloid cells, mast cells, and reproductive cells.

(b) Regulation of activin A expression. As the family of inhibin/ activins is large, this discussion will be limited to the gene regulation of Inhba, the gene subunit that comprises the activin A protein. Furthermore, as activin A is expressed in many cell types, the literature regarding gene regulation of activin A is diverse and only Inhba expression in immune cells will be discussed. In T cells differentiating along the TH_2 lineage, activin A is markedly induced, suggesting that regulation of Inhba gene expression is reminiscent of other TH_2-type genes (3). A putative NF-AT binding site was identified in the Inhba gene promoter region; however, NF-AT also activates the promoter of numerous genes (3). Further examination of the promoter region found Maf-recognition elements (MAREs) downstream of the NF-AT recognition sites. *c-Maf*, a basic region/leucine-zipper transcription factor, is preferentially found in TH_2, and not in TH_1, cells and *c-Maf* and NF-AT may work synergistically to transactivate the Inhba promoter.

There are high levels of activin A in the cerebral spinal fluid during meningitis and in the systemic circulation during sepsis (71). Primary murine microglial cells and peritoneal MΦs release activin A in response to treatment with both IFN-γ and toll-like receptor (TLR) 2, 4, or 9 agonists. TLRs 2, 4, and 9 are important TLRs in the recognition of bacterial infections; thus, MΦs and central nervous system microglial cells are thought to be important producers of activin A in response to bacterial challenge (71).

Additional studies confirm that signaling through TLR-4 and the key adaptor protein, MyD88, results in high serum levels of activin A (72).

Monocytes and bone marrow stromal fibroblasts constitutively produce activin A. Interestingly, activin A secretion is enhanced upon cognate interaction with activated T cells (73). Enhanced activin A secretion relies on interactions between the co-stimulatory molecules CD40/ CD40 ligand: Crosslinking of CD40 on monocytes or stromal fibroblasts with α-CD40 antibody or by CD40-ligand transfectants independently increases activin A secretion (76). In addition, cognate interaction of T cells with monocytes and stromal fibroblasts decreased production of the activin-A inhibitor, follistatin. T-cell secreted cytokines such as GM-CSF and IFN-γ further augment CD40/ CD40 ligand enhanced activin A secretion. CD40 stimulation on APCs enhances additional co-stimulatory molecules CD80 and CD86, which interact with CD28 on T cells and further enhances antigen-specific T cell activation. Signaling through CD40 leads to the activation of nuclear factor (NF)-κβ in fibroblasts and monocytes (74;75), and AP-1 in B cells (76). As the 3' flanking region of the Inhba gene contains an AP-1 binding site, it is plausible that CD40 ligand/ CD40 mediated activin A induction is mediated by activation of AP-1 in combination with NFκβ (77). CD80/86 may participate in a positive-feedback loop of activin A secretion (73): CD40 ligand/ CD40 interactions between activated T cells and APCs increase CD80/86 expression on APCs (78), further activating T cells via interaction with the co-stimulatory molecule CD28. Blockade of CD80/86 on monocytes or stromal fibroblasts incubated with activated T cells leads to decreased activin A secretion (73). In sum, cross-linking CD40 on APCs leads to enhanced APC CD80/86 expression, and activin A production. Enhanced

CD80/86 expression promotes T cell activation translating to more activin A production by the APCs (73). Together, these data imply a link between activated T-cells and the induction of activin A by monocytes and stromal fibroblasts in inflammatory responses such as infection and immune disorders.

Activin A is secreted by mast cells subsequent to IgE receptor cross-linking. Multivalent binding of an antigen to receptor-bound IgE initiates sequential phosphorylation by protein tyrosine kinases, leading to Ca^{2+} release from intracellular stores and an increase in cytosolic Ca^{2+} concentration. Depletion of intracellular Ca^{2+} stores drives the influx of extracellular Ca^{2+} in which drives the production and secretion of multiple cytokines (79). Presumably, cross-linking of mast cell IgE receptors leads to elevated intracellular Ca^{2}+ concentration which, through the calmodulin pathway, increases JNK and p38 kinase activity and leads to activin A gene activation (80).

(c) Signaling pathways of activin A. Activins signal through a hetero-tetrameric receptor complex comprised of two ligand-binding type II receptors and two signal transducing type I receptors. Signaling is initiated through activin binding a type II receptor, such as ActRIIA and ActRIIB, and the subsequent recruitment of a type I receptor, such as ActRIa (ALK2) and ActRIb (ALK4) (70). The type II receptor phosphorylates the type I receptor on multiple serine and threonine residues within a unique GS rich region. There is a high degree of receptor promiscuity within the TGF-β super-family, as different ligands may signal through the same receptor. For example, bone-morphogenic protein (BMP)-2 and -7 signal through ActRIIA or ActRIIB in combination with BMPRI, and Nodal signals through ActRIIA, ActRIIB, and ActRIb. Due to this redundancy of

receptors, it is thought that specificity is conferred via accessory proteins or perhaps combinations of different receptor isoforms (70). Following phosphorylation, type I receptors transmit the signal intracellularly by activating members of the SMAD family, which then transmit the signal to the nucleus. Receptor-regulated SMADs (R-SMADs), such as SMAD2 and 3, are specifically recognized by type I receptors and are phosphorylated on their C-terminal sequences by activated type I receptors, releasing them from an auto-inhibitory configuration and resulting in SMAD2/3 activation. Inhibitory SMADs (I-SMADs), such as SMAD6 and 7, can bind and form stable complexes with type I receptors but cannot be activated, preventing activation of R-SMADs. Activated SMAD2/3 form a complex with common mediator SMAD (co-SMAD) 4 translocates to the nucleus. Unlike R-SMADs, co-SMADs are not directly phosphorylated by type I receptors and are probably required for the formation of a productive transcriptional complex rather than for the actual process of nuclear translocation. Both R-SMADs and co-SMADs participate in the recruitment of transcription factors and DNA binding. SMAD binding elements, which contain the consensus sequence GTCT, are often but not always present in activin-responsive genes. The low binding affinity and short recognition sequence of SMAD binding elements insinuates the necessity of other transcriptional co-activators. The best characterized co-activator is forkhead activin signal transducer (FoxH1), a transcription factor which binds constitutively to activin-response elements (ARE) but cannot initiate transcription on its own. Activin A signaling results in the nuclear translocation of a SMAD2 or 3 / SMAD4 complex, and FoxH1 interacts with either SMAD2 or 3 while SMAD4 contributes additional DNA binding specificity and transcriptional activation functions to ARE (70).

Activin-mediated signaling can be prevented by the decoy-receptor BAMBI; although activin can bind BAMBI, this decoy receptor does not contain an active signaling domain, thus truncating the signaling cascade. In addition, inhibins can bind the same receptors as activins, and inhibit activin-mediated signaling by simple out-competition of the activins for limited receptors. Finally, activin-mediated signaling can be inhibited by follistatin, which can bind activin and 'cloak' the receptor-binding sites thus neutralizing its activity (81). Interestingly, circulating activin appears to be bound irreversibly by follistatin (82) and for activin to have distant effects it would have to be released from follistatin by a proteolytic mechanism. To date, no such mechanism has been found and most literature instead focuses on the paracrine and autocrine effects of activin (70).

(d) *Effects of activin A.* The family of inhibins and activins were initially characterized as key-regulators of follicle-stimulating hormone secretion (70). Subsequently, they were demonstrated to be important in many tissues and cells for a myriad of other non-reproductive functions, such as mesoderm formation, cell proliferation and apoptosis, wound healing, fibrosis, and inflammation. These functions of activin are discussed in extensive detail elsewhere and will only be discussed briefly (70). Activin expression is induced by TGF-β, epidermal growth factor (EGF), and platelet-derived growth factor –d all of which are released by damaged platelets upon hemorrhage (70). In addition, activin stimulates the proliferation of keratinocytes (83). Unpublished observations within our own laboratory have shown that activin A is expressed in TGF-β treated human epithelial cells. Activin A is a potent stimulator of fibroblasts (84) and increases production of

extracellular matrix proteins and collagen (85), fibronectin, and α-smooth muscle actin. Combined with the fact that activin A also affects production and actions of matrix metalloproteinases (MMPs) such as MMP-2, this suggests that activin A could be involved in the creation of extracellular matrix and scar formation at multiple levels (86). Activin A released from mast cells may play a role in the process of airway remodeling in murine models of asthma by promoting the proliferation of airway smooth muscle (79). Finally, activin A was recently demonstrated to be secreted by α-CD3 activated T cells and to skew peritoneal MΦs towards an AMA-phenotype, as characterized by Arg1 induction (3).

1.10 JUSTIFICATION OF PROJECT

It is important to continually define and then justify the context in which our experimental-transplant observations are made, and two main points about the studies conducted within this project must be made. Firstly, although the immune system of the mouse is similar in many ways to that of a human, there are important key differences; namely, Arg1 is not a marker of AMA in the human (87). However, Arg1 is arguably the most reliable and frequently used marker of AMA in the mouse, and as such is valuable as a read-out of AMA induction in our mouse-based systems. Thus, information from the studies described within this work will enhance our current understanding of AMA-induction in the mouse and will be translatable to AMA in general in the human. Secondly, it is not known whether or not the induction of Arg1 in our murine model of

renal allograft rejection is a cause or effect of severe graft necrosis and accelerated rejection. Regardless, Arg1 is an important pathogenesis-associated transcript in our studies and a more thorough understanding of its regulation is important to creating a comprehensive picture of allograft rejection. On a more broad scale, dissecting the mechanism of Arg1 induction will enhance our understanding of AMA-induction. Thus, the purpose of this project is to investigate the nature of T cell interactions and products in regulating MΦ Arg1 expression and to relate these to the mechanism of transplant rejection and AMA-induction as a whole.

1.11 FIGURES

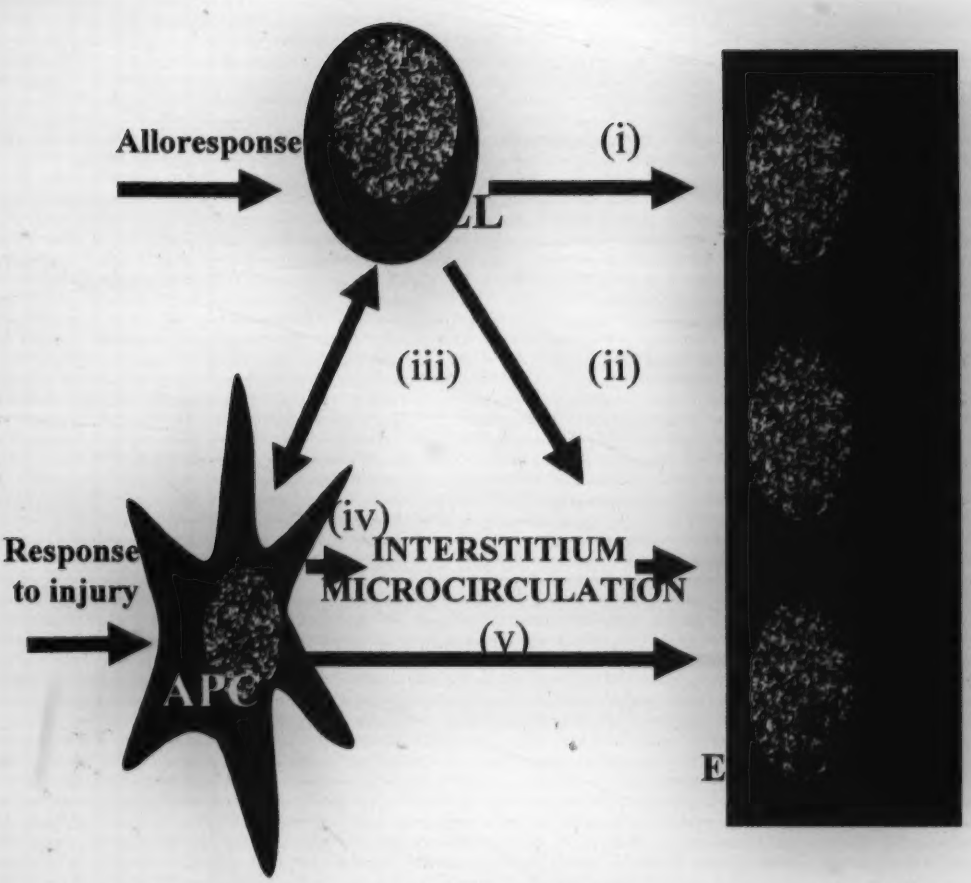

Figure 1a. General overview allograft rejection. Although the exact mechanism of rejection is not known, MΦ and T cells are the most abundant immune cells found infiltrating rejecting allografts. While largely dependent on T cells, cytolytic mediators like perforin are not essential for allograft rejection to occur. Our current view of rejection contends that effector T cells are activated in peripheral lymphoid organs upon encountering their cognate alloantigen. Activated T cells could then go on to (i) directly damage kidney epithelium, (ii) damage allograft microcirculation, and/ or (iii) activate APC. Activated APC could be activated as a non-specific response to tissue-injury incurred during transplantation or as a by-product of a specific allospecific immune response that includes specifically-activated T cells. Activated APC could then go on to (iv) damage allograft microcirculation and/ or (v) directly damage kidney epithelium.

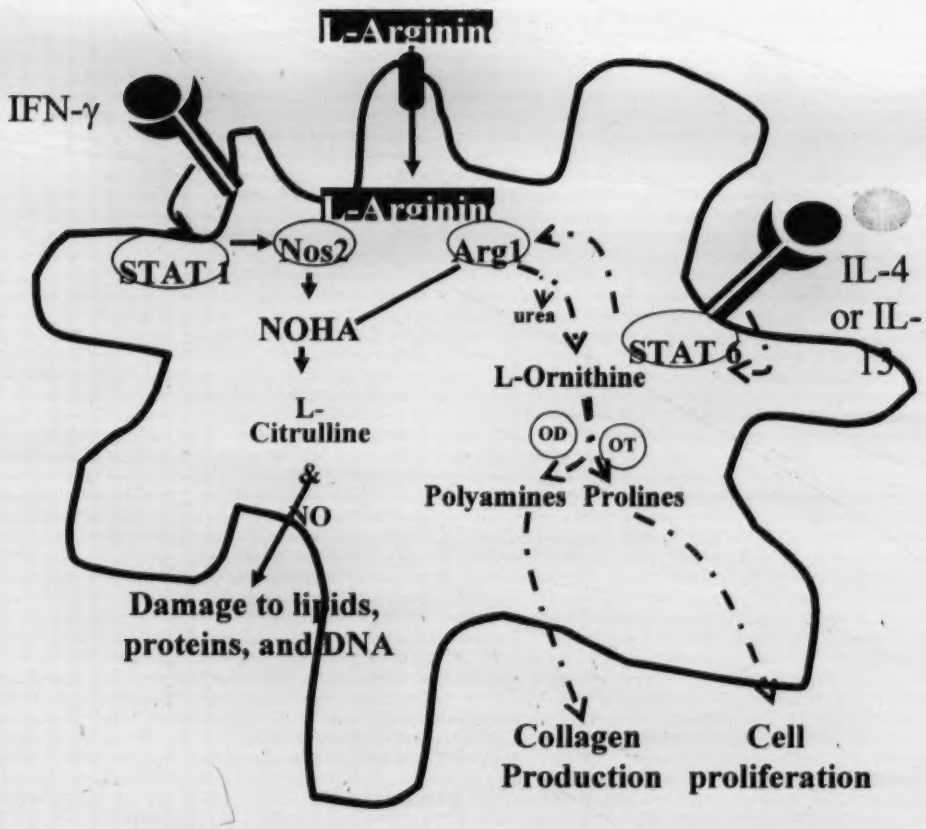

Figure 1b. Cartoon of the AMA/ CMA paradigm. L-Arginine is transported into the cell, where it is acted upon by nitric oxide synthetase (Nos2) or arginase1 (Arg1). Nos2 production is induced through a STAT1-dependent pathway instigated in response to IFN-γ. Nos2 acting on L-Arginine results in NG-hydroxy-L-arginine (NOHA) production and subsequent production of L-citrulline and nitric oxide which damage lipids, proteins, and DNA. Conversely, Arg1 production is induced through a STAT6-dependent pathway instigated in response to IL-4 and IL-13. Arg1 acting on L-Arginine results in the production of L-orthinine. Ornithine decarboxylase (OD) and ornithine aminotransferase (OT) convert L-orthinine to polyamines and prolines which play roles in collagen production and cell proliferation respectively.

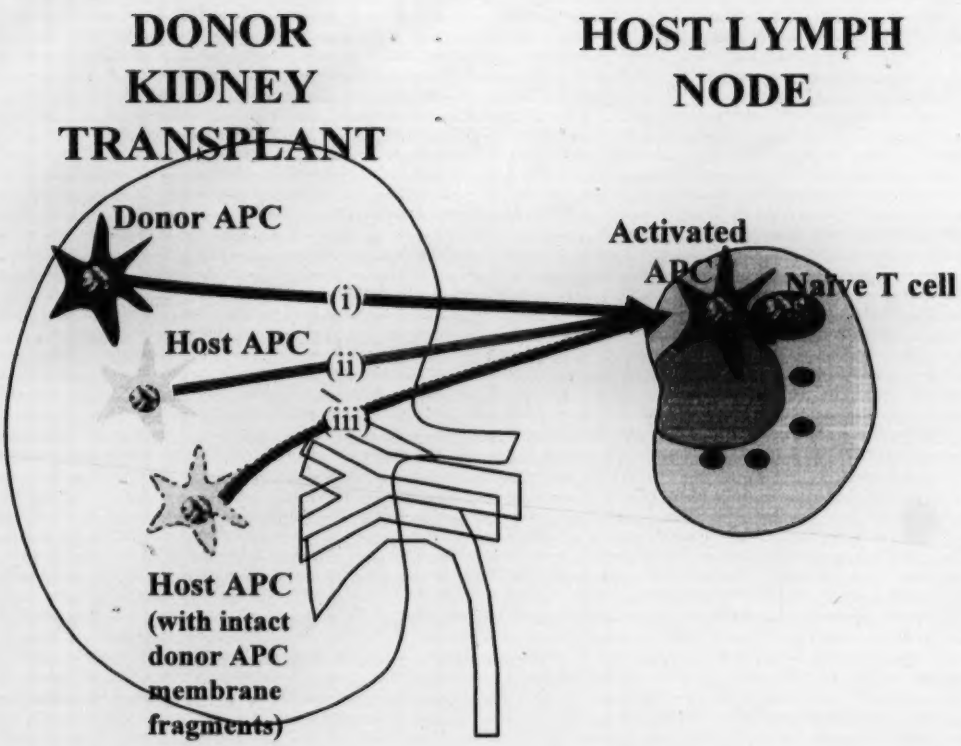

Figure 1c. Alloantigen recognition by T cells during the course of allograft rejection. Alloantigen recognition is generally grouped into three pathways: (i) Donor APC can enter host lymphoid organs and naïve host T cells recognize allogeneic MHC 'directly' on donor APC, (ii) Host APC can take-up graft-derived cells or released antigens and naïve host T cells 'in-directly' recognize allogeneic donor antigens in the context of donor APCs, and/ or (iii) Host APC could acquire donor APC membrane fragments, including allogenic MHC, and present this intact to naïve T cells in a 'combination' presentation pathway.

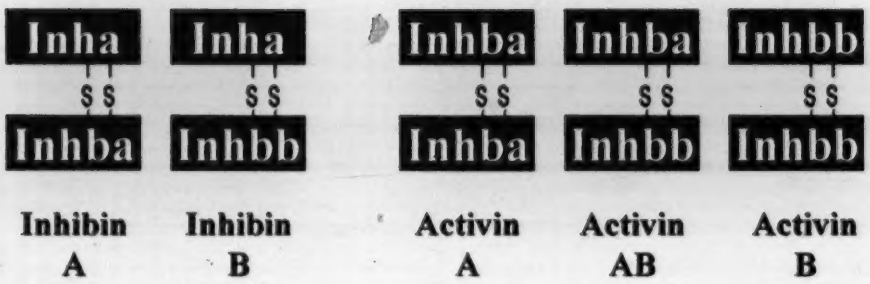

Figure 1d. General structure of the inhibins and activins. Both inhinins and activins are dimers of disulfide linked subunits; however, the inhibins are comprised of Inhb and Inha gene subunits while the activins are comprised of only Inhb gene subunits.

CHAPTER 2

MATERIALS AND METHODS

2.1 INTRODUCTION

In the following studies, I used a number of mouse strains and laboratory techniques. Our initial experiments focused on the importance of contact between macrophages (MΦ) and activated T cells (ATC), and I examined the effect of IFN-γ on *Arg1* induction using MΦ generated in either wild-type (WT) or *Ifng*$^{-/-}$ (GKO) BALB/c mice. In addition, I compared the cytokine profile of DBA/2 and WT BALB/c ATC. *Arg1* induction was compared in MΦs generated in WT or IL-4Rα$^{-/-}$ (IL-4R KO) BALB/c mice. Mice were obtained/ generated and housed as subsequently described. I used RAW264.7, a mouse MΦ-like cell line, in our initial optimization experiments and the acquisition and maintenance of this cell line will also be described in subsequent text.

I examined *Arg1* induction in MΦ by combining MΦs and ATC in an *in vitro* co-culture. MΦs were incubated with ATC in the same well under conditions that either facilitated or prevented direct-physical contact between the two cell types –'contact' or 'no contact' conditions respectively. MΦ were obtained from the peritoneal lavage fluid of thioglycollate-injected IL-4R KO or WT BALB/c mice, and ATC were generated from spleen homogenates of GKO or WT BALB/c mice. I also cultured MΦ with recombinant cytokines and neutralizing antibodies. From *in vitro* cultured cells, I extracted RNA, made corresponding cDNA, and quantified gene expression by real time polymerase

chain reaction (qRT-PCR). Surface expression of cellular markers was examined using flow cytometry. Cytokine levels in *in vitro* co- culture supernatant were measured with cytokine ELISAs.

Finally, I examined rejection in GRKO or WT CBA/J allogeneic kidneys transplanted into IL-4R$\alpha^{-/-}$ or WT BALB/c hosts by our laboratory. RNA was extracted from transplanted kidneys, cDNA prepared, and an Affymetrix microarray chip run. Gene expression was analyzed using software as described below.

2.2 REAGENTS, CELL CULTURE MAINTENANCE, AND MICE

(a) Reagents. Complete medium was comprised of RPMI medium supplemented with 2 mM L-glutamine, 10% fetal bovine serum, 1% non-essential amino acids, 1 % sodium-pyruvate, 1% antibiotic/ antimycotic (InVitrogen), and 50 μM β-mercaptoethanol. Easy-separation (Easy-sep) medium was made with HBSS, 2% fetal bovine serum, 2mM sterile EDTA (Sigma, St. Louis, MO), and 1% antibiotic/ antimycotic.

(b) Cell lines. The RAW264.7 (RAW) MΦ cell line was acquired from the American Type Culture Collection (ATCC, Rockville, MD). RAW cells were grown in tissue-culture treated 10 cm plates in complete media and passaged every three days. Similarly, primary cells were maintained in tissue culture-treated 10 cm plates and grown in complete media. All cells were incubated at 37°C at 5% CO_2.

(c) IFN-γ -/- (GKO), IL-4Rα$^{-/-}$ and WT BALB/c mice. To create the original GKO BALB/c mice, the IFN-γ gene was disrupted, a neomycin-resistance gene was inserted, and one copy of the wild-type gene was replaced with the modified gene in embryonic stem cells by homologous recombination. These stem cells were used to breed mice that were heterozygous for the disrupted gene (1). Heterozygous mice were intercrossed and offspring were selected for homozygosity (Health Sciences Laboratory Animal Services (HSLAS), University of Alberta) and IFN-γ -/- mice were identified by tail skin DNA testing. Offspring homozygosity was confirmed by additional tail skin testing. Homozygosity was confirmed in all IFN-γ -/- mice used (confirmation done by Joan Urmson). Heterozygous BALB/c mice were a generous gift from Dr. Tim Stewart (Genentech, South San Francisco, CA). Wild-type BALB/c mice were obtained from a breeding colony maintained by the University of Alberta's HSLAS or from the Jackson Laboratory (Bar Harbor, ME). IL-4Rα$^{-/-}$ BALB/c mice were also obtained from the Jackson Laboratory.

(d) Ifngr1$^{-/-}$ (GRKO) and WT CBA mice. GRKO/H-2$^{b/k}$ mice were generated by disrupting the Ifngr1 with an insertion of the neomycin-resistance gene into exon V, which encodes an extracellular domain. Dr. Michel Aguet (University of Zurich, Switzerland) provided us with homozygous GRKO/H-2$^{b/k}$ mice. GRKO (GRKO.IC5, CBA background) mice were obtained by crossing CBA mice with 129.GRKO/H-2$^{b/k}$ mice. The third homozygous generation was tested for homozygosity of the neomycin-resistance gene, the presence of H-2^{k}, and the absence of H-2^{b}. Since this time, our laboratory has maintained this strain by brother-sister mating. Wild-type CBA mice were used as

controls and were obtained from breeding colonies maintained by the University of Alberta's HSLAS.

(e) DBA2 mice. DBA2 mice were obtained from breeding colonies maintained by the University of Alberta's HSALS. All mice used in this project were male and were used for experimental purposes between 9 -12 weeks of age. Mice were maintained by the University of Alberta's Health Sciences Laboratory Animal Services, and all experimental procedures and housing conditions were in accordance with protocols enforced by Health Sciences Animal Policy and Welfare Committee of the University of Alberta. Animals were sacrificed after isoflurane (Halocarbon Laboratories, NJ, USA) anesthetization by cervical-dislocation.

2.3 RENAL TRANSPLANTATION AND SAMPLE PREPARATION

(a) Renal transplantation. As death of the mice precludes the study of pathology, our laboratory preformed renal transplantation in a non life-threatening transplant model as previously described and characterized (88). Briefly, donor kidneys were anastomosed heterotopically to the abdominal aorta and vena cava of recipient mice, without removing the recipient left kidney. All mice strain combinations were studied across full MHC disparities and compared to syngeneic controls. Immunosuppressive therapy was not used on any of the mice. At the time of harvesting, kidneys were examined histologically

and those exhibiting technical complications or infection were precluded from the study. Acceptable kidneys were snap frozen in liquid nitrogen and stored at -70°C.

(b) Microarrray pre-processing and analysis. RNA was extracted from kidneys using TRIzol™ reagent and purified using the RNAse Easy Mini kit (Qiagen). Our laboratory generated cDNA using a GeneChip Expression 3'-Amplification one-cycle cDNA synthesis kit (Affymetrix), followed by *in vitro* transcription labeling (Affymetrix). 15 μg of fragmented cRNA was run on a GeneChip Mouse Genome 430 2.0 Array (Affymetrix). Affymetrix® Moe 430 2.0 .cel files were pre-processed by robust multi-array analysis (RMA), and implemented in Bioconductor version 1.7, R version 2.2, in one batch. For each sample, there were at least three biological replicates with each sample composed of a pool of three mouse kidneys.

2.4 GENERATION OF PRIMARY IMMUNE CELLS AND *IN VITRO* CO-CULTURES

(a) Generation of activated T cells. ATC were generated from whole or CD3-enriched splenocyte preparations of WT BALB/c, GKO BALB/c, or DBA2 mice. Spleens were collected from mice and I prepared single-cell suspensions by pressing the spleens through a steel mesh, followed by red blood cell lysis using lysis buffer (0.15 M NH_4Cl, 1 mM $NaHCO_3$, 0.1 mM EDTA). Whole splenocyte preparations were subsequently resuspended at 2 x 10^6 cells/mL in 4 mL of complete media and activated at 37°C in α-

CD3 (7.5μg/well; eBioscience)-coated tissue culture-treated 6-well plates (BD Falcon). Plates were coated with antibody overnight at 4°C, and prior to use were blocked for three hours at room temperature with complete media. CD3+ splenocytes were enriched from whole spleen preparations by negative selection using magnetic beads (EasySep® Mouse T Cell Enrichment Kit; StemCell). I used flow cytometry to show that CD3+ cell purity was always between 96 – 99%. CD3+ splenocytes were activated in a manner similar to whole splenocyte preparations; however, 6-well plates were coated with α-CD3 (7.5 μg/well) and α-CD28 (3 μg/well; eBioscience). After 96 hours of stimulation by α-CD3, splenocytes were harvested for use in the *in vitro* contact assay.

(b) Generation of primary macrophages. Primary MΦs were generated by intra-peritoneal lavage of WT BALB/c or IL-4Rα$^{-/-}$ BALB/c mice that had been injected three days previously with 2mL of 4% Brewer's thioglycollate media (Sigma-Aldrich). For the intra-peritoneal lavages, I removed the fur and outer layer of the mouse's abdomen, and injected in 5 mL of EasySep media followed by 5 mL of air. After gently shaking the mouse, I removed fluid from the peritoneum with a syringe. Each 5 mL EasySep + 5 cc air wash was repeated a total of three times. F4/80^{+} cells were positively selected using magnetic bead separation using Biotin Selection Kit (StemCell) and biotinylated anti-F4/80 antibody (clone BM8, eBioscience). Purified cells were allowed to rest at 37°C in 100 mm tissue-culture treated plates for 2 days. By flow cytometry, I always observed F4/80+ cell purity between 95 -97%. Non-adherent cells were then washed away and the remaining cells were incubated at 37° C for 24 hours before use in the *in vitro* contact assay.

(c) In vitro co-cultures – ATC were incubated at 37°C with primary or RAW MΦs in tissue culture-treated 6-well plates containing immobilized α-CD3 (7.5μg/well). MΦs and ATC were incubated in a 2:1 ratio: I added 6 x 10^6 MΦs and 3 x 10^6 ATC to each well and incubated co-cultures at 37° C for 24 hours in complete RPMI media. In contact conditions, ATC were incubated in the same well as MΦs. In no-contact conditions, ATC were also incubated in the same well as MΦ, but MΦs and ATC were physically separated from each other by a 0.45 μm cell culture insert (BD Falcon).

(d) Recombinant cytokines and cytokine neutralizations. I dissolved recombinant activin A, IL-4, and IL-13 (R & D Systems) in 0.5% BSA in filter sterilized PBS and allowed the suspension to equilibrate for ten minutes at room temperature prior to aliquoting at the desired concentration. Samples were kept at -70°C until needed, and thawed slowly on ice prior to use in experiments. Cytokines were added at the indicated doses at time zero of each experiment.

I blocked CD94 and NKG2A/C/E using 10 μg/mL of anti-mouse CD94 (clone 18d3, eBioscience), and 10 μg/mL of anti-mouse NKG2A/C/E antibody (clone 20d5, eBioscience). Activin A was neutralized, , or in co-culture supernatant using 1.0 μg/mL of anti-activin A (Clone 69403R & D Systems) antibody. Antibodies were added to supernatant at time zero of co-culture.

2.5 CELL RNA EXTRACTIONS, REVERSE TRANSCRIPTASE POLYMERASE CHAIN REACTION, AND QUANTITATIVE REAL-TIME POLYMERASE CHAIN REACTION

I gratefully acknowledge Anna Hutton, Kara Allanach, and Stacey Lacoste for preparing and processing allograft tissue for microarray analysis. I preformed all other experiments discussed within this work.

(a) RNA extraction. Using TRIzol (Invitrogen), I extracted RNA from cells as per the manufacturer's directions. Briefly, after removal of supernatant of media from cells, I resuspended the cells in the residual volume of media and added 1 mL of TRIzol to the tube. After thoroughly vortexing the tubes, I froze the cell/TRIzol mixture at -20°C until RNA extraction using the RNAse Easy Micro kit (Qiagen) according to the manufacturer's directions.

(b)Reverse transcriptase polymerase chain reaction (RT-PCR). 0.5 μg of RNA were reverse transcribed in a 20 μL reaction containing 1X first strand buffer, 500 μM dNTPs, 2 μg BSA, 0.1 mM DTT, 200U M-MLV reverse transcriptase (Invitrogen), 3 ng/μL random primers and 32U RNAsin RNase inhibitor (Promega, Madison, WI). The reaction was held at 37 °C for 60 minutes before being heated to 95 °C for 5 minutes. 30 μL of RNAse-free water (AccuGene, Lonzo) was added to each resultant cDNA preparation to bring the total cDNA concentration to 10 ng/mL. UV absorbance was used to measure RNA yields, and RNA purity was assessed by the absorbance ratio at 260nm

and 280nm. RNA quality was assessed using the Agilent 2100 Bioanalyzer (Agilent Technologies, Palo Alto CA)

(c) Quantitative real time polymerase chain reaction (qRT-PCR). In triplicate, I amplified and detected cDNA on an ABI PRISM 7700 Sequence Detector (AB Applied Biosystems) with gene-specific primers and labeled probes (Table 2.1). In each 20 µl reaction was 1 x TaqMan Universal PCR Master Mix (AB Applied Biosystems), forward and reverse primers, and TaqMan quantification probe, each at their optimized concentrations, and 40 ng of cDNA template. PCR amplification conditions were as follows: 50°C for two minutes, 95°C for 10 minutes, then 40 cycles of 95°C for 15 seconds and 60°C for one minute. Amplification plots were constructed using ABI PRISM 7700 Sequence Detection System and software version 1.7 (PE Applied Biosystems). Threshold cycle numbers (Ct) were determined and transformed using the ddCt method as described by the manufacturer, using murine hypoxanthine phosphoribosyltransferase (mHPRT) as the internal reference.

Later on in this project, I used the ABI PRISM 7900 Sequence Detector (PE Applied Biosystems) to amplify and detect cDNA samples. In these cases, I used a 10 uL reaction and 40 ng of cDNA template and gene-specific primers with FAM- and VIC-labeled probes (Table 2.2). PCR amplification conditions were as follows: 50°C for two minutes, 95°C for 10 minutes, then 40 cycles of 95°C for 15 seconds and 60°C for one minute. All PCR reactions were performed in triplicate.

Finally, the following equation was used to express the relative amounts of mRNA as fold increase: $2^{-[(Ct\ target\ gene_X - Ct\ HPRT_X) - (Ct\ target\ gene_{calibr} - Ct\ HPRT_{calibr})]}$ where 'calibr'

refers to the values obtained from the unstimulated sample in the experiment. Alternately, I expressed relative amounts of mRNA as %HPRT: $2^{-[(Ct\ target\ gene_X - Ct\ HPRT_X)}$.

2.6 EXPERIMENTAL PROCEDURES ON CO-CULTURES

(a) Enzyme-Linked ImmunoSorbent Assay (ELISA). Cell culture supernatant cytokine levels were quantitated by ELISA using kits for mouse IL-4, IFN-γ (eBioscience), and IL-13 (R & D Systems) according to the manufacturer's instructions. In addition, I quantitated activin A levels in cell culture supernatants using monoclonal α-βA subunit antibody clone 69403 for the capture antibody at a concentration of 0.625 μg/mL, and biotinylated α-βA subunit antibody clone 69403 (R & D Systems) at a concentration of 0.25 μg/mL as the detection antibody (R & D Systems). Briefly, capture antibodies were diluted at the manufacturer's recommended concentration in PBS and immobilized onto Immunolon 4 HBX flat-bottomed 96-well plates (Dynatech Laboratories) at 4 °C overnight. Plates were washed once following antibody immobilization with wash buffer (0.5% PBS/Tween) and blocked with 200 μl of assay diluent (10% FBS in PBS for IL-4 and IFN-γ ELISAs, or 1% BSA in PBS for IL-13 and activin A ELISAs) between 1-2 hours at room temperature. Standards and samples were added and each well was topped up to a total volume of 100 μl per well. After incubation for 2 hours at room temperature, wells were rinsed three times with wash buffer prior to addition of detection antibodies. Detection antibodies were left on samples/ standards for one hour and, after three washes, avidin-HRP was added to each well at the recommended concentration.

Samples/ standards were incubated with avidin-HRP in the dark at room-temperature for 20 minutes and then washed three times prior to addition of TMB substrate (TetraMethylBenzidine, eBioscience). Following sufficient color development at room temperature, the reaction was stopped using 2 M H_2SO_4. Using a SPECTRAmax PLUS^{384} plate reader (Molecular Devices) I measured absorbance at 450 nm using 630 nm as a reference wavelength. Standards were plotted on a concentration versus absorbance plot and I used the linear equation of the line to determine sample concentration.

(b) Flow Cytometry. For each tube in flow cytometry experiments, $1x10^6$ cells were collected by centrifugation and washed in flow cytometry staining buffer (0.5% FBS, 0.5% EDTA, 0.05% sodium azide in PBS). To decrease the amount of non-specific staining, I blocked F_c receptors for five minutes at room temperature with anti-mouse CD16/32 (FcγRIII/II) antibody (eBioscience) prior to immunolabeling. I stained samples with various combinations of antibodies against cell-surface antigens for 20 minutes in the dark at room temperature. Antibodies, which included anti-CD3ε (clone 145-2C11), anti-Ly6G, anti-CD4, and anti-F4/80 (clone BM8). After staining, cells were washed with flow cytometry staining buffer and resuspended in PBS/1% paraformaldehyde. Cells were stored in the dark at 4˚C for no longer than 24 hours and then analyzed.

A FACScan or FACScalibur flow cytometer was used to analyze stained cell samples. I analyzed samples with the Research Edition of FCS Express, version 3 (De Novo Software, Los Angeles, California, U.S.A.).

(c) Intracellular cytokine staining: Cells of interest were stained for surface markers using the above flow cytometry protocol. Subsequently, cells were fixed with 100μL of fixative buffer (eBioscience) and incubated at room temperature in the dark for twenty minutes. After incubation, cells were centrifuged and the cell pellet was resuspended in 1 mL of permeabilization buffer (eBioscience). This step was repeated twice before final resuspension of the cell pellet in 100 uL of permeabilization buffer (eBioscience) and incubation at room temperature in the dark for 5 minutes. Biotinylated monoclonal anti-activin A antibody (R & D Systems, clone BAM3381) was added to cell suspensions at its optomized concentration and incubated at room temperature in the dark for twenty minutes. After incubation, cells were washed with 1 mL of permeabilization buffer (eBioscience) and steptavidin-PE (eBioscience) was added at 0.5 μg/ 10^6 cells. Following a twenty minute incubation at room temperature, cells were washed with 1 mL of permeabilization buffer (eBioscience) and left in 500 μL of fixation solution (eBioscience) for a maximum of twenty-four hours before being read on a FACScalibur flow cytometer.

(d) Statistical analysis. Statistical analyses were performed using Excel software. Student's *t*-test was used in the analysis of most experiments unless otherwise indicated.

2.7 TABLES

Table 2.1: Gene-specific primer and probe sequences used in quantitative RT-PCR studies using the ABI PRISM 7700 and 7900 Sequence Detector.

Primer/Probe	Sequence (5'-3')
Arg1 fwd	CAAGCCAAAGTCCTTAGAGATTATCG
Arg1 rev	CAGCAGACCAGCTTTCCTCAGT
Arg1 probe	AGCGCCTTTCTCAAAAGGACAGCCTCGA
Chi3L3 fwd	CCTCAACCTGGACTGGCAGTA
Chi3L3 rev	CTTGGAATGTCTTTCTCCACAGATT
Chi3L3 probe	TCAGTGTTCTGGTGAAGGAAATGCGTAAAGCT
Nos2 fwd	CTTTGACGCTCGGAACTGT
Nos2 rew	TGAAGTCATGTTTGCCGTC
Nos2 probe	GCAACATCAGGTCGGCCA
Emr1 fwd	TGTGGAAAGCACCATGTTAGCT
Emr1 rev	TCTGGCTGCCAAGTTAATGGA
Emr1 probe	TGATTCAGACGGAGTACCTAGACATCGAAAGCAAA
Tcrbv13 fwd	Applied Biosystems
Tcrbv13 rev	Applied Biosystems
Tcrbv13 probe	Applied Biosystems
Inhba fwd	Applied Biosystems, Assay on Demand, RefSeq: NM_008380.1
Inhba rev	Applied Biosystems, Assay on Demand, RefSeq: NM_008380.1
Inhba probe	Applied Biosystems, Assay on Demand, RefSeq: NM_008380.1
HPRT fwd	TGACACTGGTAAAACAATGCAAACT
HPRT rev	AACAAAGTCTGGCCTGTATCCAA
HPRT probe	TTCACCAGCAAGCTTGCAACCTTAACC

CHAPTER 3

EFFECTS OF T-CELL CONTACT ON MACROPHAGE ARGINASE-1 INDUCTION

3.1 ALTERNATIVE MACROPHAGE ACTIVATION MARKERS FOUND IN THE ALLOGRAFT DESPITE INTERFERON-γ.

Our laboratory has previously characterized a mouse model of kidney allograft rejection, where an allogeneic kidney is transplanted into a host that retains one native kidney (88). Using Genespring 7.3 software, we analyzed Affymetrix microarray data for expression of various genes on CBA/J kidneys transplanted into C57Bl/6 hosts. Gene expression was determined as fold-increase of raw signal compared to normal CBA kidney biopsies. CMA-associated transcripts Nos2 and Aif1 were expressed at high levels from days 5 through 42 post-transplant. In contrast, AMA-associated transcripts Arg1 and Mmp12 were initially expressed at low levels but gradually increased to the highest levels of expression by day 42 post-transplant (Figure 3a). The Th1 cytokine IFN-γ is a known inducer of CMA, and we used RT-PCR to confirm that Ifng gene expression was induced at time-points that correlate with high expression of CMA markers. On the other hand, Th2- cytokines like IL-4 and IL-13 are known inducers of AMA, and we confirmed that Il4 and Il13 gene expression was induced at time-points that correlated with high expression of AMA markers (Figure 3b). Interestingly, expression of AMA-markers was induced despite the concomitant high expression of Ifng, which the current paradigm of

macrophage activation predicts would inhibit AMA. I chose to focus on Arg1 induction as it is a well-characterized marker of AMA in the mouse (1). I hypothesized that manipulating conditions of contact between macrophages (MΦ) and activated T cells (ATC) would result in differential expression of Arg1, and lead to an explanation of allograft Arg1 expression in the allograft at time-points that correspond with high levels of Ifng transcripts.

3.2 ESTABLISHMENT OF MACROPHAGE/ T-CELL CO-CULTURES.

To test this hypothesis, I examined the induction of AMA marker Arg1 in macrophages that were incubated in 'direct contact' or 'no-contact' conditions with activated T cells. As discussed in the Materials and Methods section of this work, this was facilitated by the use of a cell-culture insert in an *in vitro* co-culture system that was carefully optimized.

I initially used RAW 264.7 cells, a MΦ cell line, or primary peritoneal MΦ subsequently in my experiments. Thioglycollate-induced peritoneal cells were generated in various mouse strains and harvested as previously described (85); however, to obtain high levels of purity I built and optimized an immunomagnetic bead-based system using biotin-conjugated antibodies and a biotin-positive selection kit (StemCell). Two strategies of purification were tested: (1) Positive selection of $F4/80^+$ cells from peritoneal lavage fluid using a biotinlylated α-$F4/80^+$ antibody, and (2) $F4/80^+$ cell enrichment by positive selection and removal of $Ly6g^+$, $CD19^+$, and CD3+ cells from peritoneal lavage fluid

using biotinlylated α-Ly6g, CD19, and CD3 antibodies, leaving behind a population which would presumably be MΦ. The first method of purification was used in subsequent experiments as it led to a higher yield and purity of $F4/80^+$ MΦ (Figure 3c).

ATCs were initially generated via mixed lymphocyte reactions (MLRs), where the responder BALB/c splenocytes were incubated with allogeneic B6 splenocytes. However, I ultimately abandoned MLRs due to poor yields and the lengthy generation time required for ATC. Instead I used whole-splenocyte cell suspensions that were activated for 96 hours with immobilized α-CD3 antibody, or $CD3^+$ enriched splenocyte preparations that were activated for 96 hours with immobilized α-CD3 and α-CD28 antibody (Figure 3d). Following initial activation, ATC were incubated with MΦ for 24 hours while concurrently being re-stimulated with α-CD3 antibody.

Each co-culture experiment included three replicate wells for each condition, and subsequent analyses was done in either triplicate (ELISA) or duplicate (RT-PCR). From each condition in the co-culture assay, supernatant was collected and analyzed using cytokine ELISA for the presence of IFN-γ, IL-4, and IL-13. In addition, RNA was extracted from cells in each culture condition, and I evaluated the expression of gene markers of MΦ activation (Arg1, Nos2) under each condition using RT-PCR.

3.3 MACROPHAGE ACTIVATION IN MACROPHAGE/ ACTIVATED T CELL CO-CULTURES.

Initial co-culture experiments were preformed using RAW264.7 MΦ and ATC generated from whole splenocytes (n = 4). All experiments are summarized in Table 3.1; however, a representative experiment is shown in figure 3e. I extracted RNA from the cells in each culture condition, and after synthesizing corresponding cDNA, I used RT-PCR to examine expression of macrophage activation genes. Compared to MΦ incubated alone, MΦ incubated in direct-contact with whole ATC had an Arg1 fold-induction of 622 ± 18, and MΦ incubated under no-contact with ATC had an Arg1 fold-induction of 76 ± 28. Despite Arg1 induction in both conditions, Arg1 induction under direct-contact conditions was statistically higher than Arg1 induction under no-contact conditions ($p < 0.005$). I examined whether Arg1 was also induced in T cells after MΦ interaction. This was done by examining induction of Arg1 expression in no-contact co-cultured ATCs by collecting cells on the ATC side of the cell-impermeable insert. Arg1 was not induced in ATCs incubated alone, similar to results observed with MΦ alone.

My results suggested that MΦ Arg1 expression was being induced in MΦ by a T cell-associated molecule or secreted product. I confirmed this by repeating the co-culture experiments with purified CD3+ cells. Finally, I repeated the co-culture experiments using primary MΦ, instead of a MΦ cell line, and ATC derived from whole-splenocytes and $CD3^+$ enriched splenocytes. Induction of Arg1 expression was higher in direct-contact conditions than in no-contact conditions when I used primary MΦ, and when I used $CD3^+$-enriched ATC and RAW MΦ (Table 3.2). However, this difference was only

significant in RAW MΦ/ $CD3^+$-enriched ATC co-cultures ($p < 0.005$) and in primary MΦ/ whole ATC co-cultures ($p < 0.05$) but not in primary MΦ/ $CD3^+$-enriched ATC co-cultures ($p>0.05$).

I also examined Ym1 expression, another marker of AMA, in co-cultured MΦ. As shown in Figure. 3f, Ym1 gene expression was not readily detectable in co-cultured cells. Finally, I examined Nos2 induction in co-cultured MΦ. Nos2 was induced under both direct-contact (74.7 ± 10.0) and no-contact conditions (130.1 ± 27.5). Nos2 expression did not vary in direct-contact and no-contact conditions and I henceforth focused on Arg1 induction.

3.4 THE CYTOKINE PROFILE IN MACROPHAGE/ ACTIVATED T CELL CO-CULTURE SUPERNATANT.

Using cytokine ELISA, I found that IL-4 was present in very low levels, if at all, in supernatant of any of the culture conditions. In the representative experiment shown in Figure 3g, IL-4 was not detectable in the supernatant of direct-contact cultures, no-contact cultures, or MΦ-only cultures, but was present at a concentration of 147 ± 18 pg/mL in T cell-only cultures. I could not detect IL-13 in MΦ-only cultures, but I determined the concentrations in direct-contact, no-contact, and T-cell only cultures to be 1392 +/- 215, 1056 ± 284, and 9568 ± 621 pg/mL respectively. IL-13 concentration was similar in the supernatant from direct-contact and no-contact co-cultures, but was higher in T-cell only cultures ($p<0.005$). I detected IFN-γ in a pattern similar to IL-13. That is,

IFN-γ was not detectable in MΦ-only cultures, but the concentrations in direct-contact, no-contact, and T-cell only cultures were 4081 ± 377, 4591 ± 247, and 6128 ± 175 pg/mL, respectively. As shown in Table 3.3, I obtained similar results in co-cultures with primary MΦ and/ or ATC generated from CD3+ enriched splenocyte preparations.

3.5 EFFECT OF INTERFERON-γ ON CO-CULTURE MACROPHAGE ARGINASE-1 INDUCTION.

My initial hypothesis stemmed from the observation that Arg1 expression was induced in the rejecting allograft despite concomitant high Ifng expression. I further examined this phenomenon *in vitro* by incubating RAW264.7 cells in co-culture with BALB/c Ifng$^{-/-}$ (GKO) ATC (n = 2). Importantly, prior to conducting this set of experiments my laboratory switched from the ABI PRISM 7700 Sequence Detector to the ABI PRISM 7900 Sequence Detector and the overall magnitude of Arg1 expression was consistently lower than seen previously. As a control, I examined Arg1 induction in RAW MΦ/ WT ATC co-cultures and I observed that, despite lower total detection, Arg1 was induced in the same pattern between co-culture conditions as seen previously. Arg1 expression was low in RAW264.7 or ATC alone (GKO or WT) cultures. Arg1 expression was induced in direct-contact (26 ± 4) and no-contact (11 ± 2) conditions in WT ATC co-cultures (Figure 3h). In GKO ATC co-cultures, Arg1 expression was also induced in direct-contact and no-contact conditions; however, Arg1 expression was similar in both conditions: Arg1 expression was induced 33 ± 9 fold in direct-contact conditions and 22

± 2 fold in no-contact conditions. That is, in the absence of IFN-γ, contact between MΦ and ATC does not enhance Arg1 expression to the same extent as it does in co-culture conditions where IFN-γ is present. Two independent experiments indicated that contact between MΦ and GKO ATC does not enhance induction of Arg1 expression (Table 3.4).

3.6 EFFECT OF INTERFERON-γ ON CYTOKINE PROFILE IN MACROPHAGE/ ACTIVATED T CELL CO-CULTURE SUPERNATANT.

I examined IL-4, IL-13, and IFN-γ levels in GKO ATC co-cultures (Figure 3i). MΦ-only cultures did not contain detectable levels of any of these cytokines. IL-4 was present in co-culture supernatants in direct-contact (190 ± 38), no-contact (364 ± 14), and T cell-only cultures (867 ± 63). IL-13 was also present in direct-contact, no-contact, and T cell-only cultures in GKO co-cultures at high levels (18,269 ± 1278, 15,121 ± 924, and 32,824 ± 492 pg/mL respectively). As expected, IFN-γ was not detectable in any condition of the GKO ATC co-cultures.

3.7 EFFECT OF H2-T23 ON CO-CULTURE MACROPHAGE ARGINASE-1 INDUCTION.

Observations from WT co-cultures suggested that, in the presence of IFN-γ, contact between ATC and MΦ enhanced MΦ Arg1 induction. Observations previously

made in our laboratory indicated a possible role for H2-T23 (Qa1) in Arg1 induction. I examined the role of CD94/ NKG2A/C/E, the receptors for H2-T23, in Arg1 induction. DBA2 mice are CD94 deficient and unable to express NKG2A/C/E. I repeated the co-culture assays using BALB/c or DBA/2- derived whole splenic ATC. I used RAW264.7 cells in place of primary MΦs in these co-cultures, keeping MΦ type homogenous and ensuring that I only examined the effects of ATC CD94/ NKG2A/C/E on Arg1 induction in MΦ, and not differential responses of BALB/c WT MΦ versus DBA/2 MΦs. In addition, co-cultures using RAW264.7 MΦ are not allogeneic: RAW264.7 cells match to both BALB/c and DBA2 cells at MHC loci.

Arg1 fold-induction in RAW264.7 MΦ/ BALB/c WT ATC co-cultures was significantly higher in direct-contact co-cultures than in no-contact co-cultures (912 ± 38 and 120 ± 20 respectively; (Figure3j). In RAW264.7 MΦ/ DBA/2 ATC co-cultures, Arg1 fold-induction was not significantly enhanced in direct-contact conditions (1189 ± 47) compared to in no-contact conditions (841 ± 58). In sum, in co-cultures where CD94/ NKG2A/C/E was absent, contact between ATC and RAW264.7 cells did not significantly enhance Arg1 induction.

3.8 EFFECT OF H2-T23 ON CYTOKINE PROFILE IN MACROPHAGE/ ACTIVATED T CELL CO-CULTURE SUPERNATANT.

I examined IL-4, IL-13, and IFN-γ levels in DBA2 co-cultures (Figure 3k). None of these cytokines were detectable in RAW264.7-only cultures. Unlike BALB/c WT co-

cultures (Figure 3g), IL-4 was detectable in DBA/2 co-cultures in direct-contact (403 ± 3 pg/mL), no-contact (392 ± 4 pg/mL), and T cell-only cultures (1023 ± 6 pg/mL). IL-13 was also detectable in direct-contact, no-contact, and T cell-only cultures: 9098 ± 95, 5854 ± 1419, and 28485 ± 1552 pg/mL respectively. Finally, IFN-γ was detectable in direct-contact (2539 ± 6 pg/mL), no-contact (2404 ± 30 pg/mL), and T cell-only cultures (2451 ± 16 pg/mL) in DBA/2 co-cultures.

3.9 NEUTRALIZING α-CD94 AND α-NKG2/A/C/E ANTIBODIES DO NOT INCREASE IL-4 PRODUCTION BY ACTIVATED BALB/C T CELLS.

Interestingly, when I examined the cytokine milieu in DBA2 co-culture supernatants, both IL-4 and IFN-γ were present at high levels. In contrast, BALB/c WT co-culture supernatant contained low levels of IL-4 and high levels of IFN-γ (Figure 3k versus Figure 3j). I postulated that the absence of CD94, and hence NKG2A/C/E, on DBA2-derived ATC led to increased levels of IL-4 in DBA2 co-culture supernatants. To mimic the effects of CD94 deficiency, I analyzed IL-4 supernatant levels in *in vitro* cultures of α-CD3 activated BALB/c ATC after 24-hours of further activation by α-CD3. Cultures were left untreated, were treated with the appropriate isotype control antibody, or with neutralizing α-CD94 or α-NKG2A/C/E antibody. I was not able to detect IL-4 in any of the cultures. Altogether, my CD94 and NKG2A/C/E neutralization studies suggest that the absence of CD94 on DBA2 ATC does not play a role in the increased IL-4

production by DBA2 ATC, compared to BALB/c WT ATC and further studies are required to fully understand this phenomenon.

3.10 TABLES

Table 3.1. Summary of Arg1 induction in co-culture experiments using RAW MΦ and whole ATC. MΦ and ATC were incubated together in direct-contact conditions or in no-contact conditions where the cells were physically separated by a cell-culture insert. Whole ATC were generated from α-CD3 antibody activated whole BALB/c WT splenocyte single cell suspensions. Induction of Arg1 transcripts is expressed as fold-increase over Arg1 expression in RAW MΦ-only cultures. Each row represents an independent experiment; all experiments (n= 4) included triplicate experimental conditions and Arg1 transcripts are quantified by RT-PCR in duplicate ± standard error. Arg1 transcripts in direct-contact conditions are significantly more abundant ($p < 0.005$) than in no-contact conditions in all experiments.

ATC and MΦ: direct-contact	ATC and MΦ: no contact
809	221
622 ± 18	76 ± 28
912 ± 38	120 ± 20
26 ± 4	11 ± 2

Table 3.2. Summary of Arg1 induction in co-culture experiments using RAW or primary MΦ and/ or 'whole' or $CD3^+$ ATC. As before, MΦ and ATC were incubated together in direct-contact conditions or in no-contact conditions. Primary MΦ were generated from $F4/80^+$-enriched BALB/c WT thioglycollate-elicited peritoneal cells, and $CD3^+$ ATC were generated from $CD3^+$-enriched whole BALB/c WT splenocyte single cell suspensions. Induction of Arg1 transcripts is expressed as fold-increase over Arg1 induction in RAW MΦ-only cultures. All results are representative of triplicate experimental conditions and Arg1 transcripts are quantified by RT-PCR in duplicate ± standard error. Arg1 transcripts in direct-contact conditions are significantly more abundant with $p < 0.005$ than in no-contact conditions when indicated by *, or with $p < 0.05$ when indicated by **.

MΦ and ATC type	ATC and MΦ: direct-contact	ATC and MΦ: no contact
RAW MΦ & $CD3^+$-enriched ATC	8207 ± 101*	1530 ± 465*
Primary MΦ & 'whole' ATC	1844 ± 517**	343 ± 7**
Primary MΦ & $CD3^+$-enriched ATC	1922 ± 770	924 ± 167

Table 3.3. Summary of IL-4, IL-13, and IFN-γ levels in co-culture supernatant in experiments using RAW or primary MΦ and/ or 'whole' or $CD3^+$ ATC. Cytokine levels are shown in pg/mL for conditions where MΦ and ATC were incubated in direct-contact conditions, in no-contact, or in instances where ATC were incubated alone. IL-4, IL-13, and IFN-γ levels were zero in every instance for MΦ-only cultures and are not shown. Results are the average of triplicate ELISA analyses of triplicate experimental replicates and are shown ± standard error. n/d indicates 'not-done' as the cytokine ELISA was not available at the time of the experiment.

	ATC and MΦ: direct-contact			**ATC and MΦ: no contact**			**ATC only**		
MΦ and ATC type	IL-4	IL-13	IFN-γ	IL-4	IL-13	IFN-γ	IL-4	IL-13	IFN-γ
RAW MΦ & 'whole' ATC	0 ± 20	1392 ± 215	2141 ± 78	0 ± 20	1056 ± 284	2066 ± 110	147 ± 18	9568 ± 621	2361 ± 70
Primary MΦ & 'whole' ATC	0 ± 59	876 ± 75	3630 ± 251	26 ± 22	319 ± 61	3721 ± 82	422 ± 210	1900 ± 134	3777 ± 199
Primary MΦ & $CD3^+$-enriched ATC	0 ± 9	n/d	3268 ± 67	8 ± 45	n/d	3378 ± 186	924 ± 167	n/d	3732 ± 230

Table 3.4. Summary of Arg1 induction in co-culture experiments using RAW MΦ and whole BALB/c WT or BALB/c Ifng$^{-/-}$ (GKO) ATC. MΦ and ATC were incubated together in direct-contact conditions or in no-contact conditions. Induction of Arg1 transcripts is expressed as fold-increase over Arg1 induction in RAW MΦ-only cultures. All results are representative of triplicate experimental conditions and Arg1 transcripts are quantified by RT-PCR in duplicate ± standard error. Arg1 transcripts in direct-contact conditions are significantly more abundant with $p < 0.05$ than in no-contact conditions for each type of ATC when indicated by *.

	ATC and MΦ: direct-contact		**ATC and MΦ: no contact**	
	WT	GKO	WT	GKO
Experiment 1	14 ± 3*	15 ± 3	5 ± 1*	8 ± 1
Experiment 2	26 ± 4*	33 ± 9	11 ± 2*	22 ± 2

3.11 FIGURES

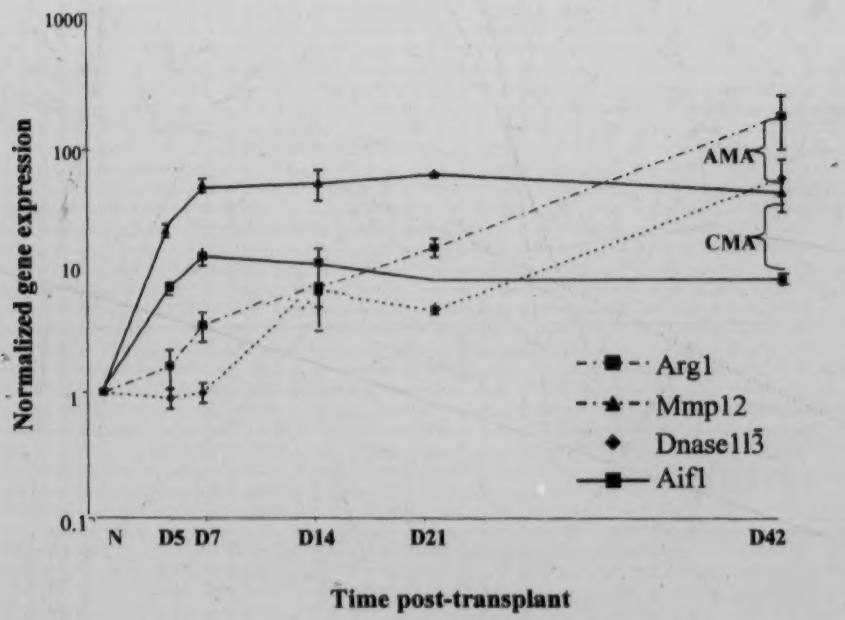

Figure 3a. Time-course of macrophage activation-associated cytokine transcripts in CBA kidney allografts transplanted into B6 hosts. RNA was extracted from kidney allografts at the indicated days and we examined gene markers of CMA (Dnase1l3, Aif1) or AMA (Arg1, Mmp12) using microarray chip analysis. Gene expression was normalized against non-transplanted (N) CBA kidneys (n=3). For each graph, numbers represent mean expression of each sample pool (n=3) ± standard error.

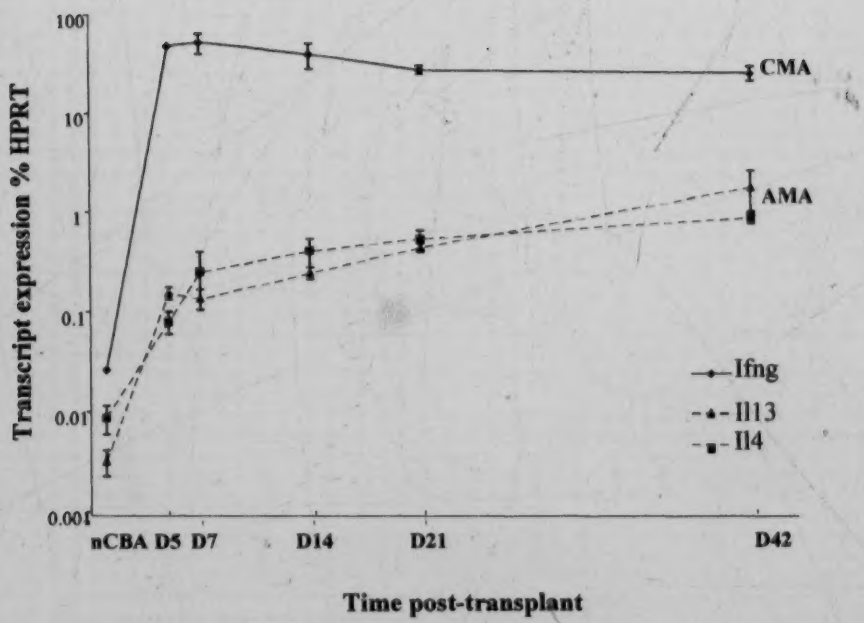

Figure 3b. Time-course of macrophage activation-associated transcripts in CBA kidney allografts transplanted into B6 hosts. We extracted RNA from kidney allografts at the indicated days and we examined gene expression of inducers of CMA (Ifng) or AMA (Il4, Il13) using RT-PCR analysis where expression of each gene is shown as percent HPRT. For each graph, numbers represent mean expression of each sample pool (n=3) ± standard error.

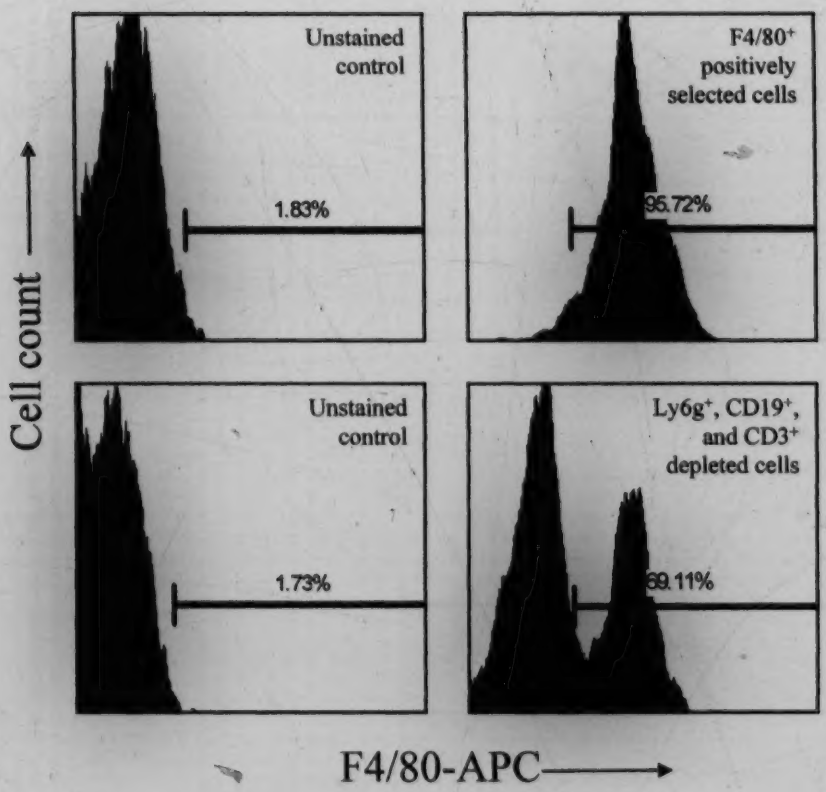

Figure 3c. Flow cytometric analysis of F4/80$^+$ purity in mouse peritoneal preparations following two different methods of macrophage purification. Unstained negative controls are shown for each method of purification: Peritoneal preparations were either postively selected for F4/80$^+$ cells using a biotinylated F4/80$^+$ antibody, or depleted of Ly6g$^+$, CD19$^+$, and CD3$^+$ cells using a cocktail of the appropriate biotinylated antibodies. Graphs shown are within a leukocyte gate that is based on side- and forward-scatter properties and show percent of F4/80$^+$ cells.

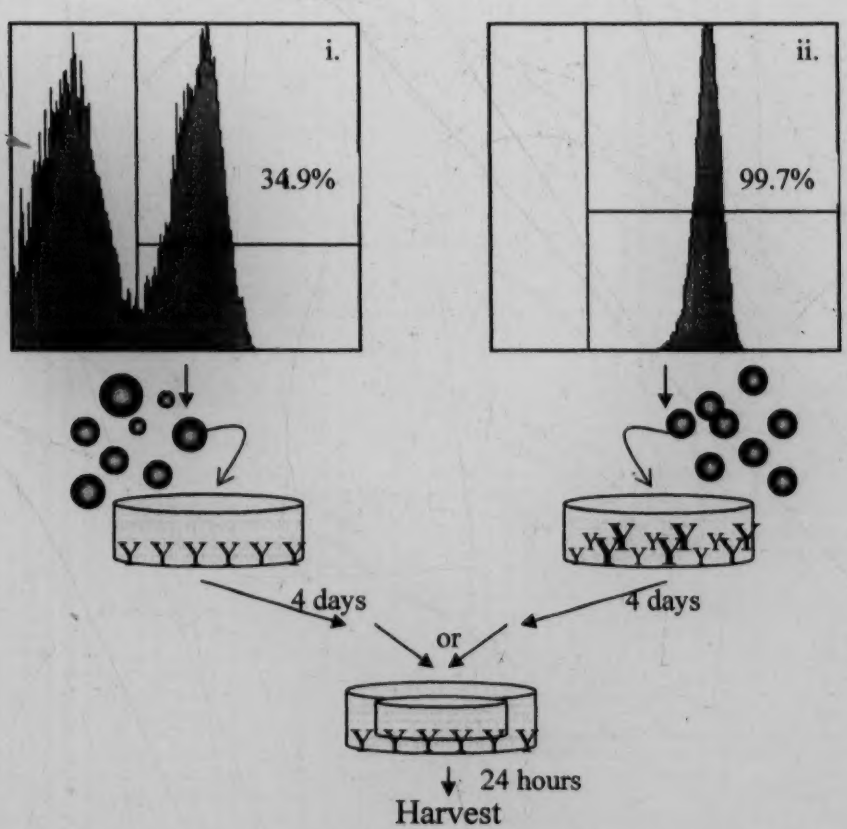

Figure 3d. Whole or $CD3^+$-enriched ATC used used in the co-culture assay. Flow cytometric analysis of % $CD3^+$ purity in BALB/c WT mouse splenocytes in whole suspensions (i) and in $CD3^+$-enriched suspensions (ii). Graphs shown are within a leukocyte gate that is based on side- and forward-scatter properties Whole ATC were stimulated for 4 days with 7.5μg of immobilized α-CD3 antibody, while $CD3^+$-enriched ATC were stimulated with 7.5μg of immobilized α-CD3 and 3μg of immobilized α-CD28 antibody. Subsequently, whole or $CD3^+$ ATC were re-stimulated with α-CD3 antibody for 24 hours whilst concurrently being incubated with macrophages.

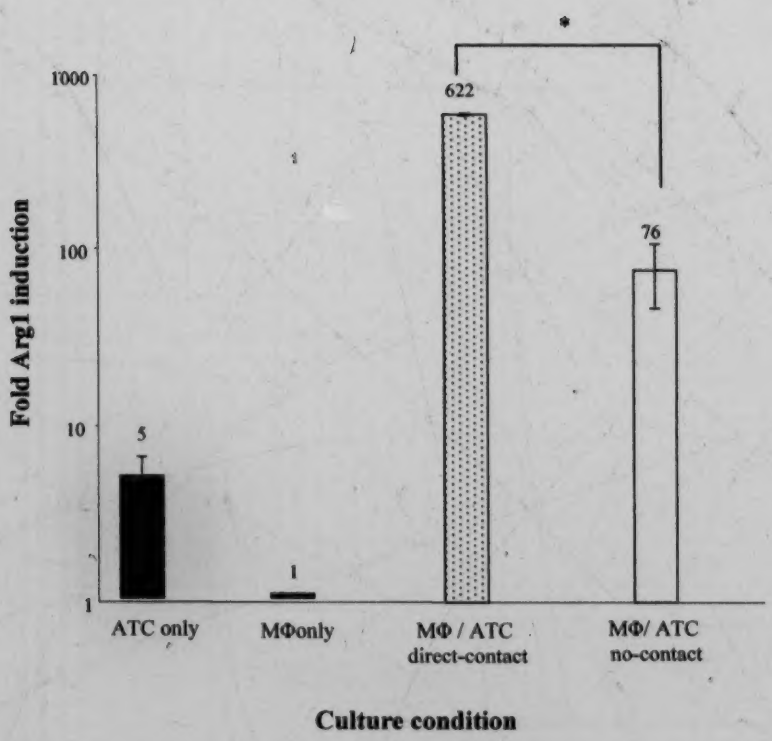

Figure 3e. Quantitative RT-PCR of AMA marker Arg1 in RAW MΦ/ whole ATC co-cultures. RNA was extracted from adherent cells under each *in vitro* co-culture assay condition and cDNA was prepared prior to quantification of Arg1 transcripts by RT-PCR using the ABI PRISM 7700 Sequence Detector. Induction of Arg1 expression in direct-contact (DCt = 17.9) and no-contact (DCt = 20.4) conditions was expressed as fold-increase compared to expression observed in RAW Mϕ -alone (DCt = 25.5) cultures. Data is ± standard error and is representative of three replicates for each condition followed by duplicate quantitative RT-PCR analysis for each replicate. Cytokine levels are significantly different, as determined by a student's T-test, at $p < 0.005$ between culture conditions where indicated by *.

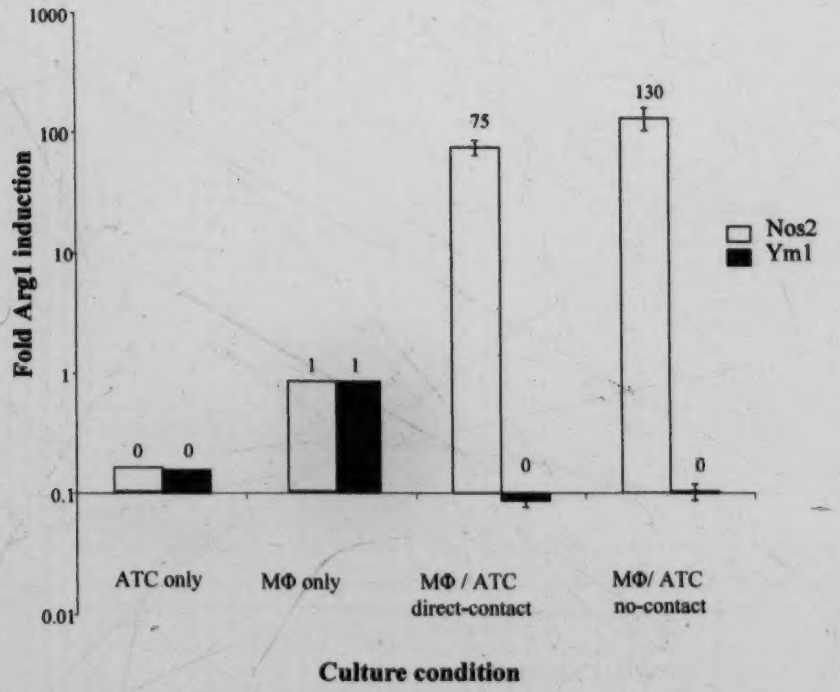

Figure 3f. Quantitative RT-PCR of AMA marker Ym1 and CMA marker Nos2 in RAW MΦ/ whole ATC co-cultures. RNA was extracted from adherent cells under each *in vitro* co-culture assay condition and cDNA was prepared prior to quantification of mRNA transcripts by RT-PCR using the ABI PRISM 7700 Sequence Detector. Induction of transcript expression was expressed as fold-increase compared to expression observed in RAW Mϕ -alone (DCt = 24.9 and 23.6 for Nos2 and Ym1, respectively) cultures. Data is ± standard error and is representative of two replicates for each condition followed by duplicate quantitative RT-PCR analysis for each replicate.

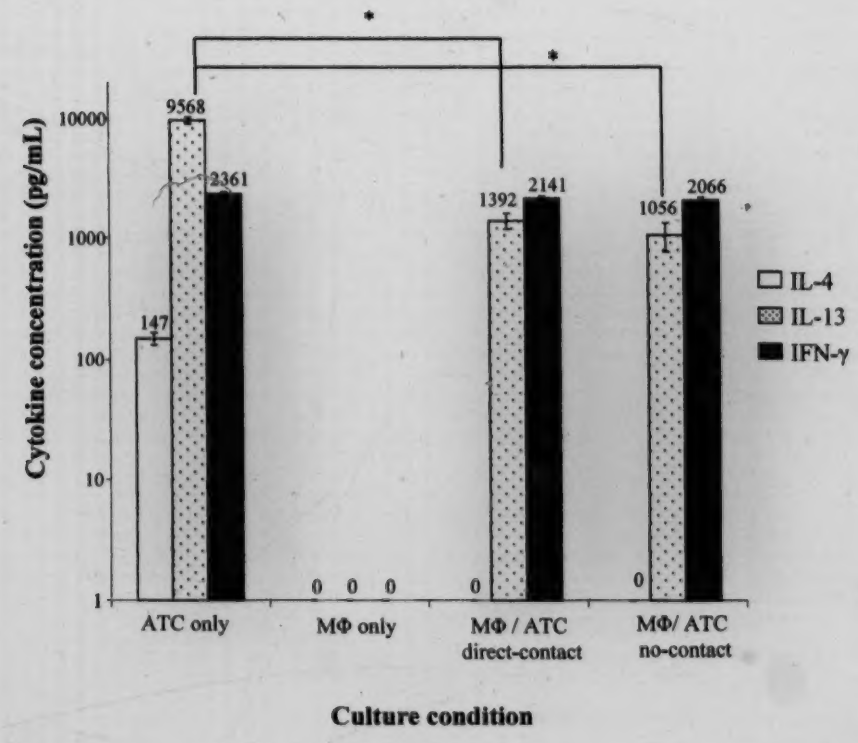

Figure 3g. ELISA analysis of cytokine levels in RAW MΦ / BALB/c WT ATC co-culture supernatant. Supernatants from co-cultures were examined for IL-4, IL-13, and IFN-γ levels in pg/mL. Each bar represents the average of triplicate ELISA analysis for each of two biological replicates and is shown ± standard deviation. Cytokine levels are significantly different, as determined by a student's T-test, at $p < 0.005$ between culture conditions where indicated by *.

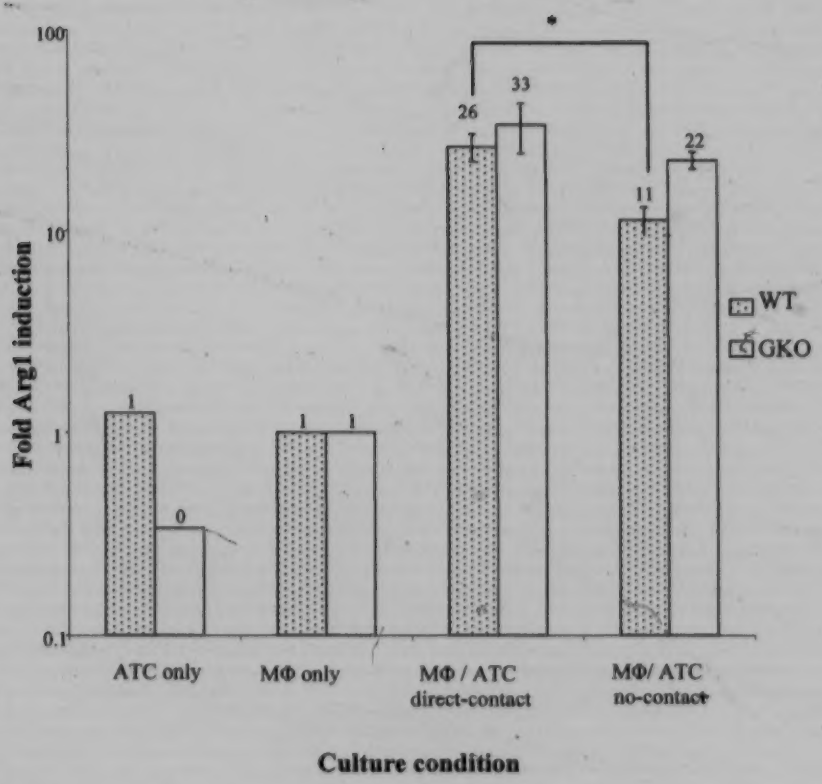

Figure 3h. Quantitative RT-PCR of AMA marker Arg1 in RAW MΦ/ whole BALB/c WT or GKO ATC co-cultures. RNA was extracted from adherent cells under each *in vitro* co-culture assay condition and cDNA was prepared prior to quantification of Arg1 transcripts by RT-PCR using the ABI PRISM 7900 Sequence Detector. Induction of Arg1 expression in WT ATC direct-contact (DCt = 20.9) and no-contact (DCt = 22.2) conditions and GKO ATC direct-contact (DCt = 20.4) and no-contact (DCt = 20.6) conditions was expressed as fold-increase compared to expression observed in RAW Mϕ -alone (DCt = 25.8) cultures. Data is ± standard error and is representative of three replicates for each condition followed by duplicate quantitative RT-PCR analysis for each replicate. Cytokine levels are significantly different, as determined by a student's T-test, at $p < 0.05$ between culture conditions where indicated by *.

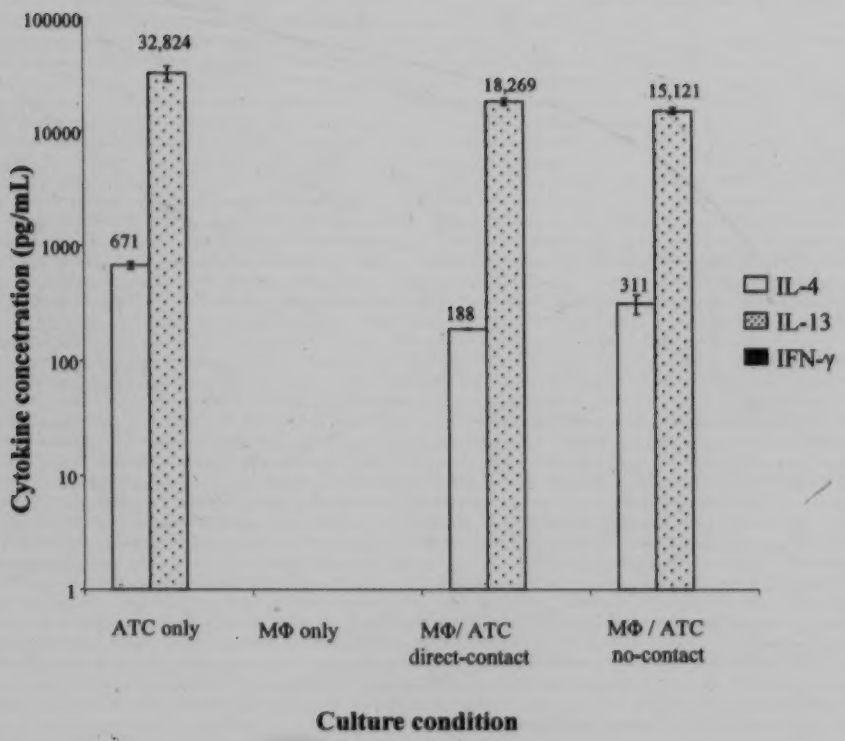

Figure 3i. ELISA analysis of cytokine levels in RAW MΦ/ BALB/c GKO 'whole' ATC co-culture supernatant. Supernatants from co-cultures were examined for IL-4, IL-13, and IFN-γ levels in pg/mL. Each bar represents the average of triplicate ELISA analysis for each of three biological replicates and is shown ± standard deviation.

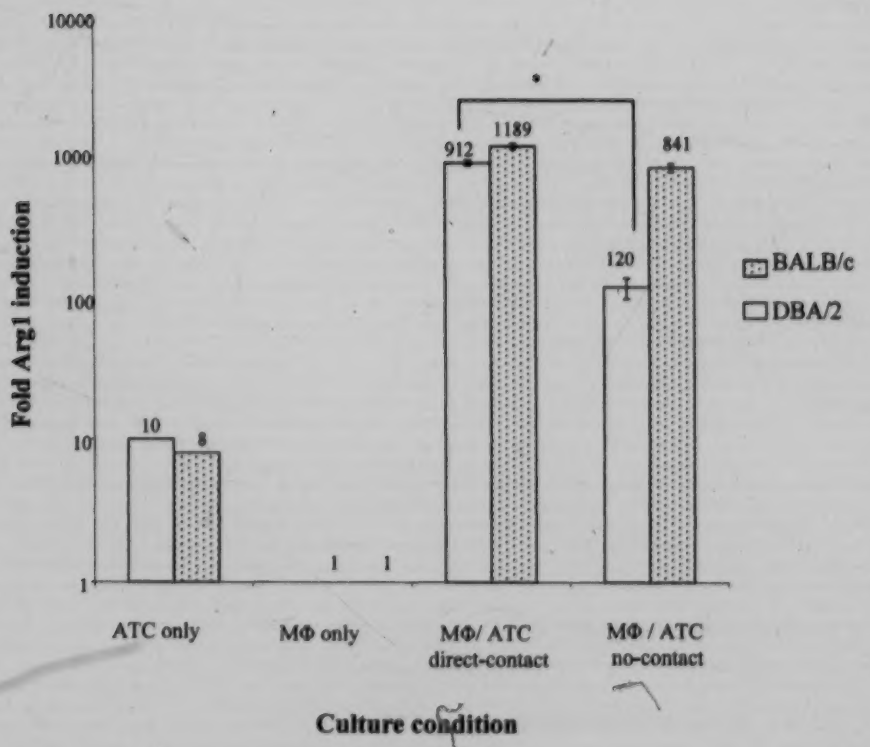

Figure 3j. Quantitative RT-PCR of AMA marker Arg1 in RAW MΦ/ whole BALB/c or DBA/2 ATC co-cultures. RNA was extracted from adherent cells under each *in vitro* co-culture assay condition and cDNA was prepared prior to quantification of Arg1 transcripts by RT-PCR using the ABI PRISM 7700 Sequence Detector. Induction of Arg1 expression in BALB/c ATC direct-contact (DCt = 17.2) and no-contact (DCt = 19.1) conditions and DBA/2 ATC direct-contact (DCt = 16.0) and no-contact (DCt = 16.2) conditions was expressed as fold-increase compared to expression observed in RAW MΦ -alone (DCt = 24.7) cultures. Data is ± standard deviation and is representative of two replicates for each condition followed by duplicate quantitative RT-PCR analysis for each replicate. Cytokine levels are significantly different, as determined by a student's T-test, at $p < 0.005$ between culture conditions where indicated by *.

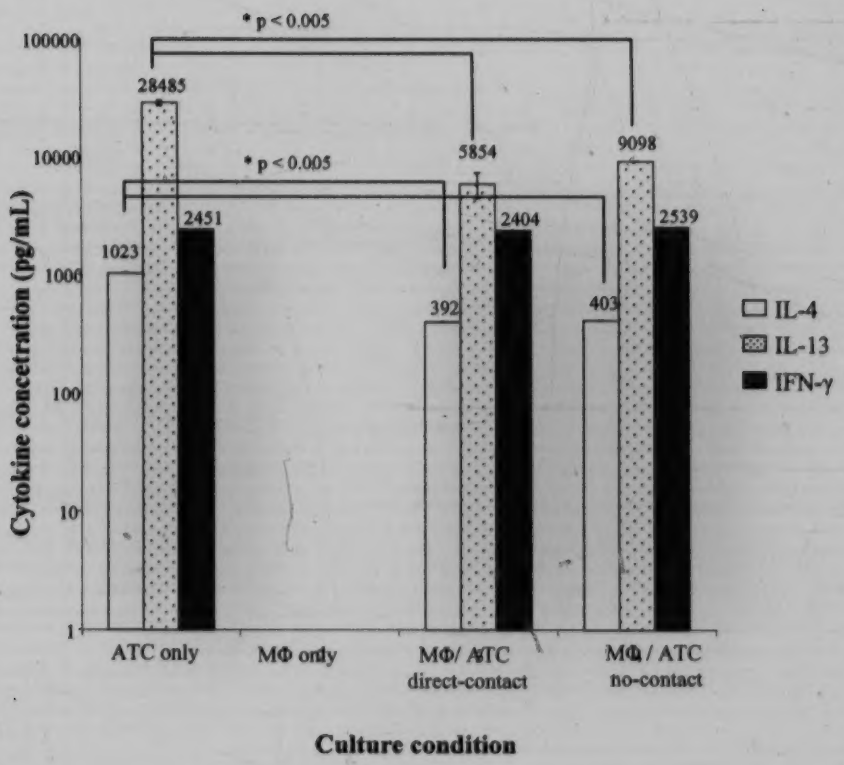

Figure 3k. ELISA analysis of cytokine levels in RAW MΦ/ DBA/2 'whole' ATC co-culture supernatant. Supernatants from co-cultures were examined for IL-4, IL-13, and IFN-γ levels in pg/mL. Each bar represents the average of triplicate ELISA analysis for each of two biological replicates and is shown ± standard deviation. Cytokine levels are significantly different at $p < 0.005$ between culture conditions where indicated by *.

CHAPTER 4

ACTIVIN-A AND THE ALTERNATIVE MACROPHAGE ACTIVATION PARADIGM

4.1 SOLUBLE T CELL-ASSOCIATED PRODUCTS INDUCE MARCOPHAGE ARGINASE-1 EXPRESSION.

MΦ Arg1 expression was increased in MΦ incubated in direct-contact and no-contact conditions with ATC in my co-culture experiments (Figure 3e). I realized that T cell-associated factors inducing Arg1 expression in MΦ incubated in direct-contact conditions were also present in no-contact conditions. Prior to dissecting contact-specific Arg1-inducing factors I first sought to understand the no-contact Arg1-inducting factors present. I turned my focus to T cell-associated soluble factors that induce Arg1.

4.2 IL-4 AND IL-13 ARE SUFFICIENT IN OUR CULTURE SYSTEM TO INDUCE MACROPHAGE ARGINASE-1 EXPRESSION.

IL-4 and IL-13 are important inducers of AMA (1). As IL-4 and IL-13 were present only at very low levels in co-culture supernatant, as determined by ELISA (Figure 3g), I sought to confirm that these cytokines were sufficient to induce Arg1 expression in my system. I treated F4/80+ primary MΦ cultures, generated as described in Chapter 2, with 0, 0.01, 0.1, 1.0, 10 ng/mL of recombinant mouse IL-4 (rmIL-4) or

with 0, 0.01, 0.1, 1.0, 10, 100 ng/mL of recombinant mouse IL-13 (rmIL-13) (Figure 4a). Each cytokine was capable of inducing Arg1 expression in a dose-dependent fashion. Low levels of cytokine failed to induce Arg1 and after a threshold level of cytokine was added, Arg1 expression spiked and then plateaued to a point from which even maximal levels of cytokine could not further increase. rmIL-4 was a more potent inducer of Arg1 expression than rmIL-13; the approximate KD_{50} of rmIL-4 was 0.1 ng/mL, whereas the approximate KD_{50} of rmIL-13 was 5 ng/mL (Figure 4a). Furthermore, I examined the effect of combining both rmIL-4 and rmIL-13 on MΦ Arg1 expression by adding rmIL-4 and rmIL-13 at a concentration equivalent to each cytokine's KD_{50} (Figure 4b). I observed a 12 ± 3.2 fold induction of Arg1 expression in MΦ treated with 0.1 ng/mL of rmIL-4, compared to untreated MΦ. A 38 ± 10 fold induction of Arg1 expression was observed in MΦ treated with 5 ng/mL of rmIL-13. Finally, MΦ Arg1 expression was induced 42 ± 16 fold in MΦ treated with both 0.1 ng/mL of rmIL-4 and 5.0 ng/mL of rmIL-13. This data suggests that Arg1 expression in MΦ is not induced by IL-4 and IL-13 in a synergistic manner.

4.3 IL-4 AND IL-13-INDEPENDENT INDUCTION OF MACROPHAGE ARGINASE-1 *IN VITRO*.

After establishing that IL-4 and IL-13 are sufficient to induce Arg1 expression in my system, I examined the necessity of these cytokines in Arg1 induction. IL-4 and IL-13 both signal through heterodimeric receptors that utilize the IL-4Rα chain as its active

component; thus MΦ deficient in IL-4Rα (IL-4RKO) cannot respond to IL-4 or IL-13 (1). I further confirmed that Arg1 expression could not be induced in IL-4RKO MΦs that were treated with IL-4 and IL-13 (Figure 4c). IL-4RKO MΦs were treated with 0 x KD_{50}, 0.1 x KD_{50}, 1.0 x KD_{50}, and 10 x KD_{50} doses of IL-4 and IL-13 to ensure that I examined MΦ responses at a gradient of cytokine doses. In IL-4RKO MΦ, Arg1 expression was not induced at any dose. In contrast, BALB/c WT MΦ Arg1 expression was induced in a dose-dependent manner. At 0.1 x KD_{50}, 1.0 x KD_{50}, and 10 x KD_{50} fold-induction of Arg1 expression was 6.0 ± 1.1, 6.5 ± 2.7, and 16 ± 4.6 respectively. These results demonstrated that IL-4RKO MΦ could not respond to IL-4 or IL-13.

I examined induction of Arg1 expression in BALB/c WT or IL-4RKO MΦ after co-culture in no-contact conditions with BALB/c WT ATC. Arg1 expression in BALB/c WT MΦ incubated in no-contact conditions with WT ATC was 189.0 ± 80.0 fold-induced compared to unstimulated WT MΦ. In BALB/C IL-4RKO MΦ incubated in no-contact conditions with ATC, Arg1 expression was 13.0 ± 1.4 fold-induced over unstimulated IL-4RKO MΦ (Figure 4d). I examined IL-4, IL-13, and IFN-γ levels in co-culture supernatant by ELISA (Figure 4e). IL-4 was present in T cell-only cultures (766 ± 23 pg/mL), but not in BALB/c WT or IL-4RKO MΦ-only cultures. In BALB/c WT and IL-4RKO MΦ no-contact co-cultures, IL-4 was present at 530 ± 13 and 497 ± 14 pg/mL respectively. Similar to IL-4, IL-13 was also present in T cell-only co-cultures (12,712 ± 402) but not in BALB/c WT or IL-4RKO MΦ-only cultures. In BALB/c WT and IL-4RKO MΦ no-contact co-cultures, IL-13 was present at 16,939 ± 398 and 14,411 ± 198 pg/mL respectively. Finally, IFN-γ was present in T cell-only cultures (2,214 ± 20

pg/mL) but not in BALB/c WT or IL-4RKO MΦ-only cultures. IFN-γ levels in supernatants of BALB/c WT and IL-4RKO co-cultures at 2,205 ± 25 and 2,240 ± 24 pg/mL respectively.

These data corroborate *in vitro* co-culture studies where I showed Arg1 induction in BALB/c WT MΦ incubated with BALB/c WT ATC, despite very low levels of IL-4 or IL-13. Taken together, my observations suggest that although the majority of Arg1 induction appears to be driven by IL-4 and IL-13, an IL-4 and IL-13-independent pathway of MΦ Arg1 induction also exists.

4.4 ACTIVIN A EXPRESSION IS FOUND IN ALLOGRAFTS AT TIME-POINTS THAT CORRESPOND WITH HIGH ARGINASE-1 AND HIGH INTERFERON-γ EXPRESSION.

TGF-β superfamily member activin A is produced by α-CD3 antibody activated ATCs and induces MΦ Arg1 expression (3). We used microarray analysis to analyze gene expression of Inhba in CBA kidneys transplanted into C57Bl/6 hosts. From days 7, 14, 21, and 42 post-transplant we found that Inhba gene expression increased at time-points that corresponded with increasing Arg1 expression (Figure 4f).

We examined the effect of host IL-4 and IL-13—associated immune responses on the allograft. Gene expression of Arg1, Ifng, Il4, Il13, and Inhba was examined by microarray analysis in CBA kidney allografts transplanted into BALB/c IL-4RKO or BALB/c WT host mice at day 7 post-transplant (Figure 4g). In normal CBA/J kidneys,

the raw probe signal of Arg1 (26), Ifng (25), Il4 (35), Il13 (46), and Inhba (124) was low. Interestingly, the raw probe signal of Arg1 and Inhba was comparable in allografts transplanted in WT and IL-4RKO hosts –Arg1 had a signal intensity of 131 or 215 and Inhba had a signal intensity of 148 or 167 respectively. Allograft Ifng gene expression was high in both WT (569) and IL-4RKO (764) hosts and Il4 and Il13 expression was negligible. When we transplanted IFN-γ receptor-deficient CBA allografts into BALB/c IL-4RKO hosts, Arg1 (5414), Inhba (1018), and Ifng (1510) gene expression was high while Il4 and Il13 gene expression was minimal. We are currently waiting to transplant and analyze IFN-γ receptor-deficient CBA allografts into BALB/c WT hosts.

Finally, we examined Arg1, Ifng, Il4, Il13, and Inhba gene expression by microarray in various culture conditions: In WT mixed-lymphocyte reactions (MLR), IFN-γ deficient MLRs, primary IFN-γ-treated MΦs, and in primary untreated MΦs (Figure 4h). BALB/c WT or $Ifng^{-/-}$ (GKO) responder cells and C57Bl/6 stimulator cells were used in MLRs, and thioglycollate-induced peritoneal F4/80+ macrophages generated in C57Bl/6 mice were used in MΦ cultures. Both WT and GKO MLRs had a strong signal for Arg1 (2824 and 3690) and similar signals for Il4 and Il13 (297 and 468 & 277 and 479) after four days of culture. Ifng signal was much stronger in WT MLRs (2066) compared to GKO MLRs (277). Inhba signal was also much higher in WT (1531) MLRs than in GKO MLRs (234). Arg1 signal was very strong in primary MΦs and, curiously, was higher in IFN-γ-treated MΦs (9994) than in untreated MΦs (5824). Interestingly, Inhba signal was also higher in IFN-γ-treated MΦs (239) than in untreated MΦs (15). The raw signal for Ifng, Il4, and Il13 was low in IFN-γ-treated and untreated MΦs.

4.5 ACTIVIN A IS PRESENT IN MACROPHAGE/ ACTIVATED T CELL CO-CULTURE SUPERNATANT.

I retrospectively analyzed activin A levels in BALB/c WT or IL-4RKO MΦ/ BALB/c WT ATC co-culture supernatants (Figure 4i). By cytokine ELISA, I observed that activin A was present at low levels in T cell-only (474 ± 41 pg/mL), WT MΦ-only (254 ± 29 pg/mL), and IL-4RKO MΦ-only (602 ± 80 pg/mL) cultures. In WT or IL-4RKO MΦ no-contact co-cultures, activin A was present at much higher levels: 3,096 ± 69 and 4,408 ± 102 pg/mL respectively. I compared activin A levels in co-culture supernatants from experiments where I compared MΦ Arg1 induction in direct-contact and no-contact conditions (Table 4.1). Co-culture supernatants from direct-contact conditions contained more activin than supernatants from no-contact conditions in co-cultures when I used BALB/c WT or IL-4RKO MΦ. For instance, in WT and IL-4RKO direct-contact co-cultures I found 2241 ± 110 and 2785 ± 95 pg/mL of activin A respectively, and in WT and IL-4RKO no-contact co-cultures I found 1024 ± 62 and 941 ± 64 pg/mL of activin A. Interestingly, in co-cultures of RAW264.7 cells and BALB/c GKO ATC, activin A was present at similar levels in direct-contact (1002 ± 171 pg/mL) and no-contact conditions (1050 ± 63 pg/mL). These results show that direct-contact between MΦ and ATC increases activin A production in conditions where IFN-γ is present.

4.6 ACTIVIN A DIRECTLY INDUCES MACROPHAGE ARGINASE-1 EXPRESSION IN VITRO.

I sought to determine if activin A could directly induce Arg1 expression in *in vitro* MΦ cultures. I treated F4/80+ MΦ, generated peritoneally as described in chapter 3, with 0, 1, 10, or 100 ng/mL of recombinant activin A. When expressed as fold-increase compared to untreated MΦ, Arg1 expression was induced in a dose-dependent manner to recombinant activin A –fold-induction of Arg1 was 3.6 ± 0.88 by 10 ng/mL of activin A and 7.1 ± 2.3 by 100 ng/mL of activin A (Figure 4j). Thus, activin A is able to induce MΦ Arg1 *in vitro*.

Lipopolysaccharide (LPS) is a bacterial endotoxin that activates MΦ towards a CMA-phenotype (1). Conversely, signaling through TLR-4 adaptor protein MyD88 increases serum concentrations of activin A (72) and I was curious about the effect of LPS on MΦ Arg1 induction in activin-A treated MΦ (Figure 4k). I examined fold-induction of Arg1 expression in peritoneal BALB/c WT MΦ treated with 100 ng/mL LPS, 100 ng/mL activin A, or 100 ng/mL of LPS & 100 ng/mL of activin A compared to Arg1 induction in untreated MΦ. In activin A treated MΦs, Arg1 expression was induced by 4.0 ± 1.2. In contrast, in LPS treated MΦs (0.9 ± 0.1) and LPS & activin A treated MΦs (0.9 ± 0.3), Arg1 expression was not induced.

I examined the effect of combining activin A with IL-4 and IL-13 on MΦ Arg1 induction. I treated BALB/c WT F4/80^{+} MΦ with 0.1 ng/mL of rmIL-4, 5.0 rmIL-13, and 100 ng/mL of recombinant activin A (Fig 4l). Compared to untreated MΦ (DCt = 28.1), Arg1 was induced in 42.3 ± 4.3 fold in MΦ treated with rmIL-4 and rmIL-13 and 8.0 ±

0.9 fold in MΦ treated with activin A. In MΦ treated with rmIL-4, rmIL-13, and activin A Arg1 was induced 45.2 ± 5.0 fold –an induction that was not a significant increase over Arg1 fold induction by rmIL-4 and rmIL-13 alone.

4.7 NEUTRALIZING ACTIVIN A IN MACROPHAGE/ ACTIVATED T CELL CO-CULTURES ATTENUATES MACROPHAGE ARGINASE-1 INDUCTION.

Activin A deficient mice are not available because Inhba$^{-/-}$ results in neonatal lethality (89). To show that activin A is important in Arg1 induction, I attempted to neutralize activin A in BALB/c WT and IL-4RKO MΦ/ BALB/c WT ATC no-contact co-cultures with neutralizing α-activin A antibody (Figure 4m). When normalized to WT MΦ-only cultures, fold-induction in WT MΦ/ ATC co-cultures was similar for untreated (189.0 ± 79), α-isotype antibody treated (158.7 ± 59.4), and neutralizing α-activin A antibody treated conditions (164.4 ± 26.8). In contrast, when normalized to IL-4RKO MΦ-only cultures, fold-induction of Arg1 in IL-4RKO MΦ/ ATC co-cultures was decreased in neutralizing α-activin A antibody treated conditions (6.7 ± 1.4; $p < 0.05$) and similar in untreated (12.5 ± 1.4) and isotype antibody (17.0 ± 3.5) treated conditions. Thus, when MΦ cannot respond to IL-4 or IL-13, activin A becomes important in induction of Arg1 expression.

I used cytokine ELISA to compare IL-4, IL-13, IFN-γ, and activin A levels in WT or IL-4RKO MΦ/ ATC no-contact co-culture supernatants treated with isotype or α-activin A antibody (Table 4.2). While activin A levels were significantly lower ($p<0.005$),

in α-activin A antibody treated conditions than in untreated and isotype antibody treated co-cultures, activin A was still detectable by ELISA after activin A neutralization. Untreated, isotype, and α-activin A antibody-treated WT MΦ/ ATC co-culture supernatant had 3,956.8 ± 207.6, 2,975.3 ± 43.8, and 645.2 ± 37.4 pg/mL of activin A respectively. In IL-4RKO MΦ/ ATC untreated, isotype-, and α- activin A antibody-treated co-culture supernatants I found 5,612.0 ± 132.6, 6,626.6 ± 175.1, and 895.3 ± 49.8 pg/mL of activin A respectively. IL-4, IL-13, and IFN-g levels were similar for WT and IL-4RKO MΦ/ ATC co-cultures in each condition.

4.8 MACROPHAGES IN CO-CULTURE WITH ACTIVATED T CELLS EXPRESS HIGH LEVELS OF ACTIVIN A.

I wanted to determine which cell type(s) in MΦ/ ATC co-cultures produced activin A so I examined gene expression of Inhba in WT or IL-4RKO MΦ/ BALB/c WT ATC co-cultures using RT-PCR. Confirming my ELISA data, Inhba gene expression was significantly increased in direct-contact and no-contact conditions of BALB/c WT and IL-4RKO MΦ/ ATC co-cultures, compared to Inhba levels in MΦ-only cultures (Figure 4n). I further examined Inhba gene expression within the specific cell-types in WT MΦ/ ATC co-cultures: The use of a cell-culture insert facilitated the easy separation of MΦ/ATC incubated under no-contact conditions. I used immunomagnetic-positive selection to separate F4/80+ MΦ from contact cultures (Figure 4o). I confirmed the purity of positively selected F4/80+ cells in purified direct-contact conditions using flow

cytometry. In unpurified direct-contact cells, 75% of cells were F4/80+, and in F4/80+ enriched faction of direct-contact cells 92% of cells were F4/80+. In the ATC faction there were only 3% contaminating F4/80+ cells (Figure 4p). I further confirmed purity of each faction by RT-PCR where I examined gene expression of Tcrbv13, a gene encoding a region of the β-chain of the T cell receptor, and Emr1, the gene for F4/80+ (Figure 4q). I examined gene expression of Inhba in each faction of co-culture cells: direct-contact ATC, direct-contact MΦ, no-contact ATC, direct-contact ATC, MΦ-only, and T cells-only (Figure 4r). As I cannot fairly normalize Inhba induction in each faction to a constant untreated condition, I expressed Inhba induction as percent HPRT expxression. HPRT is a housekeeping gene that is constitutively and constantly expressed and reporting Inhba gene expression as percent HPRT provides an accurate picture of Inhba transcript levels. Given the known ubiquitous nature of activin A, I was not surprised to find that Inhba was present in all cell factions. However, Inhba expression in MΦ-only (29.9 ± 1.9), ATC (31.5 ± 5.2), and direct-contact ATC (34.2 ± 9.6) and no-contact ATC (18.4 ± 0.9) was relatively lower than in direct-contact MΦ (749.2 ± 98.3) and no-contact MΦ (436.0 ± 69.9). That is, while Inhba transcripts are present in T cells and in MΦ-only cultures, they are greatly increased in MΦs after incubation with ATC.

4.9 TABLES

Table 4.1. Summary of activin A concentration levels in direct-contact and no-contact conditions in co-culture experiments using RAW or primary BALB/c WT or IL-4RKO MΦ / BALB/c WT or GKO 'whole' or $CD3^+$ ATC. Cytokine levels are shown in pg/mL for conditions where MΦ and ATC were incubated in direct-contact conditions, in no-contact. Results are the average of triplicate ELISA analyses of triplicate experimental replicates and are shown ± standard error. Differences in activin A levels between experimental conditions are significant at $p < 0.005$ when indicated by *.

MΦ and ATC type	ATC and MΦ: direct-contact	ATC and MΦ: no contact
BALB/c WT MΦ & $CD3^+$ -enriched BALB/c WT ATC	2241 ± 110*	1024 ± 62*
BALB/c IL-4RKO MΦ & $CD3^+$ -enriched BALB/c WT ATC	2785 ± 95*	941 ± 64*
RAW 264.7 MΦ & 'whole' BALB/c GKO ATC	1002 ± 171	1050 ± 63

Table 4.2. Summary of IL-4, IL-13, IFN-γ, and activin A levels in co-culture supernatant in BALB/c WT or IL-4RKO MΦ/ BALB/c WT $CD3^+$ ATC no-contact co-cultures. Co-cultures were either left untreated or treated with α-isotype control or neutralizing α-Inhba antibody. Cytokine levels are shown in pg/mL and results are the average of triplicate ELISA analyses of triplicate experimental replicates and are shown ± standard error. *Indicates a significant difference of $p < 0.005$ between treatments within a specific co-culture type.

	BALB/c WT MΦ/ BALB/c WT ATC				BALB/c IL-4RKO/ BALB/c WT ATC			
Treatment	**IL-4**	**IL-13**	**IFN-γ**	**Activin A**	**IL-4**	**IL-13**	**IFN-γ**	**Activin A**
Untreated co-cultures	369 ± 7	15971 ± 176	2205 ± 24	3957 ± 208*	380 ± 4	15571 ± 351	2240 ±24	5612 ± 133*
α-Isotype control treated co-cultures	485 ± 16	17754 ± 195	2138 ± 13	2975 ± 44*	424 ± 11	15949 ± 247	2246 ± 60	6627 ± 175*
α-Inhba treated co-cultures	403 ± 20	16003 ± 646	2255 ± 27	645 ± 37*	485 ± 9	15344 ± 354	2206 ± 13	895 ± 50

4.10 FIGURES

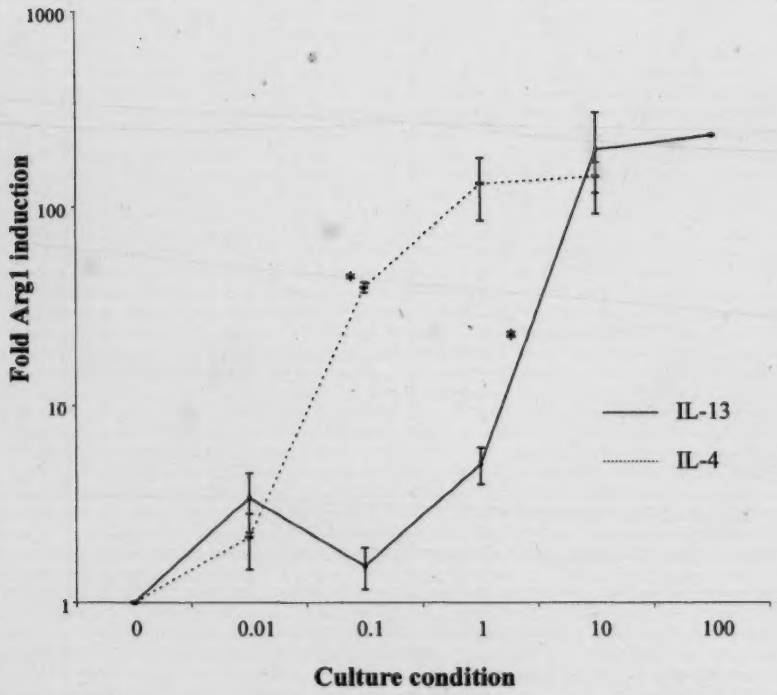

Figure 4a. Quantitative RT-PCR of AMA marker Arg1 in F4/80$^+$ peritoneal BALB/c WT macrophages treated with increasing concentrations of recombinant IL-4 or IL-13. RNA was extracted from treated MΦ and cDNA was prepared prior to quantification of Arg1 transcripts by RT-PCR using the ABI PRISM 7900 Sequence Detector. Induction of Arg1 expression was expressed as fold-increase compared to expression observed in untreated MΦ (DCt = 29.2) cultures. Data is ± standard error and is representative of three replicates for each condition followed by duplicate quantitative RT-PCR analysis for each replicate. The KD_{50} (indicated by *) of each cytokine was estimated to be the point where induction of Arg1 expression was about half of the total expression observed at the highest dose of cytokine.

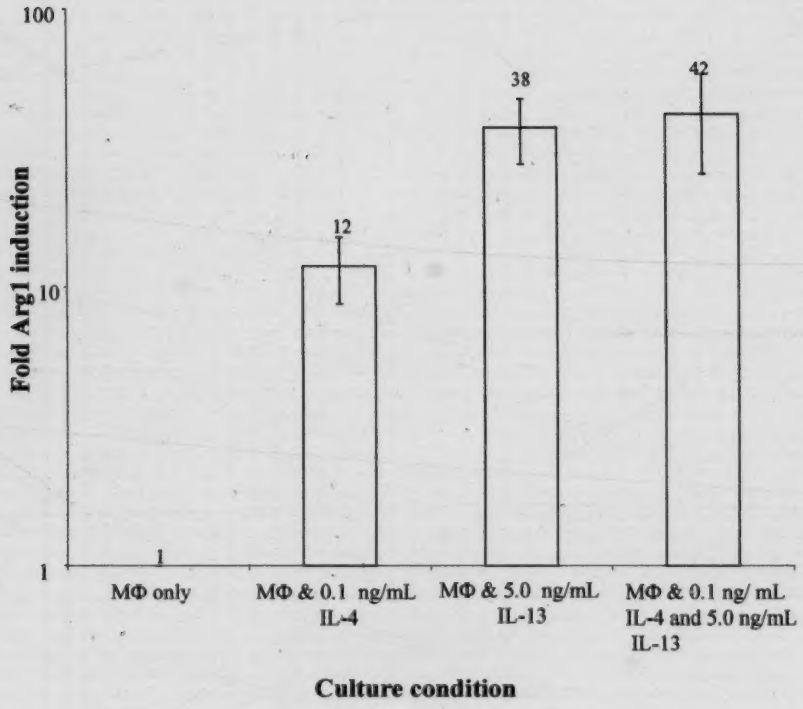

Figure 4b. Quantitative RT-PCR of AMA marker Arg1 in F4/80^{+} peritoneal BALB/c WT macrophages treated with 0.1 ng/mL IL-4 and/ or 5.0 ng/mL IL-13. RNA was extracted from adherent cells in each condition and cDNA was prepared prior to quantification of Arg1 transcripts by RT-PCR using the ABI PRISM 7900 Sequence Detector. Induction of Arg1 expression was expressed as fold-increase compared to expression observed in untreated MΦ (DCt = 28.2) cultures. Data is ± standard error and is representative of three replicates for each condition followed by duplicate quantitative RT-PCR analysis for each replicate.

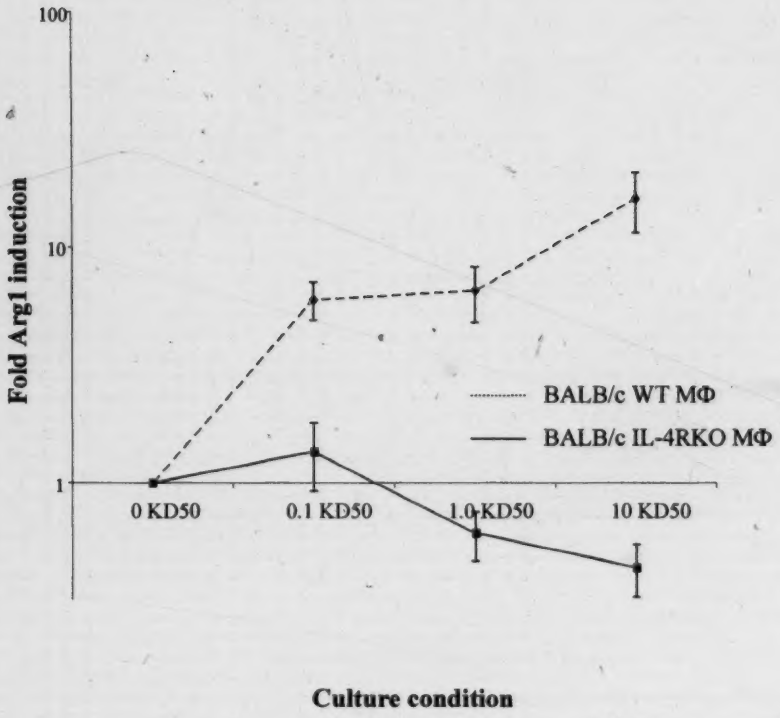

Figure 4c. Quantitative RT-PCR of AMA marker Arg1 in BALB/c WT or IL-4RKO MΦ treated with recombinant IL-4 and IL-13. RNA was extracted from MΦ treated with 0, 0.1, 1.0, or 10 times the KD_{50} of IL-4 (0.1 ng/mL) or IL-13 (5.0 ng/mL). cDNA was prepared prior to quantification of Arg1 transcripts by RT-PCR using the ABI PRISM 7900 Sequence Detector. Induction of Arg1 expression was expressed as fold-increase compared to expression observed in untreated WT (DCt = 23.4) or IL-4RKO (DCt = 24.2) MΦ cultures. Data is ± standard error and is representative of three replicates for each condition followed by duplicate quantitative RT-PCR analysis for each replicate.

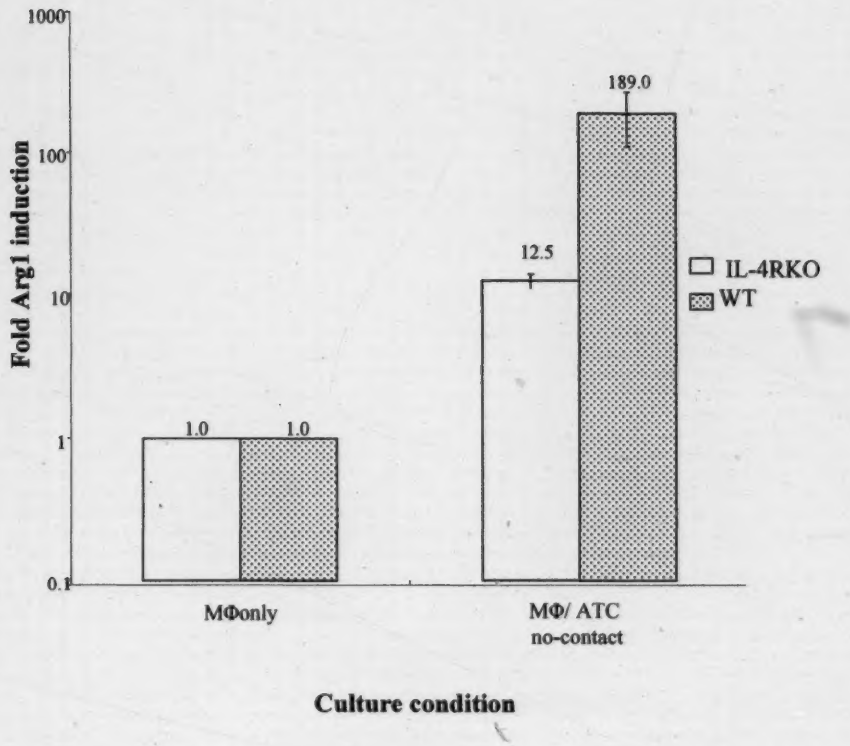

Figure 4d. Quantitative RT-PCR of AMA marker Arg1 in BALB/c WT or IL-4RKO MΦ incubated in no-contact with BALB/c WT $CD3^+$ ATC. RNA was extracted from MΦ and cDNA was prepared prior to quantification of Arg1 transcripts by RT-PCR using the ABI PRISM 7900 Sequence Detector. Induction of Arg1 expression was expressed as fold-increase compared to expression observed in untreated WT (DCt = 28.3) or IL-4RKO (DCt = 26.4) MΦ cultures. Data is ± standard error and is representative of three replicates for each condition followed by duplicate quantitative RT-PCR analysis for each replicate.

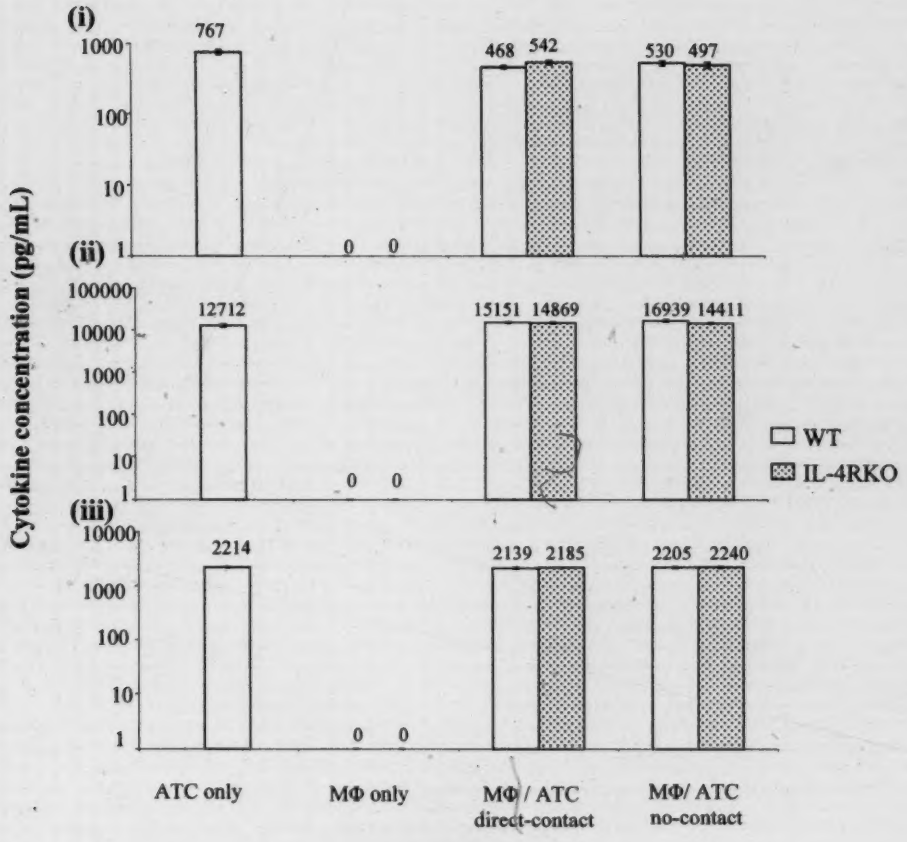

Figure 4e. ELISA analysis of cytokine levels in BALB/c WT or IL-4RKO MΦ/ BALB/c WT ATC co-culture supernatant. Supernatants from co-cultures were examined for (i) IL-4, (ii) IL-13, and (iii) IFN-γ levels in pg/mL. Each bar represents the average of triplicate ELISA analysis for each of three biological replicates and is shown ± standard deviation.

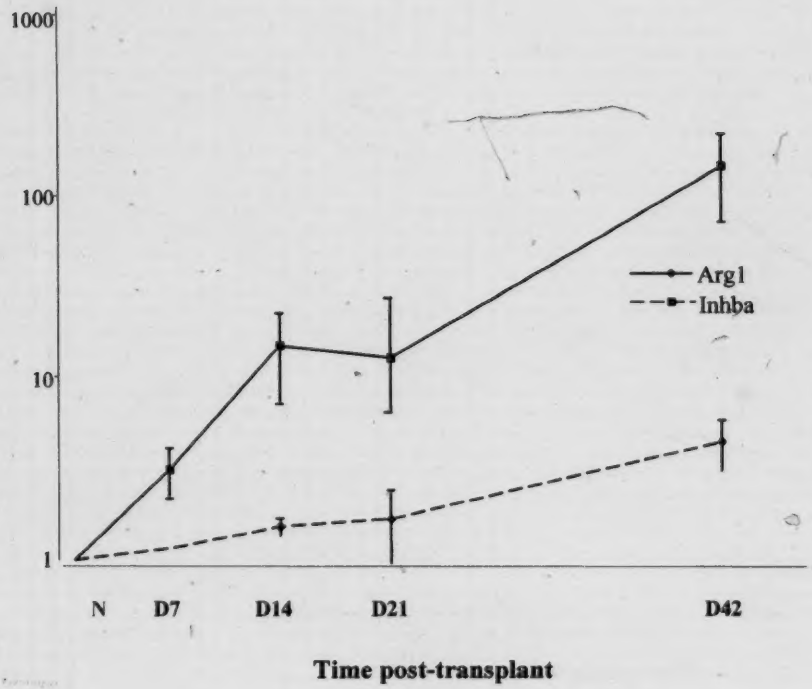

Figure 4f. Time-course of macrophage activation-associated cytokine transcripts in CBA kidney allografts transplanted into B6 hosts. RNA was extracted from kidney allografts at the indicated days and we examined gene expression of Arg1 and Inhba using microarray chip analysis. Gene expression was normalized against non-transplanted (N) CBA kidneys (n=3). For each graph, numbers represent mean expression of each sample pool (n=3) ± standard error.

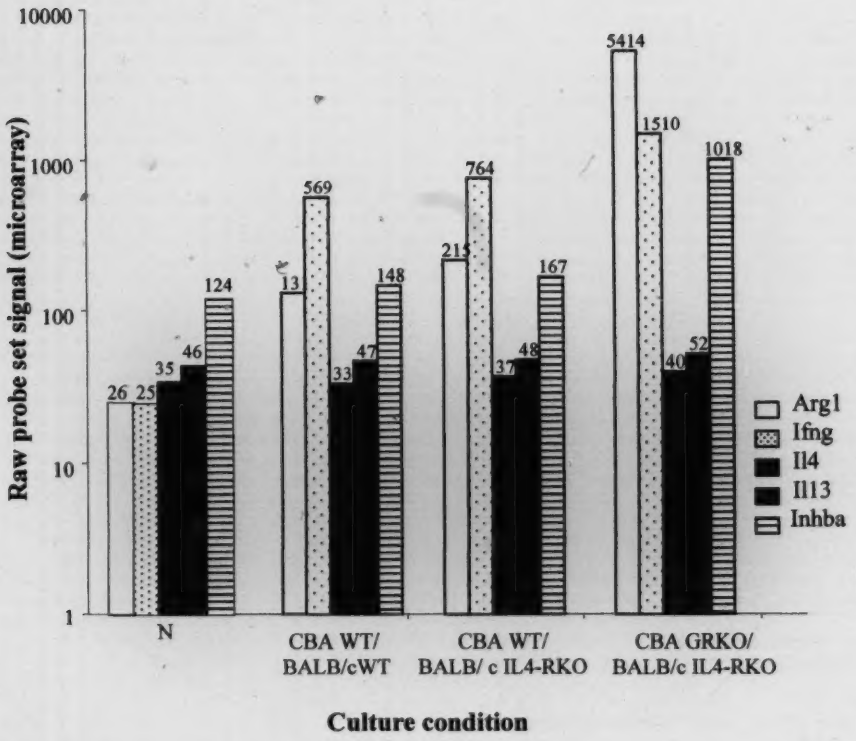

Figure 4g. Microarray analysis of transcript levels in normal (N) CBA WT kidneys, and in CBA WT or GRKO kidneys transplanted into BALB/c WT or IL-4RKO hosts. Kidney transplants were removed and examined at day 7 post-transplant. Transcript expression is shown as raw probe set signal for Arg1, Ifng, Il4, Il13, and Inhba probes.

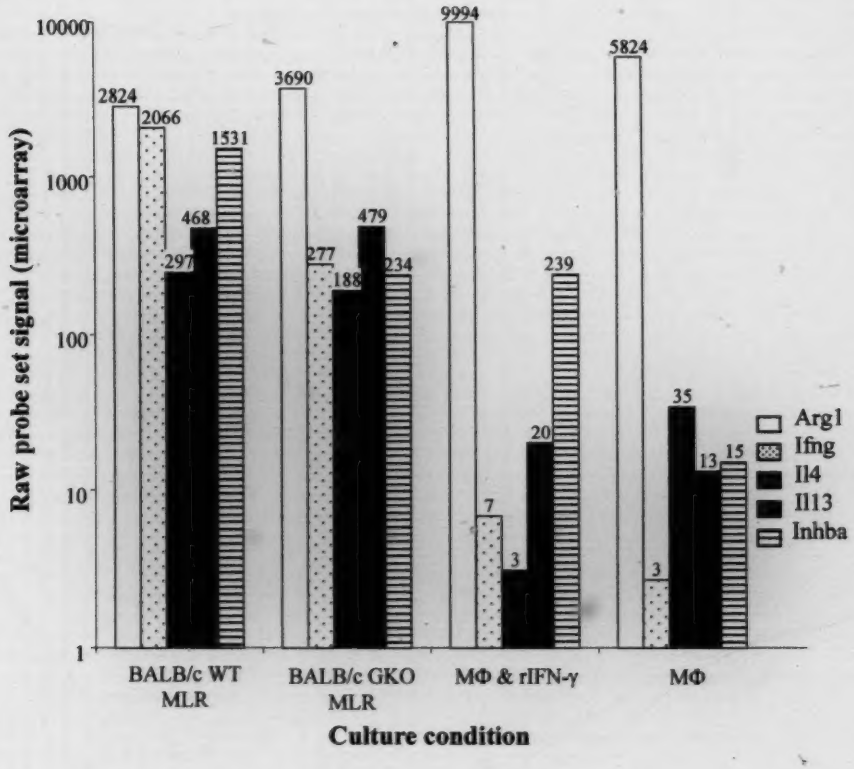

Figure 4h. Microarray analysis of transcript levels in MLRs and primary F4/80+ MΦ cultures. MLRs used either WT or GKO responder cells and MΦ cultures were either untreated or treated with 500 U of recombinant IFN-γ. Transcript expression is shown as raw probe set signal for Arg1, Ifng, Il4, Il13, and Inhba probes.

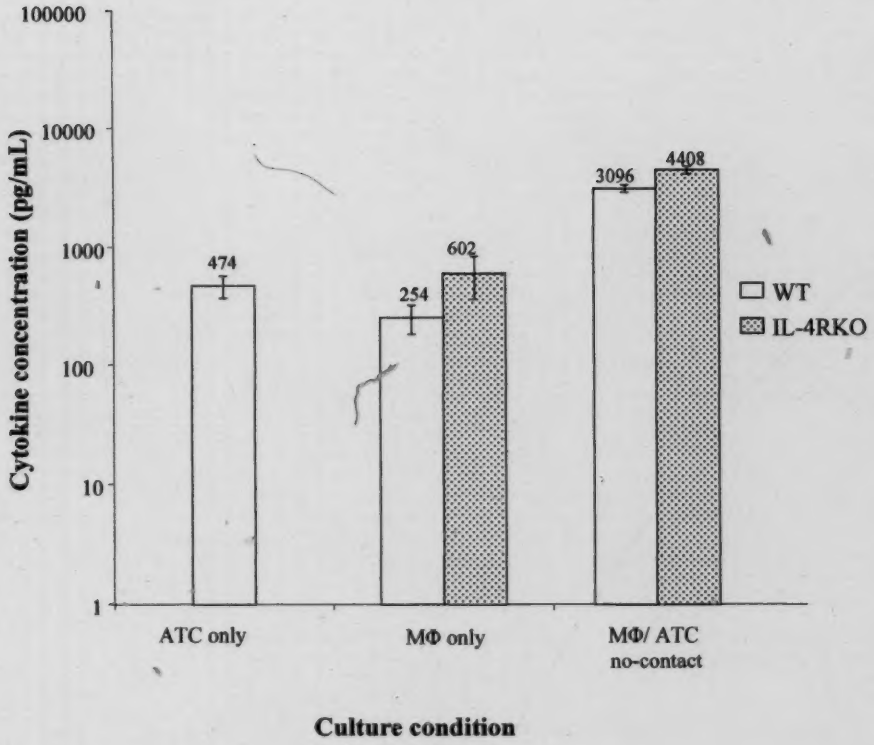

Figure 4i. ELISA analysis of cytokine levels in RAW MΦ / BALB/c WT ATC co-culture supernatant. Supernatants from co-cultures were examined for activin A levels in pg/mL. Each bar represents the average of triplicate ELISA analysis for each of two biological replicates and is shown ± standard deviation.

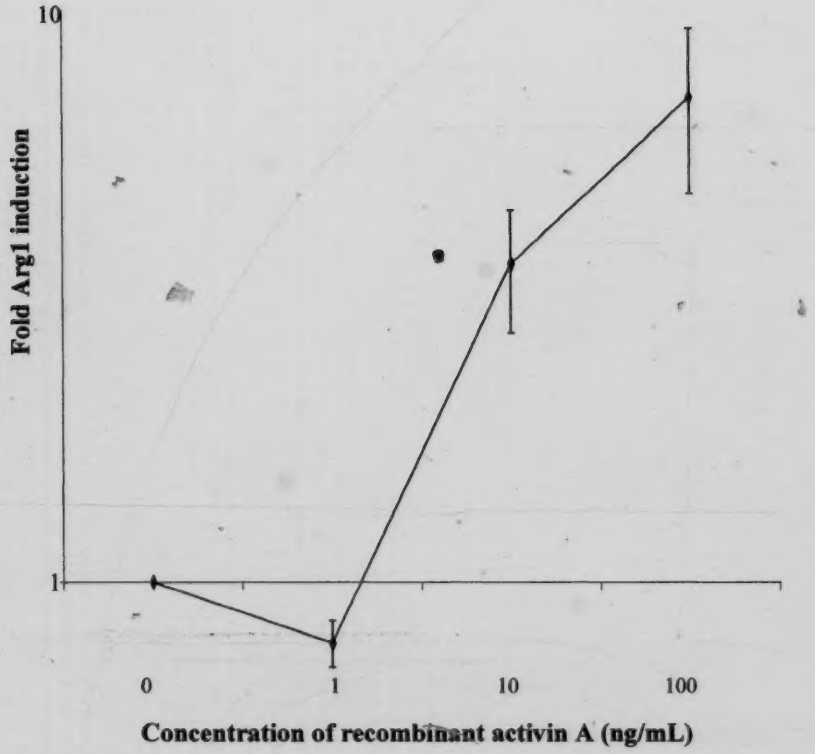

Figure 4j. Quantitative RT-PCR of AMA marker Arg1 in BALB/c WT MΦ treated with increasing doses of recombinant activin A. RNA was extracted from MΦ and cDNA was prepared prior to quantification of Arg1 transcripts by RT-PCR using the ABI PRISM 7900 Sequence Detector. Induction of Arg1 expression was expressed as fold-increase compared to expression observed in untreated WT (DCt = 28.2) MΦ cultures. Data is ± standard error and is representative of three replicates for each condition followed by duplicate quantitative RT-PCR analysis for each replicate.

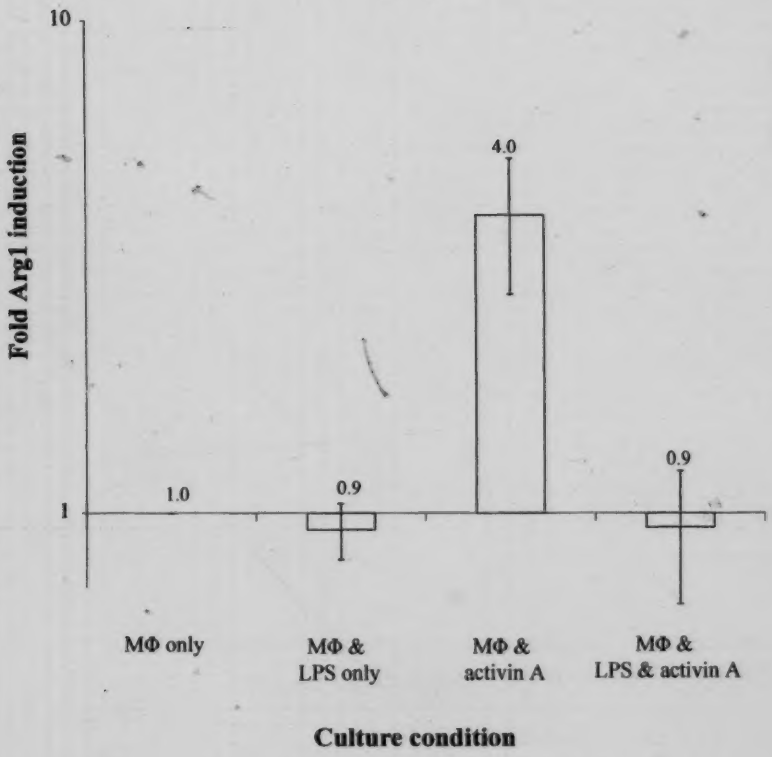

Figure 4k. Quantitative RT-PCR of AMA marker Arg1 in BALB/c WT MΦ treated with 100 ng/mL of activin A and/ or 100 ng/mL of LPS. RNA was extracted from MΦ and cDNA was prepared prior to quantification of Arg1 transcripts by RT-PCR using the ABI PRISM 7900 Sequence Detector. Induction of Arg1 expression was expressed as fold-increase compared to expression observed in untreated WT (DCt = 21.8) MΦ cultures. Data is ± standard error and is representative of three replicates for each condition followed by duplicate quantitative RT-PCR analysis for each replicate.

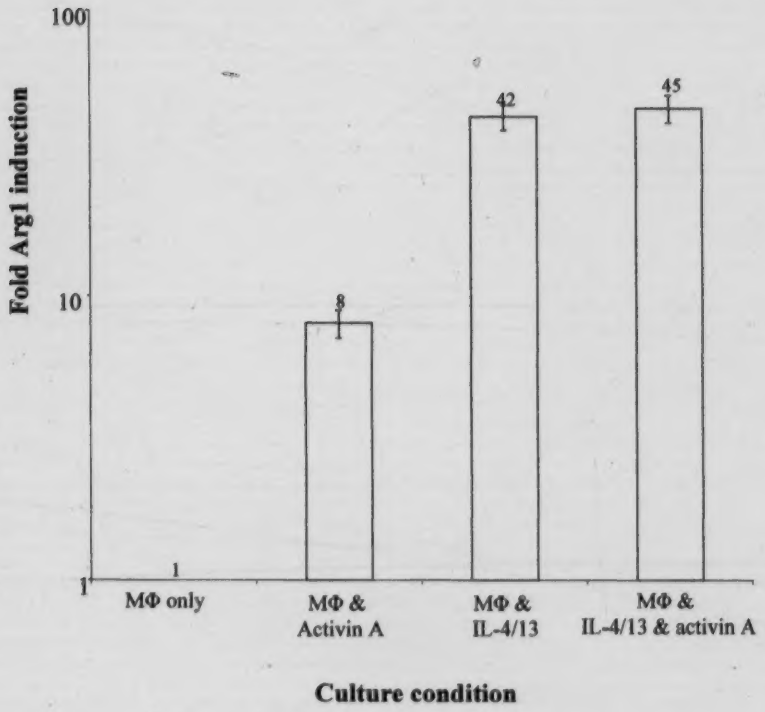

Figure 4l. Quantitative RT-PCR of AMA marker Arg1 in BALB/c WT MΦ treated with 100 ng/mL of activin A and/ or 0.1 ng/mL of recombinant IL-4 and 5.0ng/mL recombinant IL-13. RNA was extracted from MΦ and cDNA was prepared prior to quantification of Arg1 transcripts by RT-PCR using the ABI PRISM 7900 Sequence Detector. Induction of Arg1 expression was expressed as fold-increase compared to expression observed in untreated WT (DCt = 28.1) MΦ cultures. Data is ± standard error and is representative of three replicates for each condition followed by duplicate quantitative RT-PCR analysis for each replicate.

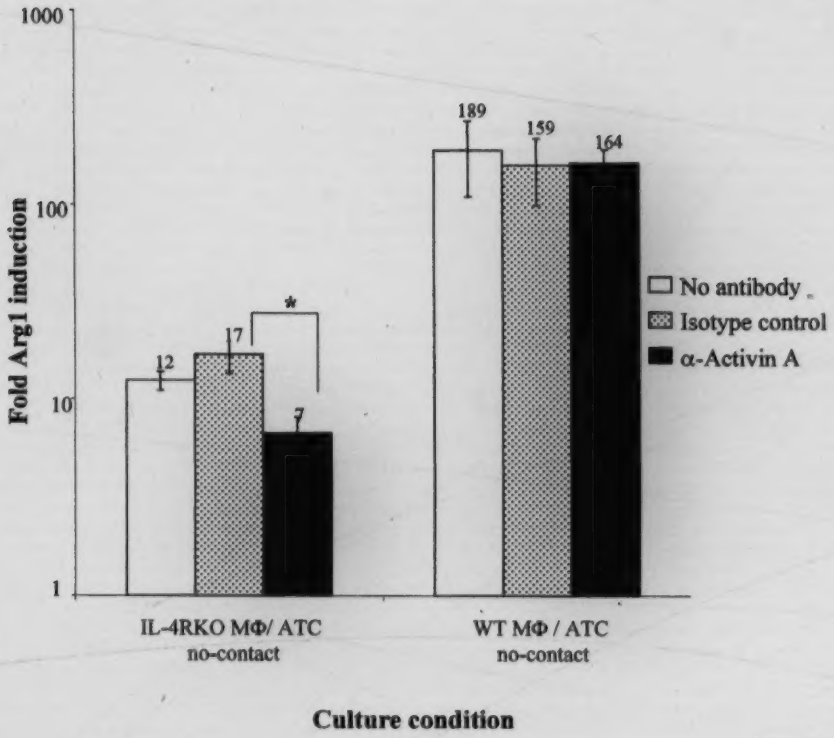

Figure 4m. Quantitative RT-PCR of AMA marker Arg1 in BALB/c WT or IL-4RKO MΦ/ $CD3^+$ BALB/c WT ATC no-contact co-cultures. MΦ cultures were untreated, treated with isotype-control antibody, or with α-Activin A antibody. RNA was extracted from adherent cells under each *in vitro* co-culture assay condition and cDNA was prepared prior to quantification of Arg1 transcripts by RT-PCR using the ABI PRISM 7900 Sequence Detector. Induction of Arg1 expression was expressed as fold-increase compared to expression observed in untreated BALB/c WT (DCt =) or IL-4RKO (DCt =) MΦ. Data is ± standard deviation and is representative of three replicates for each condition followed by duplicate quantitative RT-PCR analyses for each replicate. *Indicates a significant difference $p < 0.05$.

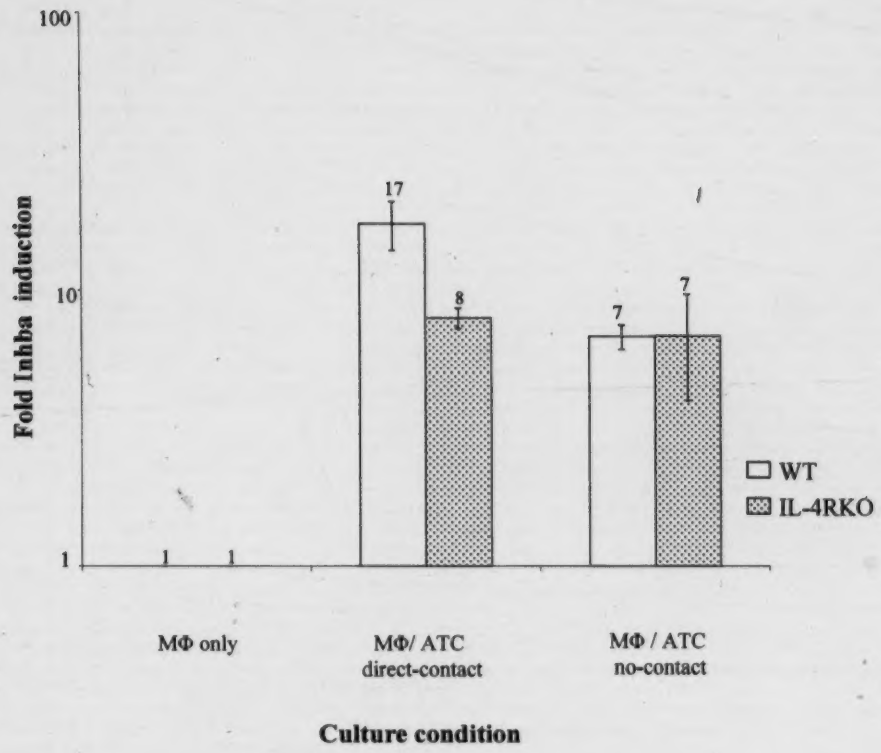

Figure 4n. Quantitative RT-PCR of Inhba in BALB/c WT or IL-RKO MΦ/ $CD3^+$ BALB/c WT ATC co-cultures. RNA was extracted from adherent cells under each *in vitro* co-culture assay condition and cDNA was prepared prior to quantification of Inhba transcripts by RT-PCR using the ABI PRISM 7900 Sequence Detector. Induction of Inhba is expressed as fold-increase compared to expression observed in BALB/c WT (DCt = 26.1) or IL-RKO (DCt = 25.9) MΦ only cultures. Data is ± standard error and is representative of three replicates for each condition followed by duplicate quantitative RT-PCR analyses for each replicate.

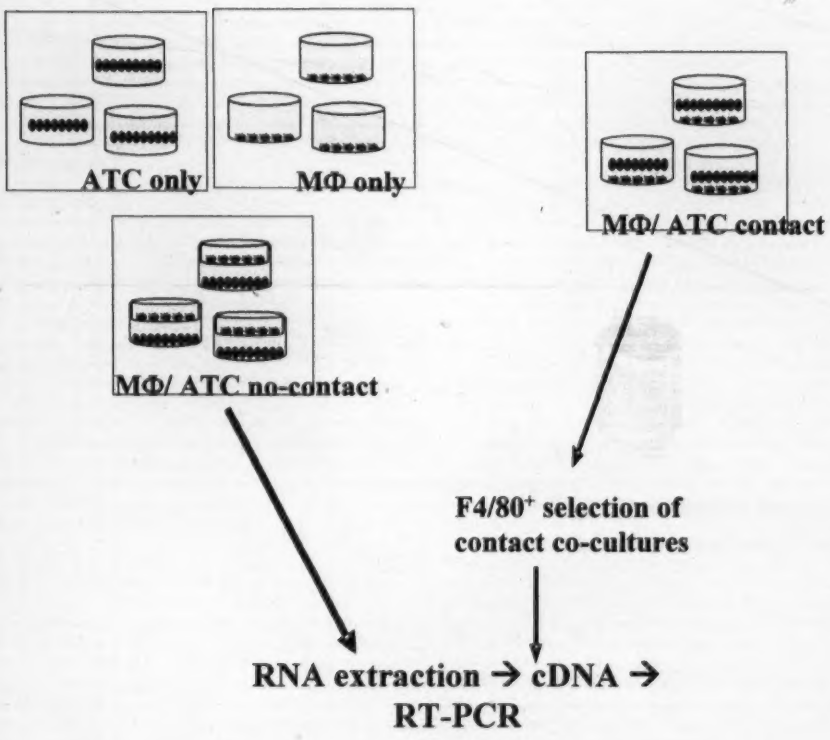

Figure 4o. Flow chart of purification protocol to re-isolate F4/80$^+$ cells from MΦ/ ATC co-cultures. Cells were collected from MΦ-only and ATC-only cultures. For no-contact conditions, MΦ and ATC were collected from the appropriate side of the cell-impermeable membrane. For direct-contact conditions, MΦ were purified from a hetergenous MΦ / ATC cell mixture by F4/80$^+$ immunomagnetic selection. Following purification, RNA was extracted from each cell population and cDNA was prepared prior to examining various transcripts using RT-PCR.

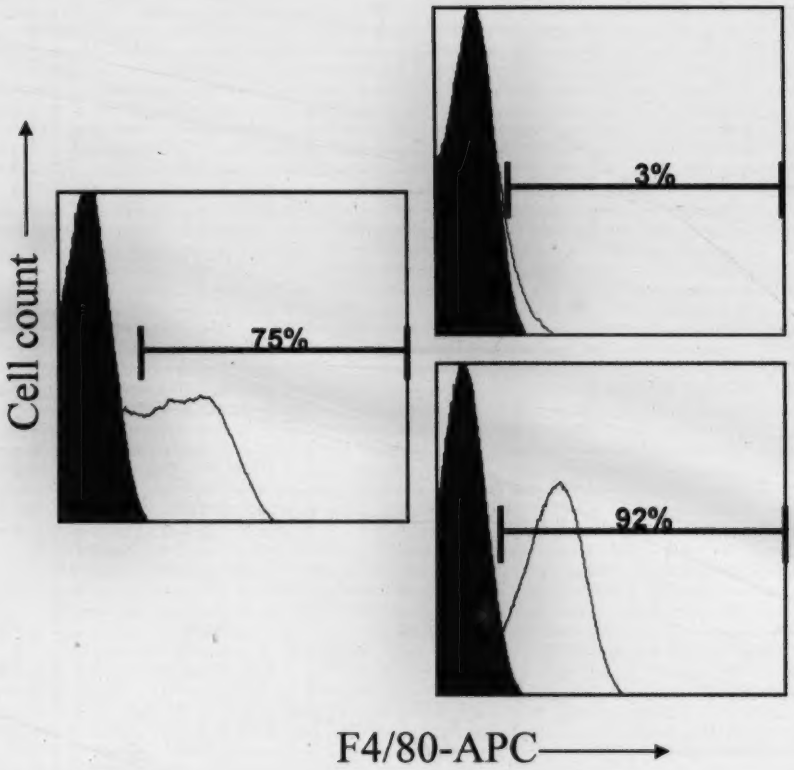

Figure 4p. Flow cytometry analysis of MΦ purity. We measured percentage of F4/80$^+$ cells in direct-contact conditions (i) prior to F4/80$^+$ purification, (ii) in the T cell-faction of purified cells, and (iii) in the MΦ-faction of purified cells. The unfilled histogram represents the F4/80$^+$-APC stained sample and the filled histogram represents the negative control for each sample. Graphs shown are within a leukocyte gate that is based on side- and forward-scatter properties.

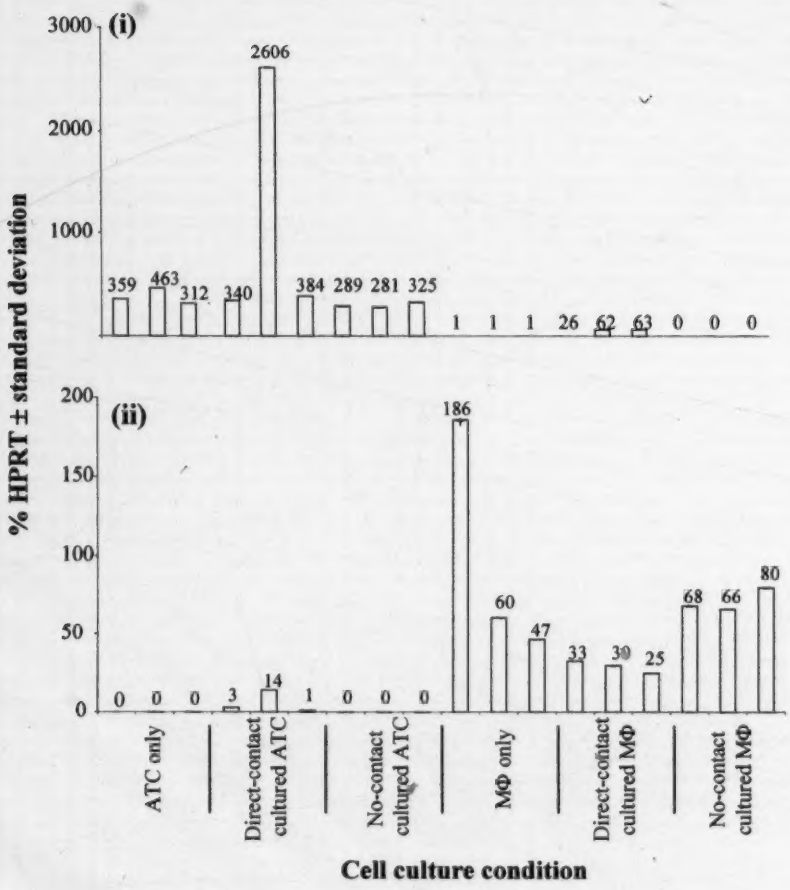

Figure 4q. Quantitative RT-PCR analysis of T cell-associated and MΦ-associated transcripts in cells from MΦ/ ATC co-cultures. We examined (i) Tcrbv13 transcripts, and (ii) Emr1 transcripts in cell factions derived from ATC-only, MΦ-only, direct-contact MΦ/ ATC, and no-contact MΦ/ATC cultures. RNA was extracted from cells and cDNA was prepared prior to quantification of transcripts by RT-PCR using the ABI PRISM 7900 Sequence Detector. Expression of each gene is shown as % HPRT. For each graph, numbers represent the average of duplicate RT-PCR analysis of each replicate ± standard deviation.

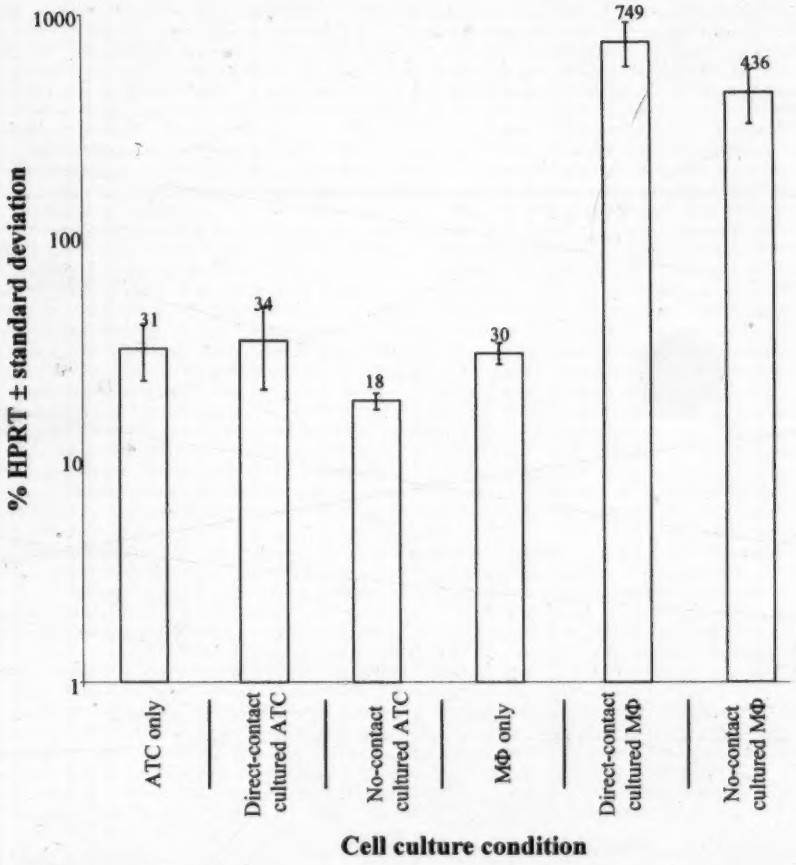

Figure 4r. Quantitative RT-PCR of Inhba in cells in BALB/c WT MΦ/ ATC co-cultures. Cell factions were derived from ATC-only, MΦ-only, direct-contact MΦ/ ATC, and no-contact MΦ/ATC cultures. RNA was extracted from cells and cDNA was prepared prior to quantification of transcripts by RT-PCR using the ABI PRISM 7900 Sequence Detector. Expression of each gene is shown as % HPRT. For each graph, numbers represent the average of duplicate RT-PCR analysis of each replicate ± standard error.

CHAPTER 5

GENERAL DISCUSSION

5.1 SUMMARY OF DATA

Macrophages (MΦ) and T cells are the most prominent immune cells present in rejecting allografts (5). Alternative macrophage activation (AMA), which is incriminated in fibrogenic disease processes (90), has not been carefully explored in allograft rejection. Our laboratory examined expression of the prototypic AMA marker arginase 1 (Arg1), and found it in our mouse model of renal allograft rejection at various times post-transplant. Unexpectedly, Arg1 was present at high levels at late time-points that correlated with severe allograft injury and with high levels of interferon-gamma transcripts (Ifng), which is usually associated with classical macrophage activation (CMA) (1). I examined Arg1 transcript expression in this project; however, Arg1 transcript expression has previously been shown to correlate with Arg1 protein expression (91).

I hypothesized that activated T cell (ATC)-associated products and MΦ/ ATC contact were responsible for MΦ Arg1 induction in the presence of Ifng. I established a co-culture assay where I incubated ATC in direct-contact or no-contact conditions with MΦ. RT-PCR analysis of MΦ/ ATC co-cultures showed that ATC-associated soluble products induced MΦ Arg1 expression and that, when MΦ and ATC were co-cultured in

direct-contact with each other, Arg1 expression was further enhanced. In co-cultures where IFN-γ was absent, preliminary results indicated that direct-contact between MΦ and ATC had no significant effect on MΦ Arg1 induction. Interestingly, in co-cultures where ATC were derived from CD94 deficient mice, direct-contact also did not have a significant effect on MΦ Arg1 induction. I realized that in order to fully understand the factors inducing MΦ Arg1 in direct-contact conditions, I had to first dissect the soluble factors responsible for MΦ Arg1 induction.

To this end, I examined ATC-associated soluble inducers of AMA and confirmed that AMA-associated recombinant cytokines IL-4 and IL-13 were sufficient to induce Arg1 (1). However, Arg1 was also mildly induced by T cell-associated products in IL-4/13 receptor-deficient (IL-4RKO) MΦ indicating an IL-4/13-independent pathway of Arg1 induction. α-CD3 ATC produce activin A and can induce MΦ Arg1 expression (3), so I examined activin A induction of Arg1 in *in vitro* MΦ/ ATC co-cultures and in MΦ cultures: Activin A was present in MΦ/ATC co-culture supernatant and recombinant activin A directly induced MΦ Arg1 in MΦ-only cultures. Neutralization of activin A in MΦ/ ATC co-cultures attenuated Arg1 induction when neither IL-4 or IL-13 were present. In MΦ/ ATC co-cultures, activin A gene expression was observed in both ATC and MΦs but was most induced in MΦs after incubation with ATC. Furthermore, I found that expression of activin A (Inhba) in murine renal allografts transplanted into WT hosts was increased at time-points that correlated with high Arg1 expression. Additionally, Inhba was expressed at time-points correlating with Arg1 induction in allografts transplanted into IL-4Rα-deficient hosts. In both instances, Inhba was expressed concurrently with high Ifng expression. Inhba and Arg1 were expressed in WT and IFN-γ

deficient MLRs, as well as in untreated primary MΦ cultures and the expression of both was further enhanced in IFN-γ-treated primary MΦ cultures.

Altogether our data indicated that regulation of AMA is more complex than currently believed. In addition to providing a basis for T cell/ MΦ contact-enhanced Arg1 expression, I showed an IL-4/13 independent pathway for Arg1 induction that appears to be mediated, at least in part, by activin A. Future studies will be required to expand on the mechanism of activin A Arg1 induction in the presence of IFN-γ.

5.2 T CELL-ASSOCIATED PRODUCTS INDUCE MACROPHAGE ARGINASE-1 EXPRESSION

(a) The role of IL-4 and IL-13 in Arg1 induction. ATC-associated products induce MΦ Arg1 expression –compared to MΦ-only cultures, as evidenced by the increased Arg1 transcript expression in MΦ/ ATC co-cultures. Arg1 expression was induced by an ATC-associated product was supported by the observation that, while Arg1 expression was induced in co-cultures when ATC were generated from whole splenocytes, it was further enhanced when ATC were generated from $CD3^+$-enriched splenocytes. T cell-cytokines IL-4 and IL-13 induce Arg1 (1), and I detected low levels of both in co-culture supernatant. However, I was surprised by the low levels of IL-4 and IL-13 in co-culture supernatants. Compared to cytokine dose-response experiments, the levels of IL-4 and IL-13 measured in co-culture seemed to be insufficient for the level of MΦ Arg1 induction observed. It is possible that IL-4 and IL-13 were present at early time-points

during MΦ/ ATC co-culture, but had been utilized past the point of detection by ELISA at the 24-hour harvest time-point. Alternatively, IL-4 and IL-13 may have been produced at low levels so that all that was produced was taken up by co-culture cells and was undetectable in co-culture supernatant. Finally, Arg1 may have been induced in our system by an ATC-associated product other than IL-4 or IL-13.

In agreement with current literature (1), I confirmed the sufficiency of IL-4 and/ or IL-13 to induce Arg1 in our culture system. WT MΦ treated with recombinant IL-4 and IL-13 expressed Arg1 in a dose-dependent manner. WT MΦ/ Ifng-deficient (GKO) ATC co-cultures, which compared to WT MΦ/ WT ATC co-cultures had high levels of IL-4 and IL-13, had corresponding high levels of Arg1. Additionally, IL-4 and IL-13 appeared to induce Arg1 expression in an additive, non-synergistic fashion.

(b) IL-4 and IL-13 –independent mechanism(s) of Arg1 induction. Surprisingly, neither IL-4 nor IL-13 were essential for Arg1 induction –when I repeated the co-culture assay using IL-4/13 receptor deficient (IL-4RKO) MΦs I still observed induction of Arg1 expression when MΦ were incubated in no-contact conditions with WT ATC. This was surprising because it is presently thought that Arg1 expression is primarily driven through pathways that directly or indirectly use IL-4 and/or IL-13 (1;45). For example, IL-10 drives Arg1 induction synergistically with IL-4 by increasing expression of the IL-4 receptor, IL-4Rα (1;92). I confirmed that Arg1 induction observed in IL-4RKO MΦ/ WT ATC co-cultures was not the result of IL-4/-13 cytokines signaling through an incompletely knocked-out IL-4Rα by checking for Arg1 induction in IL-4RKO MΦ that were treated with increasing concentrations of IL-4 and IL-13. Thus, in MΦ/ ATC co-

cultures and MΦ-only cultures IL-4 and IL-13, in addition to other soluble factor(s), induced Arg1 expression.

(c) Activin A induces Arg1 expression. Activin A, a pluripotent member of the transforming growth factor-β (TGF-β) superfamily, is produced by co-culture activated MΦs and is involved in an IL-4/13-independent pathway of Arg1 induction. Activin A was detected by ELISA at high levels in WT or IL-4RKO MΦ/ ATC. Neutralization of activin A in MΦ / ATC co-cultures significantly decreased Arg1 induction when IL-4 and IL-13 could not contribute to Arg1. I believe that the monoclonal antibody I used for activin A neutralization was not completely effective, as activin A was detectable in post-neutralization co-culture supernatant by ELISA, and that more effective neutralization of activin A would have resulted in greater attenuation of Arg1 expression. Finally, I observed that activin A induced Arg1 transcript expression in MΦ in a dose-dependent manner.

There is precedence for TGF-β superfamily member involvement in AMA, including Arg1 induction. For example, activin A is induced in tubular cells by itself or by TGF-β, and in injured kidneys it activates renal interstitial fibroblasts and contributes to fibrotic processes (84). In rat peritoneal MΦ, TGF-β enhances Arg1 activity, and in mice, activin A is produced by *in vitro* α-CD3 ATC and induces peritoneal MΦ Arg1 expression (3;93). In contrast to studies by Ogawa *et al.* (3;93) that suggested ATC-produced activin A induced MΦ Arg1, I observed high activin A gene expression only in MΦs incubated with ATC but not in α-CD3/ CD28 activated ATC or MΦ alone. However, activin A is produced by a plethora of cell types, including activated MΦs, and

in our system I believe that ATC activated MΦ produce activin A which, in turn, fed back on MΦ and acted in conjunction with ATC-produced IL-4 and IL-13 in an additive manner to induce Arg1 expression (85). In sum, our data placed in the context of current literature suggests that ATC-activated MΦ produce activin A that, in an additive manner with ATC cytokines IL-4 and IL-13, act on MΦ to induce Arg1. Thus, although the predominant pathway of Arg1 induction is IL-4 and IL-13-dependent, there appears to be an additional IL-4 and IL-13 independent pathway of Arg1 induction that includes activin A.

(d) Inhba, Arg1, and Ifng transcripts are all present in MLRs at the same time. Activin A and Arg1 production occurs in the presence of IFN-γ. Indeed, activin A transcripts were detectable in mixed lymphocyte reactions (MLRs) and MΦ cultures where both Arg1 and IFN-γ were present. Arg1 transcripts in MLRs were most likely produced by MΦ present in the splenocyte populations used as responder cells in our MLRs. As expected, I found high levels of Arg1 in IFN-γ-deficient (GKO) MLRs where transcript levels for AMA-inducing IL-4 and IL-13 are high (1). In IFN-γ competent (WT) MLRs, however, Arg1 was induced at similar levels despite lower levels of Il4 and Il13 transcripts and the ability to respond to the high levels of Ifng. This is surprising because current literature suggests that IFN-γ inhibits Arg1 induction by directing MΦ towards a CMA phenotype (94). Interestingly, Inhba transcripts were also increased in the WT MLRs, suggesting that IFN-γ might directly or indirectly increase Inhba gene expression. Indeed, activin A production can be induced in monocytes in response to IFN-γ; however the current literature is somewhat nebulous on the role of IFN-γ on Arg1 induction as it has also been

shown to inhibit activin A production in fibroblasts (73;95). I examined untreated or IFN-γ treated WT MΦ cultures and reproduced the observation that IFN-γ increased Arg1 and Inhba transcript levels. Although further study is certainly required, our results corroborate with those of others that activin A is not inhibited by IFN-γ and I propose that activin A plays an important role in Arg1 induction in the presence of IFN-γ.

(e) Activin A is present in allograft rejection. Activin A expression also correlates to IL-4 and IL-13 independent and dependent Arg1 induction *in vivo*. I examined transcript levels in allografts post-transplant into various host mice. Raw probe signal for all gene transcripts was lower than what I observed previously in MLRs and in MΦ cultures. I expect this to be because immune cell RNA in allografts is diluted by RNA derived from other non-immune cells, such as epithelial and endothelial cells, leading to a lower ratio of immune cells and thus a lower total RNA signal. In WT mouse hosts, I observed that activin A transcript expression in allografts increased at time points that corresponded to increasing Arg1 induction. In IL-4 and IL-13 receptor deficient-hosts, kidney allografts showed activin A and Arg1 transcript expression that was similar to those transplanted into WT host mice. It is not particularly surprising that activin A transcript induction is associated with IL-4 and IL-13 dependent Arg1 induction. Arg1 is induced in mononuclear cells, including MΦ, after tissue injury such as trauma or surgery –likely because injury results in an altered cytokine milieu that leans heavily towards the production of Arg1-inducing TH_2-type cytokines including IL-4 (1;41;84). In allograft rejection, Arg1 induction is enhanced by the extent of damage inflicted on the transplanted organ: Arg1 is induced at higher levels in severely rejecting allografts than

in isografts (96). TGF-β is observed in damaged epithelium and induces activin A production (70;84). Activin A has recently been grouped with other TH_2 cytokines as an inducer of Arg1 and is an important regulator of fibrogenesis in various organs, including kidney, liver, and pancreas (3;97). Additionally, activin A enhances expression of type I collagen mRNA, promotes cell proliferation, and induces the production of α-smooth muscle actin in rat kidney fibroblast cell lines and primary renal interstitial fibroblasts (84). Altogether, the current literature points to an important role for activin A in fibrosis and AMA. Activin A, together with other TH_2 type cytokines, may induce Arg1 in renal allografts and contribute to a fibrogenic disease process that is detrimental to long-term allograft survival.

In contrast to current literature, I observed strong Arg1 induction regardless of IL-4 or IL-13 (1). Furthermore, our *in vivo* data showed strong IL-4 and IL-13-independent Arg1 induction in the presence of IFN-γ. IFN-γ receptor-deficient kidneys were transplanted into IL-4 and IL-13 receptor deficient mice. The inability of the allograft to respond to IFN-γ results in enhanced Arg1 induction –independently of the host immune system's IL-4 and IL-13 responsiveness. At the present time, our laboratory is awaiting the transplantation of IFN-γ receptor-deficient allografts into WT host mice and thus cannot draw definitive conclusions from this set of transplants. However, I do know that Arg1 expression occurs in rejecting allografts independently of IL-4 and IL-13 at time-points that correspond with high Inhba and Ifng expression. IFN-γ may contribute to the high induction of Inhba, and as Inhba induces Arg1, it is possible that IL-4 and IL-13-independent Arg1 induction is mediated via the induction of Inhba by Ifng although further studies are required to validate this hypothesis(73).

5.3 MACROPHAGE/ T CELL CONTACT AND MACROPHAGE ARGINASE-1 EXPRESSION.

(a) Direct macrophage/ T cell contact enhances macrophage arginase-1 expression. Direct contact between ATC and MΦ enhances MΦ Arg1 induction. Compared to no-contact co-cultures, Arg1 induction was consistently higher in MΦ/ ATC direct-contact co-cultures. MΦ in direct-contact conditions are subjected to direct physical contact with ATC and ATC-associated cytokines. That ATC associated cytokines, particularly those of the so-called TH_2 profile, induce Arg1 induction is well established and is discussed in previous sections (1). A tentative link between direct contact of human ATC and MΦ and AMA has been proposed; as Arg1 is not a reliable marker of AMA in humans, other markers such as pro-inflammatory suppression cytokines TNF and IL-6, and upregulation of CD163, CD206, and MHC class II were examined (36;87). In this system, $CD4^+CD25^+Fox3p^+$regulatory T cells (T_{reg}) producing IL-4, 10, and 13 were shown to induce MΦ suppression of TNF and IL-6 through a mechanism that was partially dependent on direct-contact between T_{reg} and MΦ (36). The mechanism of direct-contact enhanced AMA appeared to be through adequate co-stimulation of T_{reg} by MΦ that occurred only under direct-contact co-culture conditions. Interestingly, IL-10 was detected at low levels in direct-contact conditions and not in no-contact conditions. Furthermore, neutralization of IL-4 and IL-13 did not have an effect on AMA induction and neutralization of IL-10 only partially attenuated some features of AMA. With this in mind, in our mouse-based co-culture system, MΦ/ ATC contact may have augmented IL-10 production, which increases expression of the joint IL-4 and IL-13 receptor chain, IL-

4Rα (1;98). Treating MΦ with increasing doses of recombinant IL-4 and IL-13 led to Arg1 expression that increased in a concentration-dependent manner; therefore, as more IL-10 is produced, MΦ receptivity to IL-4 and IL-13 would be increased by augmented IL-4Rα expression and lead to vigorous induction of Arg1. I also found that IL-4 and IL-13 did not appear to be essential for Arg1 induction, corroborating these authors' data and highlighting the importance of additional Arg1 inducing ATC-associated factors, such as activin A. Regardless of exactly which soluble factors are leading to Arg1 induction, I still observed that direct MΦ/ ATC contact enhanced Arg1 induction –even in IL-4Rα deficient cultures where increased production of IL-10 and thus induction of IL-4Rα would have no effect. Therefore, increased levels of IL-10 cannot be the only factor accounting for enhanced Arg1 in direct-contact conditions. In co-cultures of bone-marrow derived MΦ and Th2-skewed ATC, however, contact may not enhance Arg1 activity beyond that induced by cytokines alone (94). I believe that MΦ/ ATC contact in our co-cultures enhances uptake of scarce Arg1-promoting cytokines, leading to increased Arg1 induction. In the bone-marrow MΦ/ Th2-skewed ATC co-culture system mentioned previously, levels of IL-4 were higher than what I observed, perhaps leading to levels of Arg1 activity that could not be further enhanced by contact (94). Treating bone-marrow derived MΦs with 25% or 75% ATC supernatant led to similar levels of Arg1 activity as in MΦ incubated directly with ATC, indicating saturating levels of Arg1-inducing cytokines in their system –something which our ELISA data indicated was not a factor in our co-cultures. In our system, Arg1 induction may not have reached a maximal induction; thus, it is possible that contact improved cytokine uptake and enhanced Arg1 induction. Alternatively, direct MΦ-ATC contact could trigger a receptor-

mediated cascade that ultimately led to the increase of Arg1 induction. Further studies are required, and this possibility cannot be formally excluded at this time. In sum, MΦ Arg1 was induced by ATC-associated products and further enhanced by ATC-MΦ contact.

(b) Direct macrophage/ T cell contact enhances Arg1 expression in the presence of IFN-γ. Enhancement of MΦ Arg1 expression is increased by MΦ/ ATC direct-contact only when IFN-γ is present. In MΦ/ IFN-γ deficient ATC co-cultures, Arg1 induction was similar in no-contact and direct-contact conditions. Comparatively, Arg1 induction in MΦ/ WT ATC co-cultures was higher in direct-contact conditions than in no-contact conditions. I confirmed that IFN-γ-deficient ATC are utterly devoid of IFN-γ because IFN-γ is not produced by MΦs in our co-culture system, as confirmed by cytokine ELISAs. Furthermore, our laboratory has previously used microarray analysis to show that IFN-γ is not produced by untreated MΦ, or in MΦ treated with a combination of LPS, IFN-γ, or IL-4.

Although it is not known to increase induction of Arg1, IFN-γ influences a number of genes that could indirectly have this effect. The transcription factor T-box expressed in T cells (T-bet) drives IFN-γ production and suppresses TH_2 differentiation (99). T-bet mediates this through inhibition of GATA-3, an important transcriptional regulator of TH_2 cytokines (100). IFN-γ gene regulation is part of an autocrine loop: IFN-γ, upon binding its receptor, leads to tyrosine phosphorylation of Jak1 and Stat1, nuclear translocation and transcriptional activity of Stat1 homodimers, and expression of genes encoding proteins important for Th1 development such as T-bet. Thus, IFN-γ regulates a

transcription factor that promotes its own production (101). Observations within our laboratory have shown that kidney allografts with compromised MHC class I presentation or inability to respond to IFN-γ display accelerated graft necrosis and elevated levels of Arg1 (102). Altogether, this suggests that, in our IFN-γ deficient ATC co-cultures, T-bet expression is not enhanced by IFN-γ and cannot subsequently inhibit GATA-3. Thus, much higher levels of IL-4 and IL-13 are observed in IFN-γ deficient co-cultures. Furthermore, IFN-γ induces synthesis of suppressor of cytokine signaling (SOCS)-1, a negative regulatory factor that suppresses tyrosine phosphorylation and subsequent activation of STAT-6 (62). As many IL-4 and IL-13 responsive genes have STAT-6 binding sites, inhibition of STAT-6 equates to inhibition of many IL-4 and IL-13 responsive genes. Together with the higher levels of IL-4 and IL-13, decreased SOCS-1 inhibition of STAT-6 in IFN-γ deficient co-cultures could explain the overall higher levels of Arg1 induction compared to WT co-cultures. Furthermore, the levels of IL-4 and IL-13 in IFN-γ deficient co-cultures were likely high enough that a maximum level of Arg1 expression had been reached beyond which not even contact could further increase. Evidence of a ceiling of Arg1 induction was demonstrated by our IL-4 and IL-13 dose-response experiments where Arg1 expression increased in a dose-dependent manner until a maximum level of Arg1 expression. Beyond this point, Arg1 could not be further increased even upon treatment with additional cytokine. As discussed in a previous section, direct-contact in the WT co-cultures may simply enhance uptake of available Arg1-inducing cytokine leading to higher levels of Arg1 induction. When there is IFN-γ in the co-culture system, availability of these cytokines is limiting and thus contact is an important enhancer of Arg1.

Activin A levels were higher in direct-contact co-cultures than in no-contact co-cultures. Activin A is markedly induced in monocytes and fibroblasts by a cognate interaction with ATC, likely by an interaction of CD40 with its ligand CD40L and by concomitantly produced T cell cytokines –which include IFN-γ (73). Thus, direct-contact and IFN-γ in WT co-cultures may explain contact-enhanced Arg1 induction. An additional possibility is that direct-contact enhancement of Arg1 expression is the result of an IFN-γ-controlled molecule. In IFN-γ-deficient co-cultures this hypothetical molecule would not be altered by IFN-γ and, in conditions of direct-contact, would not enhance Arg1 expression. I investigated the role of H2-T23 (Qa1) contact-enhanced Arg1 induction as our laboratory has previously observed that kidney allografts with compromised MHC class I presentation machinery express less H2-T23 than WT kidney allografts. H2-T23 associates preferentially with a peptide, Qdm, that is derived from class I signal sequences; thus IFN-γ and H2-T23 are linked because class I MHC expression is induced in response to IFN-γ, by interferon-regulatory factor 1 recognizing an interferon consensus sequence and initiating gene expression (103;104). H2-T23 is a ligand for the CD94/NKG2 receptors, including the inhibitory receptor CD94/NKG2A (103). As CD94/NKG2 receptors are expressed on NK cells as well as a peripheral blood population of predominantly CD8+ αβ-T cells (105), it is plausible that one of the CD94/NKG2 receptors on alloreactive T cells is involved in MΦ Arg1 induction (105). In contact assays using CD94-deficient ATC, derived from DBA2 mice, I found Arg1 expression to be similar in direct-contact or no-contact conditions. This suggests that enhancement of Arg1 expression by direct-contact between ATC/ MΦ could be due to interactions between H2-T23 and CD94/NKG2A/C/E. Alternatively, the lack of effect of

ATC/ MΦ contact on Arg1 induction in DBA2 co-cultures could be a result of a different cytokine milieu. Indeed, compared to BALB/c co-cultures, IL-4 and IL-13 concentrations in DBA2 co-cultures were high which could lead to maximal induction of Arg1 regardless of direct-contact or no-contact conditions. Further studies will be required to determine the role of H2-T23 –CD94/NKG2A/C/E interactions on Arg1 induction. In conclusion, contact-dependent Arg1 enhancement only occurs in the presence of IFN-γ and the mechanism for Arg1 enhancement remains unclear.

5.4 FUTURE DIRECTIONS

Our results indicated a role for T cell contact in MΦ Arg1 induction. However, I first sought to completely understand the soluble factors present in both the direct-contact and no-contact conditions prior to attempting to dissect the mechanism(s) of contact-dependent Arg1 induction. Future studies will focus directly on the role of T cell contact on MΦ Arg1 expression. Indeed, our laboratory is currently waiting the arrival of H2-T23 deficient mice, which I anticipate will have an effect on Arg1 expression. Our laboratory will transplant H2-T23-deficient kidneys into allogeneic hosts and use microarray analysis to examine induction of macrophage activation genes. In addition, it would be of scientific merit to repeat the co-culture assays using MΦs generated in H2-T23 mice.

Arg1 is a reliable marker of AMA in mice. However, it is not a marker of AMA in humans (87) and our ultimate hope is to translate the immunological lessons learned in

our mouse-based systems into something that will be of clinical relevance to humans. Thus, subsequent studies should examine a broader array of AMA markers that are also found in humans. More to the point, our *in vitro* co-culture studies should be repeated using human-derived cells. For example, T cells and MΦ purified by immuno-magnetic bead selection from human-peripheral blood can easily be obtained. Such studies are currently ongoing.

I derived our primary MΦ from peritoneal cells from mice that had been injected with thioglycollate medium. This is a commonly used method of obtaining MΦs. However, our microarray studies on untreated MΦ indicated a constitutive level of MΦ Arg1 expression which is contradictory to literature suggesting that Arg1 expression in resting MΦ is not constitutive and must be induced (92). It would be useful, however, to repeat the co-culture assays using MΦs generated in a different manner –perhaps bone-marrow derived MΦs which should show the lowest level of activation.

The correlations of Ifng and Inhba expression was surprising, and it would be interesting to observe the direct effects of IFN-γ on Inhba expression, and, consequently, on Arg1 expression. This could be accomplished by addition of recombinant IFN-γ to co-culture supernatant at various times post-incubation and measuring Inhba and Arg1 gene expression by RT-PCR.

I could examine both mRNA and protein expression of activin A, IL-13, IL-4, and IFN-γ due to the bio-distribution of these molecules and the availability of reliable ELISA antibodies and RT-PCR/ microarray probe sets. However, I only examined the mRNA level of Arg1 expression in co-culture because Arg1 is not secreted into co-culture supernatant. Future studies would benefit from examining Arg1 protein

expression in each co-culture conditions directly. This could be accomplished by Western blot or, alternatively, by enzyme-based systems (106).

I was not able to attain complete neutralization of Arg1 expression by addition of α-activin A antibody. This could be due to another molecule inducing Arg1 expression in the absence of IL-4, IL-13, and activin A. Incomplete neutralization of activin A would be a simple explanation of the residual Arg1 induction observed post-anti-activin A antibody treatment. Follistatin binds the activin A receptor with high affinity and thus is a competitive inhibitor of activin A (81). It would be edifying to repeat the neutralization studies using follistatin.

5.5 CONCLUSIONS

The initial studies described herein characterized a reliable MΦ/ ATC co-culture system that allowed for the dissection of the ATC-associated factors under direct-contact and no-contact MΦ/ ATC co-culture conditions that contributed to Arg1 induction. Our results indicated a previously undocumented role of ATC contact on MΦ Arg1 induction. Furthermore, I described IL-4 and IL-13 dependent and independent mechanisms of AMA induction that were relevant both in *in vitro* and *in vivo* and that appeared to operate despite, and perhaps even in conjunction with, simultaneous Ifng expression. Preliminary studies within our laboratory by Gunilla Einecke have shown that human kidney epithelium can be induced to express Inhba transcripts by TGF-β and injured kidney epithelium can produce TGF-β (84). Together with these studies, this observation

has very important implications for human kidney allograft rejection: One could imagine a situation where TGF-β secreted by infiltrating allogeneic ATC and damaged kidney epithelium could induce kidney epithelium to produce activin A. Furthermore, IFN-γ and other T cell-associated molecules produced by ATC would provoke MΦs into producing more activin A. Together with activin A produced by kidney epithelium, the activin A produced by infiltrating MΦs could induce Arg1 in the same population of MΦs. In fully immuno-competent hosts, traditional AMA-inducing cytokines IL-4 and IL-13 produced by allogeneic ATC would be a major contributor to Arg1 induction.

Initially, our laboratory was of the opinion that the correlation of high Arg1 with severe allograft damage was due to Arg1-mediated depletion of L-Arginine thus compromising the allograft microcirculation. However, unpublished observations showed that Arg1 inhibitor L-NOHA had no effect on the severity of kidney rejection as scored by histology suggesting that Arg1 may not be a direct-inducer of allograft rejection. Rather, it may be a response of immune cells to damaged, rejecting kidney epithelium. Arg1 and other AMA products are associated with fibrogenic disease processes, and fibrogenesis is associated with poor long term prognosis and quality of life in kidney transplant patients (107). Understanding the regulation of Arg1 and other AMA markers is thus important to promoting long-term graft survival, and these studies have indicted additional players in the AMA-paradigm. The specific findings of this project are summarized below and are depicted in Figure 5a:

1) ATC-associated products induce MΦ Arg1 expression

2) In addition to IL-4 and IL-13, activin A is present in MΦ/ ATC co-cultures and contributes to the induction of MΦ Arg1 expression

3) Activin A is present at time-points that correspond with induction of Arg1 expression in *in vivo* allografts

4) MΦ Arg1 expression is further enhanced by direct MΦ/ ATC cell contact

5) Enhancement of MΦ Arg1 induction by MΦ / ATC cell contact is dependent on ATC IFN-γ production

5.6 FIGURES

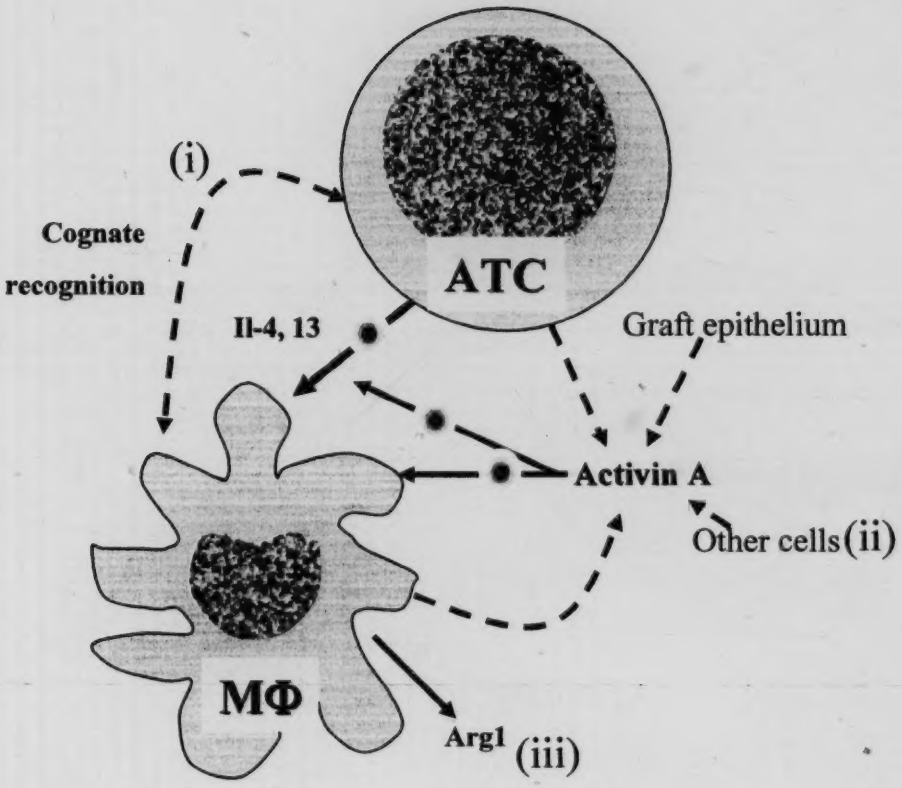

Figure 5a. Activin A in the context of an immune response. Our experimental results indicate that (i) cognate interaction between ATC and MΦ enhances production of activin A by MΦs. Additionally, (ii) multiple cell types are known to produce activin A, including kidney epithelium (21). Finally, (iii) activin A, both on its own and in conjunction with IL-4 and IL-13 induce Arg1 expression by MΦ.

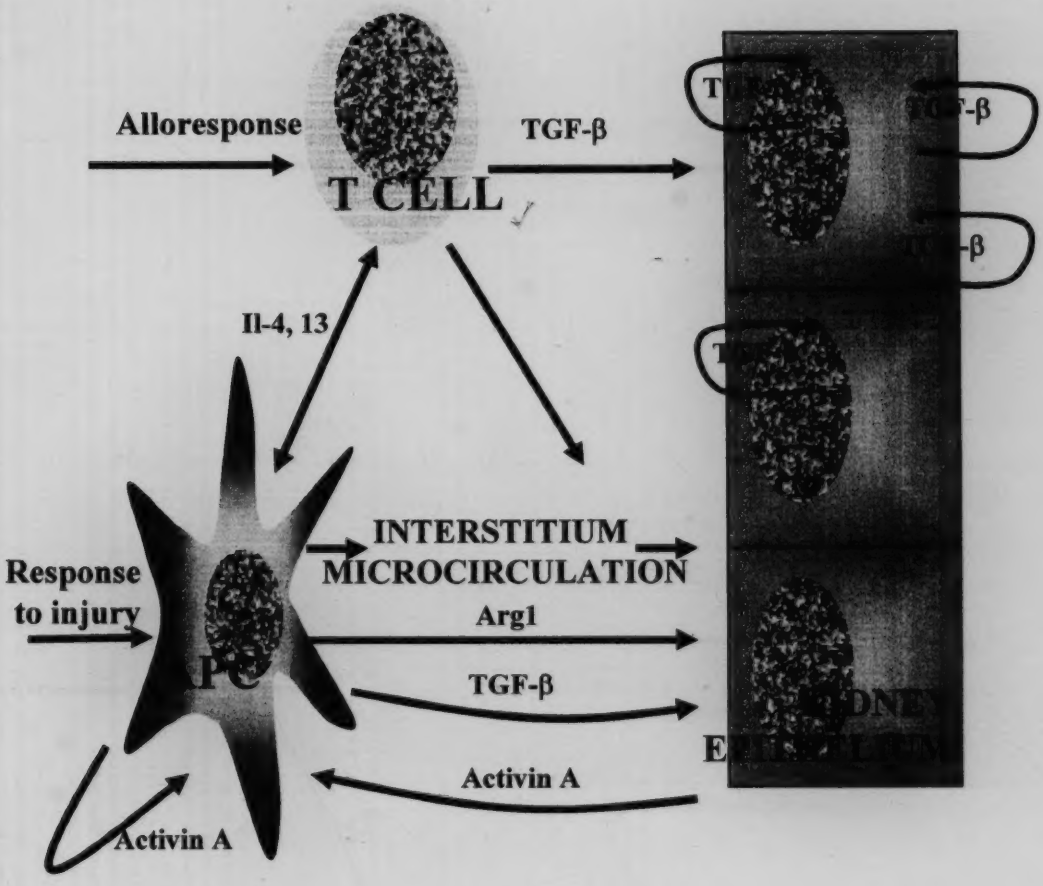

Figure 5b. The big picture of allograft rejection. As depicted in Figure 1a, allograft rejection is believed to be a process mediated largely by T cells and MΦ. We have shown that Activin A, together with IL-4 and IL-13, acts on MΦ to induce Arg1 expression (Figure 5a). Futhermore, TGF-β, which is produced by T cells, MΦ, and damaged kidney epithelium, induces activin A expression by epithelium and presumably feeds back to enhance MΦ Arg1 expression. At this point in time, it is not known whether Arg1 is an inducer or a consequence of allograft damage, but its expression is associated with rejection events such as loss of transcripts, change in cell polarity, cell death, epithelial-mesenchyme transition, atrophy, tubulitis, and nephron shutdown.

Reference List

(1) Gordon S. Alternative activation of macrophages. Nat Rev Immunol 2003; 3(1):23-35.

(2) Sis B, Famulski KS, Allanach K, Zhu L-F, Halloran PF. IFN-γ prevents early perforin-granzyme-mediated destruction of kidney allografts by inducing donor class I products in the kidney. Am J Transplant 2007; 7(10):2301-2310.

(3) Ogawa K, Funaba M, Chen Y, Tsujimoto M. Activin A functions as a Th2 cytokine in the promotion of the alternative activation of macrophages. Journal of Immunology 2006; 177(10):6787-6794.

(4) O'Connor KJ, Delmonico FL. Increasing the supply of kidneys for transplantation. Seminars in Dialysis 2005; 18(6):460-462.

(5) Hancock WW, Thomson NM, Atkins RC. Composition of Interstitial Cellular Infiltrate Identified by Monoclonal-Antibodies in Renal Biopsies of Rejecting Human Renal-Allografts. Transplant 1983; 35(5):458-463.

(6) Einecke G, Fairhead T, Hidalgo LG, Sis B, Turner P, Zhu LF et al. Tubulitis and Epithelial Cell Alterations in Mouse Kidney Transplant Rejection Are Independent of CD103, Perforin or Granzymes A/B. Am J Transplant 2006; 6(9):2109-2120.

(7) Halloran PF, Urmson J, Ramassar V, Melk A, Zhu LF, Halloran BP et al. Lesions of T-cell-mediated kidney allograft rejection in mice do not require perforin or granzymes A and B. Am J Transplant 2004; 4(5):705-712.

(8) Cozzi E, Seveso M, Hutabba S, Fabris S, Cavicchioli L, Ancona E. An update on Xenotransplantation. Veterinary Research Communications 2007; 31:15-25.

(9) Martina Y, Kurian S, Cherqui S, Evanoff G, Wilson C, Salomon DR. Pseudotyping of porcine endogenous retrovirus by xenotropic murine leukemia virus in a pig islet xenotransplantation model. Am J Transplant 2005; 5(8):1837-1847.

(10) Shoskes DA, Parfrey NA, Halloran PF. Increased Major Histocompatibility Complex Antigen Expression in Unilateral Ischemic Acute Tubular-Necrosis in the Mouse. Transplant 1990; 49(1):201-207.

(11) Goes N, Urmson J, Ramassar V, Halloran PF. Ischemic acute tubular necrosis induces an extensive local cytokine response: evidence for induction of interferon-γ, transforming growth factorβ-1, granulocyte-macrophage colony-stimulating factor, interleukin-2 and interleukin-10. Transplant 1995; 59:565-572.

(12) Medzhitov R, Janeway CA, Jr. Innate immune recognition and control of adaptive immune responses. Semin Immunol 1998; 10(5):351-353.

(13) Vongwiwatana A, Tasanarong A, Hidalgo LG, Halloran PF. The role of B cells and alloantibody in the host response to human organ allografts. Immunol Rev 2003; 196:197-218.

(14) Einecke G, Melk A, Ramassar V, Zhu LF, Bleackley RC, Famulski KS et al. Expression of CTL associated transcripts precedes the development of tubulitis in T-cell mediated kidney graft rejection. Am J Transplant 2005; 5(8):1827-1836.

(15) Hidalgo LG, Halloran P. Comprehensive Clinical Nephrology. 2 ed. Mosby, 2008.

(16) Gordon S, Taylor PR. Monocyte and macrophage heterogeneity. Nat Rev Immunol 2005; 5(12):953-964.

(17) Hume DA, Ross IL, Himes SR, Sasmono RT, Wells CA, Ravasi T. The mononuclear phagocyte system revisited. J Leuk Biol 2002; 72(4):621-627.

(18) Unanue ER. Antigen-Presenting Function of the Macrophage. Annual Review of Immunology 1984; 2:395-428.

(19) McKnight AJ, Gordon S. The EGF-TM7 family: unusual structures at the leukocyte surface. J Leuk Biol 1998; 63(3):271-280.

(20) Morris L, Graham CF, Gordon S. Macrophages in haemopoietic and other tissues of the developing mouse detected by the monoclonal antibody F4/80. Development 1991; 112(2):517-526.

(21) Lin HH, Faunce DE, Stacey M, Terajewicz A, Nakamura T, Zhang-Hoover J et al. The macrophage F4/80 receptor is required for the induction of antigen-specific efferent regulatory T cells in peripheral tolerance. The Journal of Experimental Medicine 2005; 201(10):1615-1625.

(22) Ezekowitz RA, Austyn J, Stahl PD, Gordon S. Surface properties of bacillus Calmette-Guerin-activated mouse macrophages. Reduced expression of mannose-specific endocytosis, Fc receptors, and antigen F4/80 accompanies induction of Ia. The Journal of Experimental Medicine 1981; 154(1):60-76.

(23) Ravetch JV, Bolland S. IGG FC RECEPTORS. Annual Review of Immunology 2001; 19(1):275-290.

(24) Bajtay Z, Jozsi M, Banki Z, Thiel S, Thielens N, Erdei A. Mannan-binding lectin and C1q bind to distinct structures and exert differential effects on macrophages. Eur J Immunol 2000; 30(6):1706-1713.

(25) Balagopal A, MacFarlane AS, Mohapatra N, Soni S, Gunn JS, Schlesinger LS. Characterization of the Receptor-Ligand Pathways Important for Entry and Survival of Francisella tularensis in Human Macrophages. Infection and Immunity 2006; 74(9):5114-5125.

(26) Duffield JS. The inflammatory macrophage: a story of Jekyll and Hyde. Clin Sci 2003; 104(1):27-38.

(27) Farraris JR, Day PF, Gutman R, Granillo E, Ramirez J, Ruiz S et al. Effect of therapy with a new glucocorticoid, deflazacort, on linear growth and growth hormone secretion after renal transplantation. J Pediatr 1992; 121:809-813.

(28) Ma J, Chen T, Mandelin J, Ceponis A, Miller NE, Hukkanen M et al. Regulation of macrophage activation. Cell Mol Life Sci 2003; 60(11):2334-2346.

(29) Duffield JS, Erwig LP, Wei XQ, Liew FY, Rees AJ, Savill JS. Activated macrophages direct apoptosis and suppress mitosis of mesangial cells. Journal of Immunology 2000; 164(4):2110-2119.

(30) Gibbs DF, Warner RL, Weiss SJ, Johnson KJ, Varani J. Characterization of matrix metalloproteinases produced by rat alveolar macrophages. American Journal of Respiratory Cell and Molecular Biology 1999; 20(6):1136-1144.

(31) Mariani TJ, Sandefur S, Roby JD, Pierce RA. Collagenase-3 induction in rat lung fibroblasts requires the combined effects of tumor necrosis factor-alpha and 12-lipoxygenase metabolites: A model of macrophage-induced, fibroblast-driven extracellular matrix remodeling during inflammatory lung injury. Mol Biol Cell 1998; 9(6):1411-1424.

(32) Kitamura M. TGF-beta 1 as an endogenous defender against macrophage-triggered stromelysin gene expression in the glomerulus. Journal of Immunology 1998; 160(10):5163-5168.

(33) Mantovani A, Sica A, Locati M. New vistas on macrophage differentiation and activation. Eur J Immunol 2007; 37(1):14-16.

(34) Pender MP, Rist MJ. Apoptosis of inflammatory cells in immune control of the nervous system: Role of glia. Glia 2001; 36(2):137-144.

(35) Tesch GH, Schwarting A, Kinoshita K, Lan HY, Rollins BJ, Kelley VR. Monocyte chemoattractant protein-1 promotes macrophage-mediated tubular injury, but not glomerular injury, in nephrotoxic serum nephritis. J Clin Invest 1999; 103(1):73-80.

(36) Tiemessen MM, Jagger AL, Evans HG, van Herwijnen MJ, John S, Taams LS. CD4+CD25+Foxp3+ regulatory T cells induce alternative activation of human monocytes/macrophages. Proc Natl Acad Sci U S A 2007; 104(49):19446-19451.

(37) Raes G, Noel W, Beschin A, Brys L, De Baetselier P, Hassanzadeh GH. FIZZ1 and Ym as tools to discriminate between differentially activated macrophages. Dev Immunol 2002; 9(3):151-159.

(38) Holscher C, Arendse B, Schwegmann A, Myburgh E, Brombacher F. Impairment of alternative macrophage activation delays cutaneous leishmaniasis in nonhealing BALB/c mice. Journal of Immunology 2006; 176(2):1115-1121.

(39) Christianson DW. Arginase: Structure, mechanism, and physiological role in male and female sexual arousal. Accounts of Chemical Research 2005; 38(3):191-201.

(40) Pauleau AL, Rutschman R, Lang R, Pernis A, Watowich SS, Murray PJ. Enhancer-mediated control of macrophage-specific arginase I expression. Journal of Immunology 2004; 172(12):7565-7573.

(41) Ochoa JB, Bernard AC, O'Brien WE, Griffen MM, Maley ME, Rockich AK et al. Arginase I expression and activity in human mononuclear cells after injury. Ann Surg 2001; 233(3):393-399.

(42) Morris SM. Regulation of Enzymes of Urea and Arginine Synthesis. Annual Review of Nutrition 1992; 12:81-101.

(43) Gray MJ, Poijakovic M, Kepka-Lenhart D, Morris SM. Induction of arginase I transcription by IL-4 requires a composite DNA response element for STAT6 and C/EBP beta. Gene 2005; 353(1):98-106.

(44) Hesse M, Modolell M, La Flamme AC, Schito M, Fuentes JM, Cheever AW et al. Differential regulation of nitric oxide synthase-2 and arginase-1 by type 1/type 2 cytokines in vivo: granulomatous pathology is shaped by the pattern of L-arginine metabolism. Journal of Immunology 2001; 167(11):6533-6544.

(45) Iniesta V, Gomez-Nieto LC, Molano I, Mohedano A, Carcelen J, Miron C et al. Arginase I induction in macrophages, triggered by Th2-type cytokines, supports the growth of intracellular Leishmania parasites. Parasite Immunology 2002; 24(3):113-118.

(46) Bansal V, Ochoa JB. Arginine availability, arginase, and the immune response. Current Opinion in Clinical Nutrition and Metabolic Care 2003; 6(2):223-228.

(47) Meurs H, Mckay S, Maarsingh H, Hamer MAM, Macic L, Molendijk N et al. Increased arginase activity underlies allergen-induced deficiency of cNOS-derived nitric oxide and airway hyperresponsiveness. Br J Pharmacol 2002; 136(3):391-398.

(48) Morelli AE, Thomson AW. Tolerogenic dendritic cells and the quest for transplant tolerance. Nat Rev Immunol 2007; 7(8):610-621.

(49) Verginis P, Li HS, Carayanniotis G. Tolerogenic semimature dendritic cells suppress experimental autoimmune thyroiditis by activation of thyroglobulin-specific CD4(+)CD25(+) T cells. Journal of Immunology 2005; 174(11):7433-7439.

(50) Green DR, Droin N, Pinkoski M. Activation-induced cell death in T cells. Immunological Reviews 2003; 193(1):70-81.

(51) Heeger PS, Greenspan NS, Kuhlenschmidt S, Dejelo C, Hricik DE, Schulak JA et al. Pretransplant frequency of donor-specific, IFN-gamma-producing lymphocytes is a manifestation of immunologic memory and correlates with the risk of posttransplant rejection episodes. Journal of Immunology 1999; 163(4):2267-2275.

(52) Bingaman AW, Farber DL. Memory T cells in transplantation: generation, function, and potential role in rejection. Am J Transplant 2004; 4(6):846-852.

(53) Jiang S, Herrera O, Lechler RI. New spectrum of allorecognition pathways: implications for graft rejection and transplantation tolerance. Curr Opin Immunol 2004; 16(5):550-557.

(54) O'Farrell AM, Liu Y, Moore KW, Mui ALF. IL-10 inhibits macrophage activation and proliferation by distinct signaling mechanisms: evidence for Stat3-dependent and -independent pathways. Embo Journal 1998; 17(4):1006-1018.

(55) Moore KW, Malefyt RD, Coffman RL, O'Garra A. Interleukin-10 and the interleukin-10 receptor. Annual Review of Immunology 2001; 19:683-765.

(56) Zuegg J, Webb DC, Foster PS, Casarotto MG. Structural model of human IL-13 defines the spatial interactions with the IL-13R alpha/IL-4R alpha receptor. Immunology and Cell Biology 2001; 79(4):332-339.

(57) Kelly-Welch AE, Hanson EM, Boothby MR, Keegan AD. Interleukin-4 and interleukin-13 signaling connections maps. Science 2003; 300(5625):1527-1528.

(58) Murphy KM, Ouyang W, Farrar JD, Yang JF, Ranganath S, Asnagli H et al. Signaling and transcription in T helper development. Annual Review of Immunology 2000; 18:451-494.

(59) Masuda A, Yoshikai Y, Kume H, Matsuguchi T. The interaction between GATA proteins and activator protein-1 promotes the transcription of IL-13 in mast cells. Journal of Immunology 2004; 173(9):5564-5573.

(60) Takemoto N, Kamogawa Y, Lee HJ, Kurata H, Arai K, O'Garra A et al. Cutting edge: Chromatin remodeling at the IL-4/IL-13 intergenic regulatory region for Th2-specific cytokine gene cluster. Journal of Immunology 2000; 165(12):6687-6691.

(61) Hidalgo LG, Halloran PF. Role of IFN-gamma in allograft rejection. Crit Rev Immunol 2002; 22(4):317-349.

(62) Dickensheets HL, Venkataraman C, Schindler U, Donnelly RP. Interferons inhibit activation of STAT6 by interleukin 4 in human monocytes by inducing SOCS-1 gene expression. Proceedings of the National Academy of Sciences of the United States of America 1999; 96(19):10800-10805.

(63) Mueller TD, Zhang JL, Sebald W, Duschl A. Structure, binding, and antagonists in the IL-4/IL-13 receptor system. Biochim Biophys Acta 2002; 1592(3):237-250.

(64) Hsieh FH, Lam BK, Penrose JF, Austen KF, Boyce JA. T helper cell type 2 cytokines coordinately regulate immunoglobulin E-dependent cysteinyl leukotriene production by human cord blood-derived mast cells: Profound induction of leukotriene C-4 synthase expression by interleukin 4. J Exp Med 2001; 193(1):123-133.

(65) Finkelman FD, Urban JF. The other side of the coin: The protective role of the T(H)2 cytokines. Journal of Allergy and Clinical Immunology 2001; 107(5):772-780.

(66) Fujitsu Y, Fukuda K, Kumagai N, Nishidaa T. IL-4-induced cell proliferation and production of extracellular matrix proteins in human conjunctival fibroblasts. Experimental Eye Research 2003; 76(1):107-114.

(67) Pernis AB, Rothman PB. JAK-STAT signaling in asthma. J Clin Invest 2002; 109(10):1279-1283.

(68) Minty A, Chalon P, Derocq JM, Dumont X, Guillemot JC, Kaghad M et al. Interleukin-13 is a new human lymphokine regulating inflammatory and immune responses. Nature 1993; 362:248-250.

(69) Punnonen J, Aversa G, Cocks BG, McKenzie ANJ, Menon S, Zurawski G et al. Interleukin-13 Induces Interleukin-4-Independent Igg4 and Ige Synthesis and Cd23 Expression by Human B-Cells. Proceedings of the National Academy of Sciences of the United States of America 1993; 90(8):3730-3734.

(70) Welt C, Sidis Y, Keutmann H, Schneyer A. Activins, inhibins, and follistatins: From endocrinology to signaling. A paradigm for the new millennium. Experimental Biology and Medicine 2002; 227(9):724-752.

(71) Ebert S, Zeretzke M, Nau R, Michel U. Microglial cells and peritoneal macrophages release activin A upon stimulation with Toll-like receptor agonists. Neuroscience Letters 2007; 413(3):241-244.

(72) Jones KL, Mansell A, Patella S, Scott BJ, Hedger MP, de Kretser DM et al. Activin A is a critical component of the inflammatory response, and its binding protein, follistatin, reduces mortality in endotoxemia. Proceedings of the National

Academy of Sciences of the United States of America 2007; 104(41):16239-16244.

(73) Abe M, Shintani Y, Eto Y, Harada K, Kosaka M, Matsumoto T. Potent induction of activin A secretion from monocytes and bone marrow stromal fibroblasts by cognate interaction with activated T cells. J Leuk Biol 2002; 72(2):347-352.

(74) Hess S, Rensingehl A, Schwabe R, Bufler P, Engelmann H. Cd40 Function in Nonhematopoietic Cells - Nuclear Factor Kappa-B Mobilization and Induction of Il-6 Production. Journal of Immunology 1995; 155(10):4588-4595.

(75) Kiener PA, Morandavis P, Rankin BM, Wahl AF, Aruffo A, Hollenbaugh D. Stimulation of Cd40 with Purified Soluble Gp39 Induces Proinflammatory Responses in Human Monocytes. Journal of Immunology 1995; 155(10):4917-4925.

(76) Huo L, Rothstein TL. Receptor-Specific Induction of Individual Ap-1 Components in B-Lymphocytes. Journal of Immunology 1995; 154(7):3300-3309.

(77) Tanimoto K, Murakami K, Fukamizu A. Possible Roles of the 3'-Flanking Sequences of the Human Activin Beta-A-Subunit Gene in Its Expression. Arch Biochem Biophys 1993; 302(2):409-416.

(78) Yang Y, Wilson JM. CD40 ligand-dependent T cell activation: requirement of B7-CD28 signaling through CD40. Science 1996; 273:1862-1864.

(79) Cho SH, Yao ZB, Wang SW, Alban RF, Barbers RG, French SW et al. Regulation of activin A expression in mast cells and asthma: Its effect on the proliferation of human airway smooth muscle cells. Journal of Immunology 2003; 170(8):4045-4052.

(80) Funaba M, Ikeda T, Ogawa K, Abe M. Calcium-regulated expression of activin A in RBL-2H3 mast cells. Cellular Signalling 2003; 15(6):605-613.

(81) Butler CM, Gold EJ, Risbridger GP. Should activin beta C be more than a fading snapshot in the activin/TGF beta family album? Cytokine & Growth Factor Reviews 2005; 16(4-5):377-385.

(82) Schneyer AL, Rzucidlo DA, Sluss PM, Crowley WF. Characterization of Unique Binding-Kinetics of Follistatin and Activin Or Inhibin in Serum. Endocrinology 1994; 135(2):667-674.

(83) Munz B, Tretter YP, Hertel M, Engelhardt F, Alzheimer C, Werner S. The roles of activins in repair processes of the skin and the brain. Mol Cell Endocrinol 2001; 180(1-2):169-177.

(84) Yamashita S, Maeshima A, Kojima I, Nojima Y. Activin A is a potent activator of renal interstitial fibroblasts. JASN 2004; 15(1):91-101.

(85) Ogawa K, Funaba M, Mathews LS, Mizutani T. Activin A stimulates type IV collagenase (matrix metalloproteinase-2) production in mouse peritoneal macrophages. Journal of Immunology 2000; 165(6):2997-3003.

(86) McLean CA, Cleland H, Moncrieff NJ, Barton RJ, de Kretser DM, Phillips DJ. Temporal expression of activin in acute burn wounds—From inflammatory cells to fibroblasts. Burns : journal of the International Society for Burn Injuries 2008; 34(4):50-55.

(87) Raes G, Van den Bergh R, De Baetselier P, Ghassabeh GH. Arginase-1 and Ym1 are markers for murine, but not human, alternatively activated myeloid cells. Journal of Immunology 2005; 174(11):6561.

(88) Halloran PF, Afrouzian M, Ramassar V, Urmson J, Zhu LF, Helms LM et al. Interferon-gamma acts directly on rejecting renal allografts to prevent graft necrosis. Am J Pathol 2001; 158(1):215-226.

(89) Brown CW, Houston-Hawkins DE, Woodruff TK. Insertion of Inhbb into the Inhba locus rescues the Inhba-null phenotype and reveals new activin functions. Nat Genet 2000; 25(4):453-457.

(90) Song EW, Ouyang N, Horbelt M, Antus B, Wang MH, Exton MS. Influence of alternatively and classically activated macrophages on fibrogenic activities of human fibroblasts. Cellular Immunology 2000; 204(1):19-28.

(91) Morris SM, Jr., Kepka-Lenhart D, Chen LC. Differential regulation of arginases and inducible nitric oxide synthase in murine macrophage cells. Am J Physiol 1998; 275(5 Pt 1):E740-E747.

(92) Munder M, Eichmann K, Moran JM, Centeno F, Soler G, Modolell M. Th1/Th2-regulated expression of arginase isoforms in murine macrophages and dendritic cells. Journal of Immunology 1999; 163(7):3771-3777.

(93) Boutard V, Havouis R, Fouqueray B, Philippe C, Moulinoux JP, Baud L. Transforming Growth-Factor-Beta Stimulates Arginase Activity in Macrophages - Implications for the Regulation of Macrophage Cytotoxicity. Journal of Immunology 1995; 155(4):2077-2084.

(94) Munder M, Eichmann K, Modolell M. Alternative metabolic states in murine macrophages reflected by the nitric oxide synthase/arginase balance: competitive regulation by CD4+ T cells correlates with Th1/Th2 phenotype. Journal of Immunology 1998; 160(11):5347-5354.

(95) Abe M, Shintani Y, Eto Y, Harada K, Fujinaka Y, Kosaka M et al. Interleukin-1 beta enhances and interferon-gamma suppresses activin A actions by reciprocally

regulating activin A and follistatin secretion from bone marrow stromal fibroblasts. Clinical and Experimental Immunology 2001; 126(1):64-68.

(96) Famulski K, Sis B, Billesberger L, Halloran P. Interferon-γ and donor MHC class I control alternative macrophage activation and activin expression in rejecting kidney allografts: a shift in the TH1-TH2 paradigm . Am J Transplant 2008; 8:547-556.

(97) Werner S, Alzheimer C. Roles of activin in tissue repair, fibrosis, and inflammatory disease. Cytokine Growth Factor Rev 2006; 17(3):157-171.

(98) Lang R, Patel D, Morris JJ, Rutschman RL, Murray PJ. Shaping gene expression in activated and resting primary macrophages by IL-10. Journal of Immunology 2002; 169(5):2253-2263.

(99) Szabo SJ, Kim ST, Costa GL, Zhang X, Fathman CG, Glimcher LH. A novel transcription factor, T-bet, directs Th1 lineage commitment. Cell 2000; 100(6):655-669.

(100) Yin Z, Chen C, Szabo SJ, Glimcher LH, Ray A, Craft J. T-Bet expression and failure of GATA-3 cross-regulation lead to default production of IFN-gamma by gammadelta T cells. Journal of Immunology 2002; 168(4):1566-1571.

(101) Lighvani AA, Frucht DM, Jankovic D, Yamane H, Aliberti J, Hissong BD et al. T-bet is rapidly induced by interferon-gamma in lymphoid and myeloid cells. Proc Natl Acad Sci U S A 2001; 98(26):15137-15142.

(102) Famulski KS, Sis B, Billesberger L, Halloran PF. Interferon-gamma and donor MHC class I control alternative macrophage activation and activin expression in rejecting kidney allografts: a shift in the Th1-Th2 paradigm. Am J Transplant 2008; 8(3):547-556.

(103) Vance RE, Jamieson AM, Raulet DH. Recognition of the class Ib molecule Qa-1(b) by putative activating receptors CD94/NKG2C and CD94/NKG2E on mouse natural killer cells. J Exp Med 1999; 190(12):1801-1812.

(104) Hobart M, Ramassar V, Goes N, Urmson J, Halloran PF. IFN regulatory factor 1 (IRF-1) plays a central role in the regulation of the expression of class I and II MHC genes in vivo. Journal of Immunology 1997; 158:4260-4269.

(105) Braud VM, Aldemir H, Breart B, Ferlin WG. Expression of CD94-NKG2A inhibitory receptor is restricted to a subset of CD8+ T cells. Trends Immunol 2003; 24(4):162-164.

(106) Boucher JL, Custot J, Vadon S, Delaforge M, Lepoivre M, Tenu JP et al. N omega-hydroxyl-L-arginine, an intermediate in the L-arginine to nitric oxide pathway, is a strong inhibitor of liver and macrophage arginase. Biochem Biophys Res Commun 1994; 203(3):1614-1621.

(107) Eugui EM. Fibrogenesis in chronic allograft rejection: underlying mechanisms and pharmacological control. Transplant Proc 2002; 34(7):2867-2871.